

# VERIFICATION OF A CO<sub>2</sub> VOLUMETRIC ADSORPTION SYSTEM

**Mulanga Maphada**

A Dissertation submitted to the Faculty of Engineering and the Built Environment,  
University of the Witwatersrand, in fulfilment of the requirements of the degree of  
Master of Science in Engineering

Johannesburg 2013

## DECLARATION

I declare this dissertation is my own unaided work. It is being submitted for the degree of Master of Science in Engineering to the University of the Witwatersrand, Johannesburg. It has not been submitted before for any degree or examination to any other University.

.....  
(*Signature of Candidate*)

This ..... day of ..... year .....  
(*day*)                      (*month*)                      (*year*)

## ABSTRACT

Carbon dioxide (CO<sub>2</sub>) atmospheric emissions are regarded as the major cause of global climate change. South Africa aims to reduce its current emissions of over 400 Mton per annum through carbon dioxide capture and storage (CCS) technology by initially implementing the storage phase. Storage of captured CO<sub>2</sub> into various sites (such as coal, rocks, aquifers and etc) is a globally accepted means to mitigate the accumulation of greenhouse gases (GHG) in the atmosphere.

Before storing CO<sub>2</sub>, adsorption isotherms must be generated using a volumetric adsorption system (VAS). A VAS is used to determine the CO<sub>2</sub> storage capacity of coal, and other materials, by monitoring the uptake of a known amount of CO<sub>2</sub> under pressure, generating adsorption isotherms. This research aims to commission and verify the reliability of a VAS constructed at the University of the Witwatersrand, Johannesburg, by in-house and external repetitive adsorption tests - using CO<sub>2</sub> as an adsorbate and a homogeneous Witbank basin bituminous coal sample as an absorbent, in pressure steps from 10 bar up to 50 bar.

The operating procedure for the VAS is detailed. The average adsorption of the (in-house) repeatability runs was 0.0411 g CO<sub>2</sub> per g coal (at 50 bar). The inter-laboratory comparison run from an external lab at Aachen University of Technology had maximum adsorption capacity of 0.0250 g CO<sub>2</sub> per g coal. The difference in values is due to a variety of reasons, but essentially can be concluded that the VAS is able to generate CO<sub>2</sub> adsorption isotherms.

## Table of Content

DECLARATION.....	ii
ABSTRACT .....	iii
List of Figures.....	viii
List of Tables.....	ix
Nomenclature .....	x
Symbols .....	x
Subscripts .....	x
Units.....	x
Abbreviations .....	xi
1 INTRODUCTION .....	1
1.1 Background and motivation.....	1
1.2 Problem Statement .....	3
1.3 Research Questions.....	4
1.4 Aim and Objectives .....	4
1.4.1 Aim.....	4
1.4.2 Objectives .....	4
1.5 Scope of the Project.....	5
2 LITERATURE REVIEW .....	6
2.1 Equipment for CO <sub>2</sub> Adsorption Studies .....	6
2.1.1 History of the Equipment.....	6
2.1.2 Cases of using the VAS .....	6
2.1.3 Gravimetric Adsorption System.....	8
2.1.4 Concept of the VAS .....	9
2.1.4.1 Excess Isotherm.....	10
2.1.4.2 Absolute Isotherm .....	10
2.1.5 Pros and Cons of the VAS .....	10
2.1.5.1 Advantage .....	10
2.1.5.2 Disadvantages.....	11
2.2 Adsorption Isotherms .....	11
2.2.1 Definition of adsorption isotherms.....	11
2.2.2 Types of adsorption .....	12
2.2.3 Thermodynamics of adsorption.....	13
2.2.4 Kinetics of adsorption.....	14
2.2.5 Porosity in Adsorption .....	15
2.2.6 Interface action in adsorption .....	16

2.2.7	Moisture effect on Adsorption .....	16
2.3	Properties of CO <sub>2</sub> .....	17
2.4	Properties of coal .....	18
2.5	Theories of adsorption .....	18
2.5.1	Langmuir Isotherm .....	18
2.5.2	BET Isotherm .....	19
2.5.3	Dubinin-Radushkevich .....	20
2.6	Summary of the Literature review .....	21
3	EXPERIMENTAL PROCEDURE .....	22
3.1	Overall structure of the Equipment.....	22
3.1.1	Description of the Volumetric Adsorption Equipment .....	22
3.1.1.1	Gas Vessels .....	22
3.1.1.2	Temperature Sensor .....	23
3.1.1.3	Pressure Transducer .....	23
3.1.1.4	Valves, Electro-valve and piping equipment.....	26
3.1.1.5	Oven.....	26
3.1.2	Data acquisition and control system .....	26
3.2	Material and Sample preparation .....	27
3.2.1	Materials .....	27
3.2.2	Sample Preparation .....	27
3.2.3	Characterisation.....	28
3.2.4	BET and proximate analysis .....	29
3.3	Experimental Procedure for the VAS .....	29
3.3.1	Volume determination of the cells .....	29
3.3.2	Degassing procedure.....	31
3.3.3	Manual Operation .....	32
3.3.4	Automated Operation.....	33
3.3.4.1	Main virtual interface.vi.....	35
3.4	Safety Precautions .....	40
3.5	Tips on Avoiding Leaks .....	40
3.6	Data analysis.....	41
3.6.1	Isotherm Calculations .....	41
3.6.2	Standard Deviation .....	42
3.6.3	Correlation Coefficient .....	42
3.6.4	Reliability Measurement.....	43
3.6.5	T-TEST .....	43
3.7	Chapter Summary.....	46
4	RESULTS AND DISCUSSION .....	48
4.1	Analysis.....	48

4.1.1 Proximate analysis.....	48
4.1.2 BET analysis.....	49
4.1.2.1 Surface Area .....	49
4.1.2.2 Pore Volume.....	49
4.2 Commissioning of the VAS.....	49
4.2.1 Leaks and Pressure .....	49
4.2.2 Oven .....	50
4.2.3 LabVIEW.....	50
4.2.4 Inequality of pressures between the reference and sample cells.....	50
4.2.5 Pump .....	51
4.3 Verification of the VAS .....	52
4.3.1 Adsorption Isotherms for manual operation .....	52
4.3.1.1 Run I.....	55
4.3.1.2 Run II.....	55
4.3.1.3 Run III.....	55
4.3.1.4 Run IV .....	55
4.3.1.5 Run V .....	56
4.3.1.6 Run VI .....	56
4.3.1.7 Run VII .....	56
4.3.1.8 Run VIII .....	56
4.3.1.9 Run IX .....	56
4.3.2 Average Isotherm.....	57
4.3.3 Automated Run.....	59
4.3.4 Inter-laboratory results .....	63
4.3.5 T-TEST .....	64
4.4 Chapter Summary.....	65
5 SUMMARY AND CONCLUSIONS.....	66
6 RECOMMENDATIONS .....	69
7 ACKNOWLEDGEMENTS.....	71
REFERENCES.....	72
APPENDICES .....	80
Appendix 1: MSDS.....	80
MSDS of Coal .....	80
MSDS of CO <sub>2</sub> .....	85
Appendix 2: Derivation of Isotherms .....	92
Langmuir Derivation .....	92
Thermodynamics Derivation .....	92
BET isotherm derivation.....	94
Dubinin-Radushkevich isotherm derivation .....	94

Appendix 3: BET and proximate analysis methodology .....	95
BET Analysis Methodology .....	95
Proximate Analysis .....	96
Appendix 4: Adsorption Experiment Script for a Single Pressure Set .....	98
Appendix 5: Density of the Bulk Gas at 27 °C .....	100
Appendix 6: Example of the independent two-sample T-TEST .....	101
Appendix 7: Proximate Analysis.....	104
Appendix 8: Results Data of the Generated Isotherms .....	105
Appendix 9: The AUT isotherm results .....	107
Appendix 10: Operational Procedure .....	108
Appendix 11: Documents about the VAS and Automatic Pump .....	109
Appendix 12: Runs.....	110

## List of Figures

Figure 2.01: Profile of Gas Density at Gas-Solid Interface .....	9
Figure 2.02: Temperature-Pressure Profile with respect to depth .....	17
Figure 2.02: The Phase Diagram for CO <sub>2</sub> .....	17
Figure 3.01: Volumetric Measurement Instrument with Data Acquisition, Measurement Display and Control and Costs .....	22
Figure 3.02: The Schematic Diagram of the CO <sub>2</sub> -on-Coal Volumetric Adsorption System .....	23
Figure 3.03: The Images of the Experimental Setup .....	24
Figure 3.04: The overall structure displaying the sample preparation procedure .....	28
Figure 3.05: The Simplified Version of Section Number 12 in Figure 3.02 .....	35
Figure 3.06: Systematic View of the Controlled Experimental Setup .....	36
Figure 3.07: The Interface of Main.vi. The Tab of Display.....	39
Figure 3.08: The Interface of Main.vi. The Tab of the Script Code.....	40
Figure 3.09: The Interface of Filezilla .....	41
Figure 4.01: Comparison of D-R adsorption capacities and EXC isotherm adsorption capacity for all the run .....	50
Figure 4.02: Nine comparisons of the excess adsorption isotherms (adsorption amount) and Langmuir and BET adsorption isotherm models with respect to the relative pressure.....	51
Figure 4.03: The average isotherm which was derive by averaging each pressure point for all the experimental runs .....	54
Figure 4.04: Pressure-Temperature profile of the first point at 28 °C and reference pressure of 10 bar (the 1 <sup>st</sup> 150 seconds of this pressure step) and the equilibration pressure amounting to 4 bar .....	55
Figure 4.05: Pressure-Temperature profile of the second point at 28 °C and reference pressure of 35 bar (the 1 <sup>st</sup> 150 seconds of this pressure step) and the equilibration pressure amounting to 20 bar .....	56



Figure 4.06: Pressure-Temperature profile of the third point at 28 °C and reference pressure of 38 bar (the 1st 150 seconds of this pressure step) and the equilibration pressure amounting to 32 bar .....	56
Figure 4.07: Pressure-Temperature profile of the fourth point at 28 °C and reference pressure of 50 bar (the 1st 150 seconds of this pressure step) and the equilibration pressure amounting to 41 bar .....	57
Figure 4.08: Pressure-Temperature profile of the fifth point at 27 °C and reference pressure of 50 bar (the 1st 150 seconds of this pressure step) and the equilibration pressure amounting to 45 bar .....	57
Figure 4.09: Pressure and Adsorbed amount profile as a function of time .....	58
Figure 4.10: Comparison of the inter-laboratory results (35 °C) and the average isotherm in Figure 4.03 (27 °C) .....	59

## List of Tables

Table 2.01: Comparison between Chemisorption and Physisorption .....	12
Table 3.01: Summary of Instrument Specification .....	27
Table 3.02: Determination of the average $V_B:V_A$ .....	33
Table 3.03: The Volume of the Reference Cell .....	34
Table 4.01: Proximate Analysis of the coal adsorbent .....	46
Table 4.02: The comparison of relative pressures for all nine runs at different experimental points of each run .....	49
Table 4.03: The comparison of excess mass (adsorbed mass) of all the runs at the average relative pressure .....	49
Table 4.04: The population D-R adsorption capacities for all the runs at the average relative pressure .....	50
Table 4.05: The results of the T-TEST on the last column of the table. ....	60

## Nomenclature

### Symbols

CL	confidence limit
D	Constant for a particular adsorbent-adsorbate system
E	Characteristic energy of the adsorption system
m	number of machines required in the test
N	Number of mole/s (mol)
P	Pressure (bar)
Q	Volume of the adsorbed phase per mass of the adsorbent (ml)
Q <sub>m</sub>	The amount of the adsorbate after the whole monolayer is covered (ml)
Q <sub>o</sub>	The volume of micropores (ml)
R	Gas constant (kJ/mol-K)
T	Temperature (deg Celcius)
V	Volume (ml)
R <sub>t</sub>	true reliability
γ	Structural heterogeneity parameter - varies from 1 – 4
β	Adsorbate affinity coefficient

### Subscripts

ads	adsorbed gas
G	bulk gas
ref	Reference
VAP	Vapour pressure
Vessel	Vessel
sam	Sample

### Units

°C	degree Celsius
bar	bars
g	gram
K	Kelvin
kPa	kilopascal

l	litre
m <sup>3</sup>	cubicmetre
mg	milligram
mol	moles
ml	millilitre
mm	millimetre
mmol	millimole
µm	micrometre
Pa	Pascals

## **Abbreviations**

AUT	Aachen University of Technology
BET	Isotherm theory developed by Brunauer S., Emmett P. H. and Teller E.
CDM	Clean Development Mechanism
cRIO	Compact RIO
CSIR	The Council of Scientific and Industrial Research
D-R	Dubnin-Radushkevich Isotherm
DMR	Department of Mineral Resource
DOE	Department of Energy
EXC	Excess Isotherm
GHG	Greenhouse Gases
IPCC	Intergovernmental Panel of Climate Change
LAN	Langmuir Isotherm
NECSA	The South African Nuclear Energy Corporation
NI	National Instruments
NIST	The National Institute of Standard and Technology
UIG	Universal Industrial Gas
VAS	Volumetric Adsorption System
vi	Virtual Interface
Wits	University of Witwatersrand

# 1 INTRODUCTION

## 1.1 Background and motivation

Although there are some who appear to disagree on the topic of global warming or global climate change, generally it is considered to be a dilemma which few can deny. There are two main schools of thoughts from the scientific arena regarding the major cause of global warming (Schneider, 1990; Viljoen et al., 2010). Some attribute the warming to solar rays, while others attribute it to the increase in GHG due to anthropogenic (produced by human activities) activities (Lashof and Ahuja, 1990; Viljoen et al., 2010). Apart from water vapour, CO<sub>2</sub>, CH<sub>4</sub>, NO, and O<sub>3</sub> are the main gases which retain heat in the earth's atmosphere (Viljoen et al., 2010). However, CO<sub>2</sub> has a higher concentration relative to the rest, after H<sub>2</sub>O (Viljoen et al., 2010).

The Republic of South Africa relies heavily on fossil fuels to meet its energy requirements, and is expected to emit 441 Mton of CO<sub>2</sub> per year from energy production and other fossil fuel based processes (Viljoen et al., 2010). South Africa has agreed to the Kyoto Protocol as a non-Annex I country, and its participation is initially and primarily through the Clean Development Mechanism (CDM) (Engelbrecht et al., 2004; Viljoen et al., 2010). South Africa is a member of the Carbon Sequestration Leadership Forum (CSLF). The responsible government department for the whole Carbon Dioxide Capture and Storage (CCS) value chain (regulation and policy derivation) in South Africa is the Department of Energy (DOE) (Engelbrecht et al., 2008; Viljoen et al., 2010). In 2010, when launching the South African atlas for potential CO<sub>2</sub> sequestration sites, the Minister of Energy (Minister Dipuo Peters) affirmed the intentions of South Africa towards mitigating GHG atmospheric emissions (Cloete, 2010).

Carbon Capture Storage is divided into three phases: capture, transport, and storage (Metz, Davidson, de Coninck, Loos, & Meyer, 2005). Storage is globally accepted as a proper procedure to mitigate the accumulation of GHG in the atmosphere (Metz et al., 2005); this is the phase of current activity in South Africa. Storage is a geo-engineering process where the gas is stored in geological sites for the long-term (Metz et al., 2005). Storage by adsorption in geological mediums is of interest due to the associated low

energy consumption, low equipment cost, and ease of application (Bahadori and Vuthaluru, 2009). Anthropogenic CO<sub>2</sub> emissions can be captured by various costly physical or chemical (such as adsorption and absorption) technological processes, and then transported to various suitable geological sites for storage by either pipelines or shipping to the storage sites (Bahadori and Vuthaluru, 2009; Metz et al., 2005). South Africa has an advantage as it has a large storage-ready CO<sub>2</sub> stream from the Sasol process, with 90 – 98 % purity (Viljoen et al., 2010); however, a suitable storage location needs to be sought. A possible advantage of CO<sub>2</sub> sequestration in geological sites is the future potential ease of extraction of CO<sub>2</sub> when seeking to restore carbon in the inorganic gas into another useful form.

The storage sites for CO<sub>2</sub> include coal seams (in unminable or abandoned mines), depleted oil and gas wells, as well as saline aquifers (Engelbrecht et al., 2008; Viljoen et al., 2010). However, for South Africa, the depleted oil and gas wells option is not readily viable, while the coal seam storage is an option worthy of further exploration (Engelbrecht et al., 2008; Viljoen et al., 2010). The difficulty lies in the fact that coal is one of the major export commodities in South Africa, is necessary for energy production, and is used in metallurgical and gasification processes. The definition of an unmineable coal seam is constantly changing. It is necessary to calculate CO<sub>2</sub> uptake in geological materials prior to injection at site, to estimate the volume available for storage.

In the past four years, the Coal and Carbon Research Group (CCRG) at the University of Witwatersrand (Wits) has developed an interest in the aspect of CO<sub>2</sub> storage in geological materials, specifically coal. Bhebhe (2008) undertook a preliminary assessment of the effect of coal composition on CO<sub>2</sub> adsorption (South African coals), and this work forms an on-going PhD project. A PhD student is considering the effect CO<sub>2</sub> may have on coal properties over time. Three other MSc students are investigating the effect of in-situ moisture in CO<sub>2</sub> adsorption in coal, potential adsorption of CO<sub>2</sub> into coal ash, and impact of non-pure CO<sub>2</sub> gas mixtures on adsorption.

The intention of this study is to commission a volumetric adsorption system (VAS), and to verify the reliability of the system using a South African bituminous coal sample as the adsorbent and CO<sub>2</sub> as an adsorbate. A VAS is used to determine the CO<sub>2</sub> storage capacity of coal, and other materials, by monitoring the uptake of a known amount of CO<sub>2</sub> under pressure, generating adsorption isotherms. Although this study also seeks to prove the

reliability of the VAS, the most reliable validity of the generated isotherms might be determined in the future projects as more information pertaining to CO<sub>2</sub> adsorption becomes available, and the database is enhanced.

There are a handful of VASs that are currently in operation the world for the generation of CO<sub>2</sub> adsorption isotherms. The Aachen University of Technology (AUT), Germany, has used VASs for ten years or so, and the CCRG has designed and constructed a comparable system using a local engineering company. Chemvac in South Africa was contracted to build the equipment, and the certification was done by the South African Nuclear Energy Corporation (NECSA).

The results obtained were subjected to comparisons with the models already available in the literature in order to determine the best fit. In this case, the selected models are Langmuir, BET<sup>1</sup> and Dubinin–Radushkevich isotherms. Although the VAS cannot fully imitate the exact CO<sub>2</sub> isotherm in underground coal seams, the temperatures and pressures during the experiment were adjusted such that they can simulate the underground coal seam conditions as far as possible. Based on the literature, a suitable underground depth for CCS is estimated at 800 m, which approximates the pressure and temperatures of 190 bar and 70 °C (Metz et al., 2005).

As the South African government is intentionally seeking to reduce CO<sub>2</sub> emissions, an instrument for estimating adsorption capacity is necessary to generate data on South African coals and other potential geological adsorbents.

## **1.2 Problem Statement**

In order to effectively determine CO<sub>2</sub> adsorption, it is necessary to obtain data from a VAS, and to simulate the underground conditions as far as possible in a laboratory environment.

The VAS is an instrument which is used to generate CO<sub>2</sub> adsorption isotherms, and thus the instrument is able to determine theoretical estimations of adsorption isotherms which can be modified into practical estimation by applying scaling factors. Scaling factors account for in-situ parameters which are generally neglected during laboratory experiments. With incorrect estimations and/or measurements and assumptions, CO<sub>2</sub> geo-

---

<sup>1</sup> BET is an Isotherm theory developed by Brunauer S., Emmett P. H. and Teller E. in 1938

storage could be highly inaccurate. The project at hand concerns a high pressure CO<sub>2</sub>-on-Coal adsorption study using a VAS , and provides a foundation for further research projects on related topics.

### **1.3 Research Questions**

The following questions were addressed during the course of the research:

1. How many runs need to be performed in order to test each variable (temperature, volume, flow rate, pressure and time) to provide a degree of confidence using the VAS?
2. Does the designed volumetric equipment measure CO<sub>2</sub> adsorption as expected?
3. What is the consistency of the results when the experiment is reproduced?
4. Which isotherm model (BET, Langmuir and Dubinin-Radushkevich) best predicts the generated isotherm?
5. Does LabView monitor and control the equipment effectively?
6. Do the results from an inter-laboratory comparison match the results generated at the Wits?

### **1.4 Aim and Objectives**

#### **1.4.1 Aim**

The aims of the project were to commission a VAS operating up to 100 bar, and to verify the reliability of the instrument using a South African coal sample and CO<sub>2</sub> gas at various temperatures and pressures. This research project fits into a larger initiative under-way with the CCRG at Wits.

#### **1.4.2 Objectives**

In order to achieve the above aims, the following objectives were addressed:

1. Prepare a suitable laboratory environment with a specific focus on the safety aspects.
2. Gain an understanding of the VAS by working with Chemvac during the design, construction, and commissioning stages.
3. Prepare homogeneous coal samples for the use of the project and inter- laboratory comparisons.
4. Automate the equipment using LabView so that data acquisition can be quick and computer based.
5. Verify the reliability of the equipment by consistency mapping of variables, namely: temperature, pressure, volume, flow rate and time.
6. Perform an inter-laboratory comparison to verify the results

## **1.5 Scope of the Project**

There are two phases involved in this project:

**Phase I** of the project included the commissioning and verification of a volumetric adsorption instrument using coal and CO<sub>2</sub> as adsorbent and adsorbate respectively. The exercise was performed at Wits. All the results generated were fitted with the Langmuir, BET and Dubinin–Radushkevich models. The methodology designed to operate the VAS is explained in detail.

**Phase II** involved an inter-laboratory comparison where a representative sample was sent to AUT. The set of conditions which were used during the comparison were specified by Wits, based on the conditions determined during Phase I. The Phase II exercise was undertaken to determine an international comparison of the results generated from the CCRG equipment, and thus increase the degree of confidence.



## **2 LITERATURE REVIEW**

The aim of the research is to commission and verify the reliability of an automated volumetric adsorption isotherm instrument used to measure CO<sub>2</sub> storage capacities in coal. The literature review explores the theory behind the equipment, adsorption and adsorption isotherms, and briefly considers the properties of coal and CO<sub>2</sub>.

### **2.1 Equipment for CO<sub>2</sub> Adsorption Studies**

There are various types of adsorption systems in the world today, namely: volumetric (sometimes known as manometric), gravimetric, carrier gas, and calorimetric methods (Keller and Robens, 2003). However, the most commonly used are volumetric (or manometric) and gravimetric systems, and this project is focused at experimenting with the former.

#### **2.1.1 History of the Equipment**

According to Kiefer and Robens (2008), the measurement of adsorption isotherms by the adsorption systems goes back all the way to ancient times. In the Bible, Judges 12 has one of the earliest records of an adsorption experiment between dew and dry wool (Kiefer and Robens, 2008). One of the observed natural phenomena which revealed the vitality of adsorption is salt water which becomes much less salty due to the presence of sand, which adsorbs the salts in the medium. The large-scale World War I applications of the adsorption phenomenon were in gas masks filtering unwanted gases and purifying air in submarines (Kiefer and Robens, 2008).

#### **2.1.2 Cases of using the VAS**

Volumetric adsorption systems has been used for various purposes, including sorption measurements using coal as adsorbent and CO<sub>2</sub> as absorbate. When measuring sorption rates, the results are usually fitted to various theories of adsorption isotherms – e.g. Langmuir, BET and Dubinin-Radushkevich (see *Section 2.5* for more details). Following is a list of VAS setups commissioned across the world for adsorption measurements on various adsorbents.

#### **Coal substrate**

1. Gertenbach (2009) used a VAS to perform CH<sub>4</sub> and CO<sub>2</sub> sorption studies on South African coals
2. Adiraju (2010) used a VAS to measure an adsorption of CO<sub>2</sub> on Indian coals
3. Lin (2009) used the equipment to perform a study on gas sorption and the consequent volumetric and permeability change of coal

#### **Other substrates**

4. Parseresht et al. (2002) used the system in order to assess the equilibrium isotherms for CO, CO<sub>2</sub>, CH<sub>4</sub> and C<sub>2</sub>H<sub>4</sub> on the 5A Molecular Sieve by a Simple Volumetric Apparatus.
5. Hemert et al. (2009) used the system in the determination of accurate supercritical CO<sub>2</sub> sorption utilising an improved volumetric setup (Hemert, Bruining et al., 2009).
6. Fujii et al. (2009) used the system to measure CO<sub>2</sub> sorption capacity on the rocks for CO<sub>2</sub> Geological Storage.

The VAS has also been useful in generating isotherms for inter-laboratory studies.

- a. European inter-laboratory comparison of high pressure CO<sub>2</sub> sorption isotherms. I: Activated carbon (Gensterblum et al., 2009)
- b. Inter-laboratory comparison II: CO<sub>2</sub> isotherms measured on moisture-equilibrated Argonne premium coals at 55 °C and up to 15 MPa (Goodman et al., 2007)
- c. Impact of experimental parameters for manometric equipment on CO<sub>2</sub> isotherms measured: Comment on “Inter-laboratory comparison II: CO<sub>2</sub> isotherms measured on moisture-equilibrated Argonne premium coals at 55°C and up to 15 MPa” by Goodman et al. (2007) (Yu, Guo, Cheng, and Hu, 2008)

When commissioning and verifying an instrument, it is advisable to perform an inter-laboratory study. The European Round Robin for the determination of CO<sub>2</sub> isotherms on activated carbon, using VASs, was used as a guideline (Gensterblum et al., 2009). The inter-laboratory study is necessary because it helps to formulate a standard procedure which can improve overall data quality.

### 2.1.3 Gravimetric Adsorption System

Although the gravimetric adsorption system is not utilised in this project, it is still noteworthy to explore some of the advantages and disadvantages of this equipment to enhance the understanding of the advantages of the volumetric system.

According to Keller and Staudt (2005a), the advantages of the gravimetric adsorption system are:

1. The system generates more accurate isotherms (than the VASs) due to high reproducibility.
2. The amount of the sorbent required to generate an isotherm can be very small. Hence, the gravimetric system can be advantageous when the sample available is too small.
3. Approach to equilibrium is easily attainable when coupled with data acquisition system and microbalances with alphanumerical display.
4. Wall sorption does not pose problems since gas mass balances are based on weight rather than gas phase pressure.
5. Extreme pressures (very high and very low) do not pose a problem since the adsorbed amount is based on the weight.
6. The mass of the sorbent and adsorbent can be measured throughout the experiment.

The disadvantages are (Keller and Staudt, 2005b):

1. The modern microbalances are very complex. The magnetic suspension balances microbalances are very sensitive to electromagnetic or mechanical external disturbances.
2. The measurement techniques are not easy because of the complexities of detection of thermophysical properties, necessities of various calibration, careful handling of sorbent material and requirement of a sophisticated software. Hence, automation is not easy either.
3. The gravimetric system is expensive.

#### 2.1.4 Concept of the VAS

The VAS is used to generate isotherms known as sorption or adsorption isotherms. A sorption isotherm is the amount of moles of adsorbate adsorbed by an adsorbent relative to its mole amount of different pressure steps and the same temperature. See further details about the isotherms in the adsorption isotherm

Since adsorption occurs on the surface of the adsorbent, the chemical composition and the geometry of the adsorbent is very important. The geometry of an adsorbent includes: specific surface area, pore size distribution, specific pore volume, particle size distribution and density (Keller and Robens, 2003).

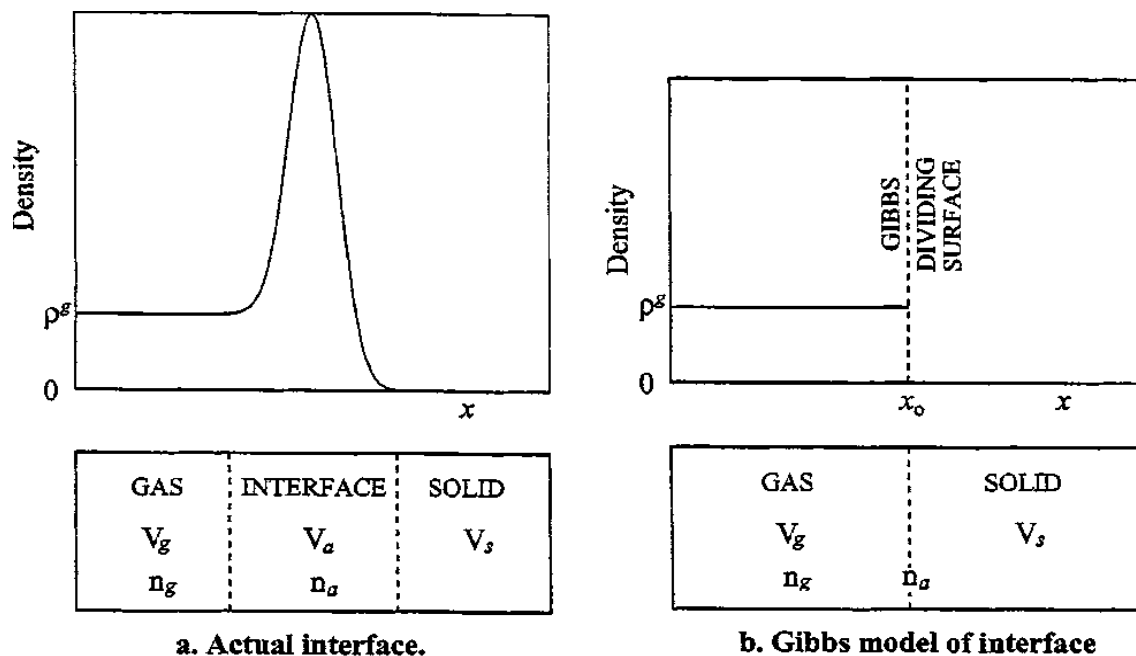


Figure 2.01: Profile of Gas Density at Gas-Solid Interface (Myers, 2002)

According to Myers (2002), the VAS is based on the principle displayed in Figure 2.01a. In Figure 2.01, adsorbed molecules are all the molecules a certain distance from the surface of the adsorbent, while the rest of the adsorbates are regarded as the bulk phase. However, the pore size of the adsorbent and the quick rate of reaction make the determination and the observation of the exact distance highly difficult the naked eye. The complication imposed by the definition of the interfacial distance was solved by Gibbs, as shown in Figure 2.01b. Gibbs proposed an 'unclear' mathematical dividing surface between the adsorbent and adsorbate (Myers, 2002). At a given conditional pressure and

corresponding temperature of an adsorption application, the mass (moles) balance surface is defined as follows (Myers, 2002):

$$\text{Adsorbed Adsorbate} = \text{Total Adsorbate (Initial)} - \text{Bulk Adsorbate (Ongoing)} \dots \dots \dots 2.01$$

$$N_{\text{ads}} = N_t - \rho_g V_g \dots \dots \dots 2.02$$

Where:  $N$  is the absorbed moles of an adsorbate,  $N_t$  is the total moles of the adsorbate,  $V_g$  is the volume of the bulk phase adsorbate and  $\rho_g$  is the density of the adsorbate in the bulk phase.

#### 2.1.4.1 Excess Isotherm

According to Gertenbach (2009), equation 2.02 is called the excess isotherm when  $V_g$  is equated to the void volume only ( $V_{\text{void}}$ ). The void volume is the absolute difference between the total volume of the sample cell ( $V_{\text{SC}}$ ) and the volume of the sample ( $V_s$ ) (Gertenbach, 2009; Myers, 2002). Equation 2.02a below depicts the phenomenon explained above (Gertenbach, 2009; Myers, 2002):

$$N_{\text{exc}} = N_t - \rho_g V_{\text{void}} \dots \dots \dots 2.02a$$

Where:  $N_{\text{exc}}$  is the number of moles excess isotherm.

#### 2.1.4.2 Absolute Isotherm

However,  $V_{\text{void}}$  in equation 2.02a is not the exact 'true' void volume ( $V_t$ ) because the adsorbed phase volume is disregarded (Gertenbach, 2009; Myers, 2002). Hence, when the  $V_g$  is equals to  $V_t$ , equation 2.02 produces the absolute isotherm (equation 2.02b).

$$N_{\text{ads}} = N_t - \rho_g V_t \dots \dots \dots 2.02b$$

Where:  $N_{\text{ads}}$  is the number of moles excess isotherm. Hence, the adsorbed phase volume ( $V_{\text{ads}}$ ) is  $V_t$  subtracted by  $V_{\text{void}}$ .

### 2.1.5 Pros and Cons of the VAS

#### 2.1.5.1 Advantage

The VAS generally selected, because of its lower cost and simplicity of construction and operation relative to the gravimetric adsorption system. The volumetric instrument does

not require high technological accessories and the experiment is simple in terms of opening the valve in between the adsorption and the gas vessel.

#### 2.1.5.2 Disadvantages

The pitfalls of the VAS are, according to (Keller and Staudt, (2005a):

1. Sorption equilibrium changes are not observable when the sample is tiny, (volume ratio of the sample to the whole adsorption chamber should not be less than 5 %)
2. Since adsorption time can take seconds, hours, and days, the establishment of the thermodynamic equilibrium cannot be easily realised. Gravimetric results can be useful in cases such as these, by its mass measurements.
3. The walls of the vessel can adsorb the adsorbate which leads further uncertainties. However, these uncertainties can be minimised by wall electropolishing and a performance of gas expansion in an empty vessel.
4. Unadsorbed gas phase in between the sorbent requires further compression.
5. Leaks pose serious uncertainties in the calculation of isotherms because of the uncertainties in the pressure of the gas.

## 2.2 Adsorption Isotherms

After understanding the VAS concept, the next topic of familiarisation is that of adsorption isotherm. This is of use because the VAS is used to generate adsorption isotherms. Hence, the following sub heading provide the definition and types of adsorption, and the other factors that are normally used to under adsorption.

### 2.2.1 Definition of adsorption isotherms

According to Mantell (1951), an adsorption isotherm is generated after measuring the adsorbed amount based on the variation of pressure at constant temperature. An adsorption isotherm is different from an adsorption isobar (measured at constant pressure and varying temperature) and an isostere (measured during simultaneous variation of both temperature and pressure). The generated plots of isobars, isotherms and isosteres are used to estimate the amount of an adsorbate which can be absorbed as a film on the surface of an adsorbent.

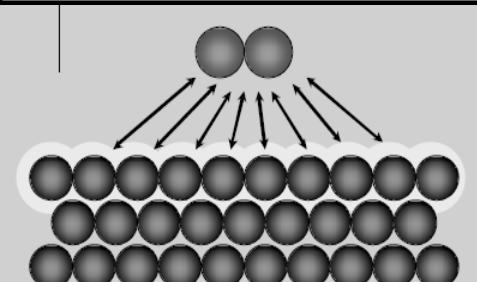
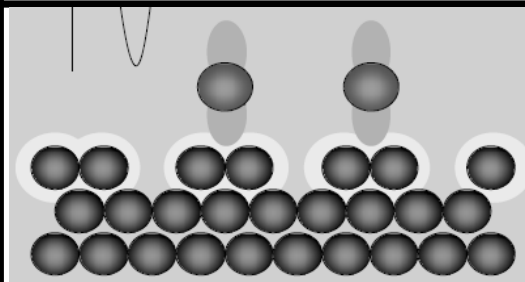
Mantell (1951) stated that an adsorbent is a solid that allows adherence of an adsorbate. During this investigation, coal is the selected adsorbent and CO<sub>2</sub> gas is adsorbate. The quantity of gas that can be adsorbed at equilibrium per mass of the adsorbent is dependent upon the temperature, the pressure, the nature of the adsorbent and the preparation and history of both adsorbent and adsorbate.

### 2.2.2 Types of adsorption

There are two types of adsorption, namely chemical and physical. The classification terminologies mostly used are chemisorption and physisorption. Chemisorption (or chemical adsorption) is adsorption in which the forces involved are valence forces of the same kind as those operating in the formation of chemical compounds (Everett et al., 2002). Physisorption (or physical adsorption) is adsorption whereby the forces involved are intermolecular forces (Van der Waals forces) of the same nature as those responsible for the imperfection of real gases and the condensation of vapours and which do not involve a significant change in the electronic orbital patterns of the species involved (Everett et al., 2002). The term “Van der Waals adsorption” is similar to “physical adsorption” (Everett et al., 2002).

Identification of the type of adsorption is done by quantifying the heat of adsorption (Mantell, 1951). Based on the energy balance of the adsorption process, the heat of adsorption is the enthalpy change that results as a difference between the final and initial states of the gas phase adsorption (Mantell, 1951). The magnitudes of heat of adsorption for chemisorption are in the orders of heat of reaction while physisorption is in the order of heat of condensation (Mantell, 1951). The summary of the adsorption types is as follows in Table 2.01.

Table 2.01: Comparison between Chemisorption and Physisorption (Everett et al., 2002)

Types of Adsorption	Physisorption	Chemisorption
<b>Bonding</b>	The bonds are weak and long range which implies the interactions is Van der Waals (e.g. London dispersion, dipole-dipole)	The bonds are strong, short range and includes orbital overlap and charge transfer.
<b>Surface Specificity</b>	It is not surface specific hence it occurs between all molecules on any surface providing the temperature is low enough.	It is site specific. For example chemisorption of hydrogen takes place on transition metals but not on gold or mercury.
<b>Models</b>		

### 2.2.3 Thermodynamics of adsorption

The thermodynamic data can be utilised to estimate the heat of adsorption. Heat of adsorption is the change in enthalpy (of CO<sub>2</sub> in the gas phase) of before and after adsorption states. However, future exploration of adsorption thermodynamics can help understand the nature of equilibrium. Mantell (1951) illustrated that at equilibrium, the rate of desorption (reverse of adsorption) and adsorption is equal, and this is when the amount adsorbed on the solid surface is no longer changing. Since the process is batch, adsorption isotherms were measured when the 'second' equilibrium of adsorption was established. Without this adsorption equilibrium the maximum capacity of an adsorbent cannot be known because physisorption is sometimes too quick, such that the rate cannot be measured.

According to Mantell (1951), physisorption is a spontaneous thermodynamic process because the entropy change is negative (due to deposition of the adsorbent onto the substrate gas a translational degree of freedom is lost), enthalpy change is negative (exothermic) and hence the Gibbs free energy change is negative (Bellert et al., 1996).



An increase in the gas temperature leads to a decrease in the adsorbed quantity, and hence a decrease in the heat of adsorption (Sakurovs et al., 2008). At low temperature, the predominant adsorption form is physical (Mantell, 1951). At high temperature, the operative forces are of the same order as those of primary chemical valence forces, which can lead to the possibility of the occurrence of chemisorptions (Mantell, 1951). Adsorption of gases by charcoal showed that as the critical temperature increases, adsorption volume increases (Mantell, 1951).

As an example, coal from Pocahontas number 3 seam (USA) had of a CO<sub>2</sub> sorption capacity decreasing with the increase in temperature at 35 and 55 °C at pressures up to 15 MPa (Day et al., 2008). The critical point of CO<sub>2</sub> is 31 °C and 73 bar. The decrease is due to the decrease in equilibrium constant which decreases with temperature (Sakurovs, 2008).

#### 2.2.4 Kinetics of adsorption

Understanding kinetics is essential, because kinetics determines the rate of adsorption. Adsorption kinetics is not very different from the normal application of kinetics theory (Nix, 2003). Hence the rate of adsorption can be expressed as any kinetics; where the kinetic rate is the product of the rate constant and partial pressure of the bulk gas phase to the power of the order of the process (Nix, 2003). The rate constant can be estimated using the Arrhenius form if applicable (Nix, 2003).

The rate of adsorption is governed by the rate of arrival of molecules at the surface and the proportion of incident molecules which undergo adsorption (Nix, 2003). The total gas molar flux in the pore is due to many transport mechanisms, namely: pore diffusion, viscous flow and surface diffusion (Mugge et al., 2000). For this project, only surface diffusion was of interest.

Saghafi et al. (2007) found that some coal samples in the Australia Basin stored twice the volume of CO<sub>2</sub> relative to CH<sub>4</sub>, and six times more CO<sub>2</sub> than N<sub>2</sub>, and CO<sub>2</sub> diffusivity was found to be twice as quick as CH<sub>4</sub>. A phenomenon like this should be carefully considered before generalising, since the quality of coal seams differs by location.

According to Shi et al. (2008), when a pore already contains CH<sub>4</sub>, CO<sub>2</sub> displaces the in situ molecules due to stronger affinity to coal. The above phenomenon is the basis for the

feasibility of enhanced coal bed methane recovery - ECBM (Shi et al., 2008). ECBM is a process where CO<sub>2</sub> is injected into a coal bed (containing in situ CH<sub>4</sub>) in order to displace the CH<sub>4</sub> already contained to recovery from the bed with CO<sub>2</sub> and hence storing the inorganic gas (Shi et al., 2008).

The report on the adsorption of gas by charcoal revealed that at least 2 times more CO<sub>2</sub> was stored than CH<sub>4</sub> (Brunauer, 1943; Mantell, 1951). For a given pressure-temperature (P-T) condition, coal can adsorb more CH<sub>4</sub> than CO<sub>2</sub> depending on the rank of the coal (Saghafi et al., 2007). High hydrogen content in coal leads to a decrease in the adsorptivity of CO<sub>2</sub> in coal (Day et al., 2008).

An experiment on Chinese coals at 45 °C with a particle size range of 0.345 – 1 mm, showed that CO<sub>2</sub> adsorption occurred quicker than CH<sub>4</sub> in anthracite and medium volatile bituminous coal (Li et al., 2010). For sub-bituminous coal, CO<sub>2</sub> reached equilibrium more quickly (Li et al., 2010). The sorption capacity reached more than 60% of its final value almost instantaneously (<10 s) while only 30 - 40 % of the final sorption capacity was occupied at the same point of time for the other two coals (Li et al., 2010). At a temperature range of 35 – 55 °C, the three different types of coal used in the experiment to show an insignificant difference of the results, as the pressure in the gas phase tends to be greater than 200 bar (Li et al., 2010).

A pressure decay expression can be utilised in order to estimate the mass of CO<sub>2</sub> adsorbed at each point of time until an equilibrium. The pressure decay function below shows an assumption which states that the decrease of mass in the free phase of an isolated system is equal to the increase of the amount of substance adsorbed:

$$\frac{M_t}{M_2} \approx \frac{P_1 - P_t}{P_1 - P_2} \dots \dots \dots 2.03$$

Where M<sub>t</sub> and M<sub>2</sub> are estimated mass amounts adsorbed at time t and t<sub>2</sub> (equilibrium time) respectively and P<sub>t</sub> is the pressure at time t (Li et al., 2010).

## 2.2.5 Porosity in Adsorption

Another important property of an adsorbent which is vital to the rate of adsorption is porosity, since it impacts the diffusivity of the gas. According to Mantell (1951), porosity determines the surface area of the adsorption sites of the adsorbent and the diffusivity

(mass transfer) of the gas through the matrix of adsorbent. Porosity can be classified in three classifications: micro-, meso- and macro-pores. At high pressure, a significant amount of gas can be stored in the pores, especially if they are not saturated with water. Amorphous solids can generally adsorb more gas than crystal solids due to their large effective surface area. Micropores have a high adsorptivity since there is high adsorbate-adsorbent interaction (Nicholson and Sing, 1976). The shape and size of the pores is important such that the pores cannot be too narrow to an extreme where the gas has a hindered passage into the pores (Mantell, 1951). Heat of adsorption is larger in narrow pores due to their large surface area, since the adsorbate is under large attractive forces (Mantell, 1951).

Day et al. (2008) performed an experiment using 30 dry coals of different origin and diversity at 53 °C and pressures up to 16 MPa. The aim of the experiment was to investigate the effect of coal properties under supercritical conditions. The results shown, two of the coals had a significant higher sorptivity of CO<sub>2</sub> when compared with the other 28. The high sorptivity was due to their high porosity.

#### 2.2.6 Interface action in adsorption

Mantell (1951) illustrated that adsorption occurs at the surface of an adsorbent where a solid and a gas come into contact with each other. The adsorbate film that is formed during adsorption is an interface between the two phases. A molecule in the body of a solid is subjected to two unbalanced forces (inward pull greater than outward pull) which lead to unbalanced forces. Due to these unbalanced forces, the surface area of a solid tends to decrease and then a solid shows surface tension just like a liquid. When gas molecules strike the adsorbent surface, they end up being adsorbed by the atoms on the surface due to saturation of unsatisfied forces resulting from the repetitive striking. This results in the decrease of surface tension.

#### 2.2.7 Moisture effect on Adsorption

Wet Selesia coal had low adsorption capacity relative to the dry sample (Busch et al., 2006). Hence, the effect of water in adsorption should not be underestimated, since it can lead to the reduction of the gas adsorption. The presence of moisture in coals can affect

the adsorption of gases in the form of gas dissolution, pore blockage or filling and structural changes due to coal swelling (Menon, Leon, Kyotani, and Radovic, 1991).

### 2.3 Properties of CO<sub>2</sub>

Carbon dioxide is a slightly toxic, odourless and colourless gas with a slightly pungent and acid taste (UIG, 2008). As stated in UIG (2008), the critical point conditions are: Temperature: 31.1 °C, Pressure: 73.82 bar and Density: 468 kg/m<sup>3</sup> ; the triple point conditions are: Temperature: -56.6 °C, Pressure: 5.173 bar; the normal boiling conditions are: Temperature: -78.5 °C, Pressure: 1 bar and Latent Heat: 571.3 kJ/kg ; and the molecular weight of CO<sub>2</sub> is 44.01 g/mol (Kobulnicky, 2008). The phase diagram is explained in Figure 2.02 (Kobulnicky, 2008):

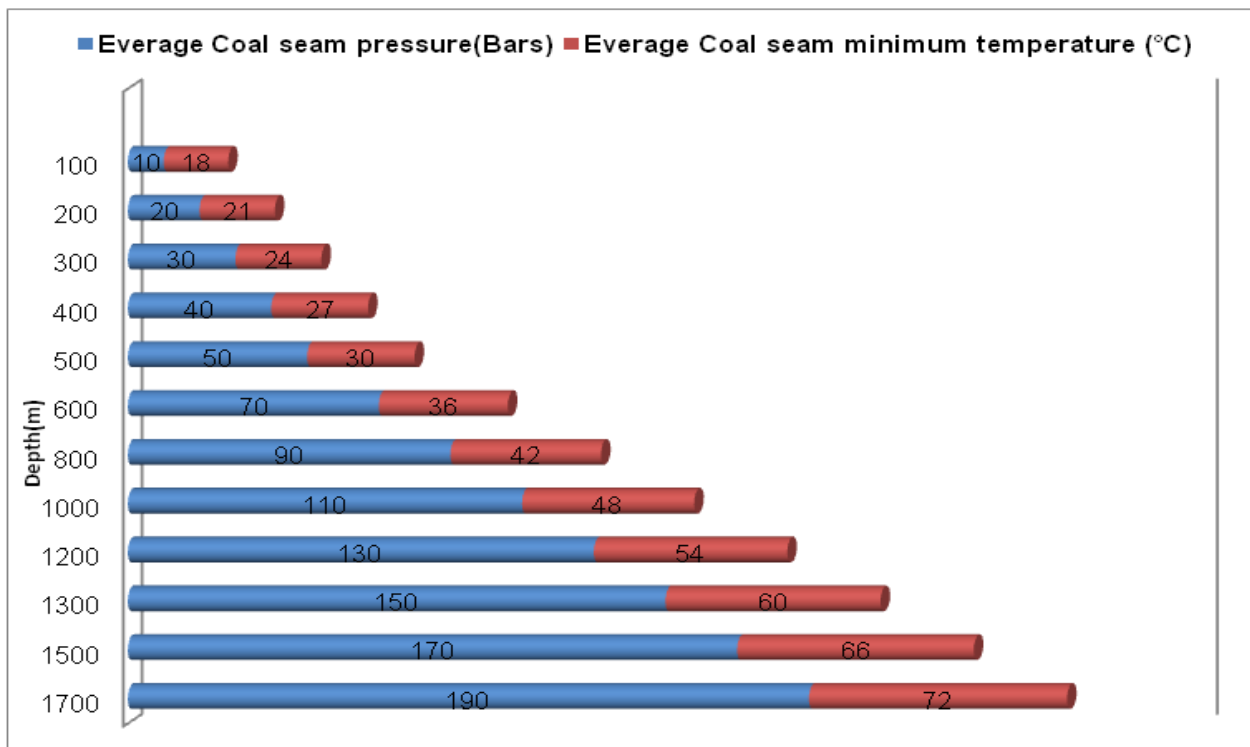


Figure 2.02: Shows Temperature-Pressure Profile with respect to depth (Qing-ling, 2008)

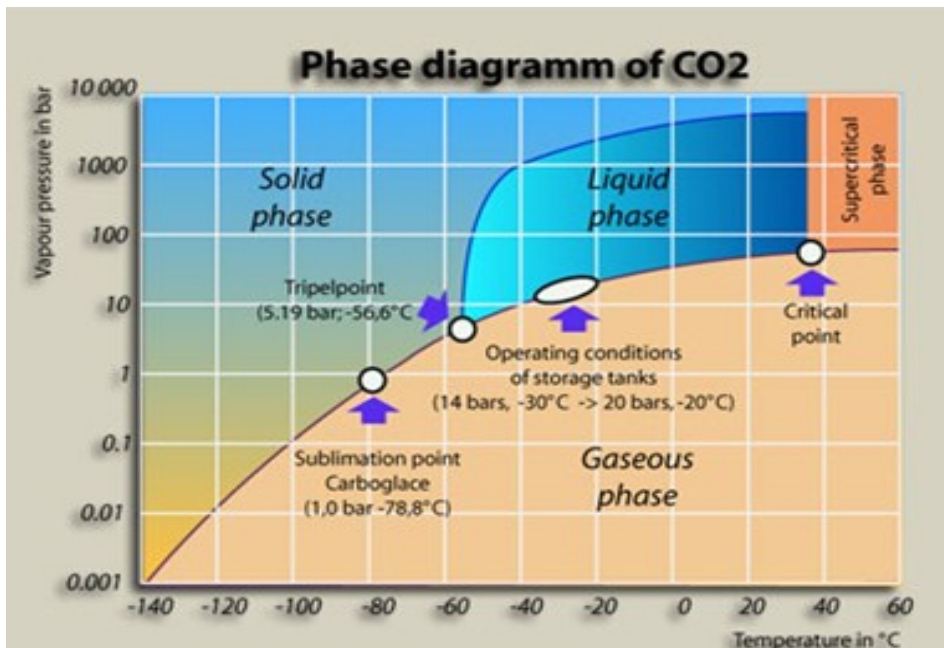


Figure 2.03: The Phase Diagram of CO<sub>2</sub> (Kobulnicky, 2008)

An MSDS for CO<sub>2</sub> is attached in Appendix 1.

## 2.4 Properties of coal

Coal is solid in form and normally found underground. One of the most hazardous forms of coal occur is when it is dust – this is due to the fact that it:

- is not easy to handle
- can be easily inhaled
- can ignite in the air as the temperature reaches 704 °C

An MSDS is attached in Appendix 1

## 2.5 Theories of adsorption

The last essential topic to grasp when dealing with isotherms is about the theories of adsorption – these are different models that are usually used in literature to display isotherms. This section will only focus on three: Langmuir, BET and D-R isotherms.

### 2.5.1 Langmuir Isotherm

According to Mantell (1951), the Langmuir model of adsorption was derived and proposed by Irvine Langmuir in 1916. Langmuir proposed that the kinds of forces that are involved in

adsorption are similar to those found during a chemical reaction. In the atomic electronic view, the acting forces in the chemical combinations are due to strong deviation of energy while adsorptive forces are due to the weak. Irvine derived the monolayer adsorption isotherm by considering the dynamic equilibrium and the rate expression during adsorption and desorption (Mantell 1951). Pakseresht et al. (2002) presented the Langmuir monolayer adsorption isotherm as follows:

$$\frac{N}{N_s} = \frac{KP}{KP + 1} \dots \dots \dots 2.04$$

See the derivation of Equation 2.04 in Appendix 2.

Where:  $N:N_s$  is a ratio of amount adsorbed and the monolayer maximum capacity respectively.  $P$  is the pressure.  $K$  is the equilibrium constant, which is the ratio of the rate constants (adsorption: desorption). The equilibrium constant is useful in determining the maximum adsorbable amount during adsorption. Following Czepirski et al., (2000), the assumptions that are considered in this expression are:

1. adsorbent's sites are equally "active" to adsorb available amount of gas;
2. adsorbed molecules have no interaction with each other and they are homogeneously energetic;
3. the adsorbed amount can only form one layer;
4. there is no phase change of both adsorbate and adsorbent (Czepirski, Balys, and Komorowska-czepirska, 2000).

The Langmuir isotherm was found applicable for low pressure (< 60 bar) of  $\text{CO}_2$  when experiments on Australian coal were carried out (Saghafi et al., 2007).

## 2.5.2 BET Isotherm

The BET isotherm is an extension of the Langmuir isotherm. According to Macmillan and Teller (1950), the BET model assumes:

1. there can be more than one adsorption layer formed;
2. the energy of the first layer is unique and for the rest of the layer the energy is that of liquefaction;
3. the effect of surface tension can be neglected.

The disadvantages of the BET isotherm are underestimating adsorbed amount at low pressure and overestimation when approaching saturation pressures (Emmett, 1977). The linearised form of the BET isotherm is (Brunauer, Emmett, and Teller, 1936):

$$\frac{P/P_{\text{VAP}}}{1 - P/P_{\text{VAP}}} \frac{1}{N} = \frac{1}{N_m C} + \frac{C - 1}{C} \frac{P}{P_{\text{VAP}}} \dots \dots \dots 2.05$$

Where:  $N_m$  is the amount of the adsorbate after the whole monolayer is covered;  $P/P_{\text{VAP}}$  is the relative pressure ( $x$ ),  $P_{\text{VAP}}$  is the saturation vapour pressure and  $C$  is a dimensionless constant greater than 1 and dependent on temperature.

$$C = \exp\left(\frac{\Delta H_{\text{ads}} - \Delta H_{\text{cond}}}{RT}\right) \dots \dots \dots 2.06$$

Where:  $\Delta H_{\text{ads}}$  is the heat of adsorption and  $\Delta H_{\text{cond}}$  is the heat of liquefaction

The vapour pressure (in bar) expression is as follows: Equation 2.07 is operational between 0 and 30 °C

$$\ln(P_{\text{VAP}}) = 3.56131 + 0.02418T \dots \dots \dots 2.07$$

### 2.5.3 Dubinin-Radushkevich

Harpalani (2003) illustrated that the Dubinin-Rudushkevich (D-R) isotherm is derived based on the assumption that solid surfaces possess a potential field in which every adsorbed molecule falls into in order for multilayer adsorption to occur. The theory is called Polanyi's Potential Theory. An adsorption potential is defined as the amount of work done per mole of the adsorbate in transferring molecules from the gaseous phase to the adsorbed phase and represents the work done by the temperature-independent dispersion forces. The gaps between each set of equipotential surfaces correspond to a definite adsorbed volume. In order to apply this theory for a microporous adsorbent, Dubinin introduced the Theory of Volume Filling of Micropore (TVFM). Dubinin postulated that the adsorbate occupies the pore (micropore) volume by the mechanism of volume filling which implies the formation of a discrete monolayer in the pores does not occur: The resulting expression is the Dubinin-Astakhov (D-A) (Harpalani, Prusty, and Dutta 2006):

$$N = N_0 \exp\left[-D \left[\ln\left(\frac{P_{\text{VAP}}}{P}\right)\right]^\gamma\right] \dots \dots \dots 2006$$

Where:  $\gamma$  is the structural heterogeneity parameter varying from 1 – 4;  $D$  is a constant for a particular adsorbent-adsorbate system and is equal to  $(RT/\beta E)^\gamma$ ,  $E$  is the characteristic

energy of the adsorption system and  $\beta$  is the adsorbent affinity coefficient;  $N_0$  is the moles in the volume of micropores.

For the Dubinin-Radushkevich (D-R) model,  $\gamma$  is replaced by 2. This was due to the suggestion of Dubinin and Radushkevich that 2 can be appropriate in some cases. Therefore the Dubinin-Radushkevich (D-R) equation is (Harpalani, Prusty, and Dutta 2006):

$$\ln N = \ln N_0 - D \ln \left[ \left( \frac{P_{\text{VAP}}}{P} \right)^2 \right] \dots \dots \dots 2.09$$

Both D-A and D-R equations are also known as the Dubinin-Polanyi (D-P) equations.

These models should be linearised in order get slopes and intercepts which aided in getting the parameters of the equations. Since there are only two parameters per model, the linearisation should be possible. The respective parameters are utilised to plot the models.

## 2.6 Summary of the Literature review

Isothermal adsorption increases with an increase in the gas pressure. Coal has twice the adsorption capacity of  $\text{CO}_2$  gas relative to  $\text{CH}_4$ . High porosity and surface area increases the sorption capacity of an adsorbent. Langmuir, BET and Dubinin–Radushkevich are the most commonly used isotherms in literature. A VAS is used in this research.

High moisture content in the pores of an adsorbent is proportional to low gas adsorption capacity. Moisture content in the laboratory environment can distort the adsorption capacity of an adsorbent; hence it advisable that inter laboratory studies are conducted in a moisture calibrated environment. Based on previous research using a VAS, an inter-laboratory study is necessary in order to confirm the reliability of the instrument.



### 3 EXPERIMENTAL PROCEDURE

The aim of this chapter is to discuss the overall schematic structure of the VAS, material and sample preparation, manual and automatic safe operating procedure, and experimental data analysis.

#### 3.1 Overall structure of the Equipment

Figure 3.01 is a schematic diagram of the volumetric adsorption isotherm measurement instrument developed during this project – it also includes data acquisition and measurement control and display. Figure 3.02 is the engineering diagram of the VAS. Photographs of the system are shown in Figure 3.03.

##### 3.1.1 Description of the Volumetric Adsorption Equipment<sup>2</sup>

A VAS consists of an adsorption chamber and gas vessel linked by a tube with a valve. In order to ensure isothermal conditions during the experiment, the instrument was placed inside an air heated oven manufactured by Labcon (Figure 3.03b, and No. 12 in Figure 3.02).

###### 3.1.1.1 Gas Vessels

Figure 3.02 shows the vessels containing manometers for pressure measurement and thermometers for temperature. Each vessel has four  $6.35 \times 10^{-3}$  m tubes. The tubes and the vessels are made out of stainless steel as the operation pressures are above ambient (up to 190 bar). The inside surface of the vessel is electropolished in order to avoid surface adsorption. The choice of the sealing material of the gas vessels is dependent on the nature of the adsorbate and the operating conditions. Since the operating range is 0 – 60 °C and 160 bar, stainless steel was the selected material for that duty. Dry CO<sub>2</sub> is not a corrosive gas, which implies the equipment should have a relatively long life span. The internal volume of the sample vessel is 17 ml, suitable for powdered samples; however, for lump particles, it is recommended that a high volume chamber is used.

---

<sup>2</sup> Note for this section, the temperature and pressure units mostly used are °C and bar respectively but for very small values K and Pa are utilised

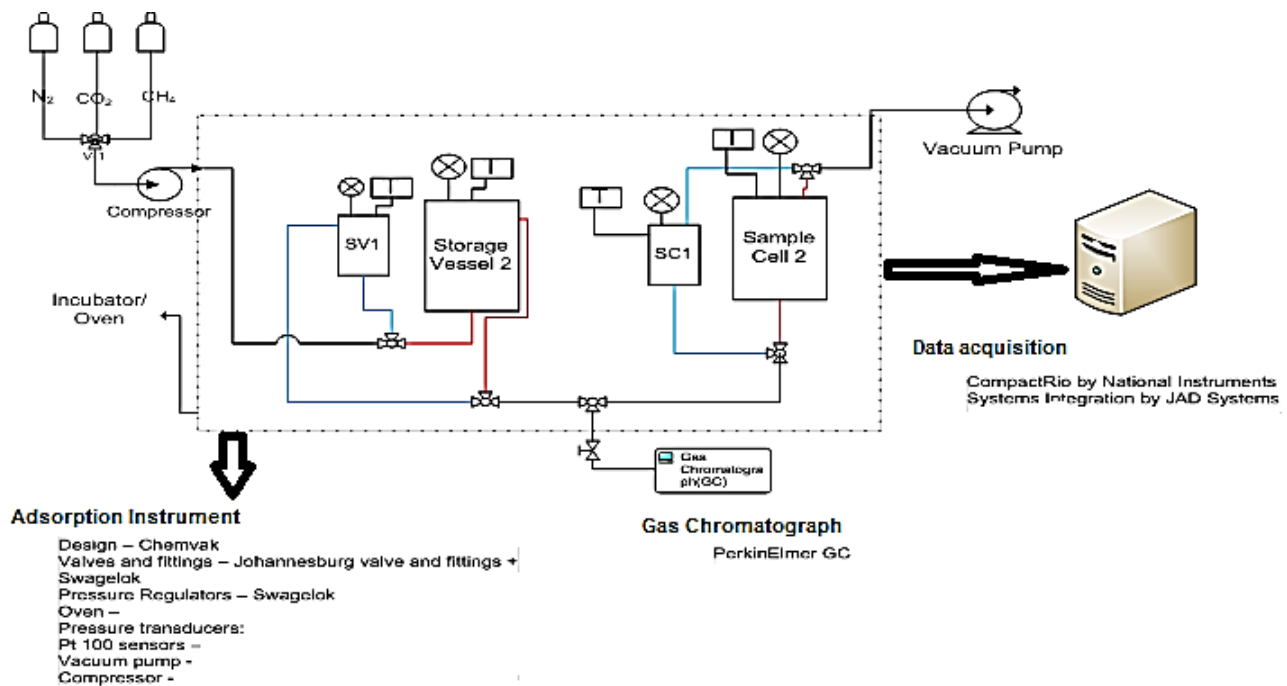


Figure 3.01: Volumetric measurement instrument for mixed gases incl. data acquisition, measurement display and control and costs

### 3.1.1.2 Temperature Sensor

A 4 wire Pt100, RTD sensor with 6.35E-03 m NPT is installed in the gas and the adsorption vessel for temperature measurements in the equipment. This sensor can operate between -40 and 220 °C and has an absolute accuracy of 0.1 K. These wires are inserted in both vessels as shown in Figure 3.03b and Figure 3.02 No 12.

### 3.1.1.3 Pressure Transducer

At least two pressure transducers are necessary for the experiment for most of the experimental procedure is automated. A pressure transducer converts the system pressure into an analog electrical signal. The pressure transducer utilised in this project has a sensor operating on the piezoresistive principle using a polysilicon sensor (Endress + Hauser, Cerabar S PMP 71). The operating limit of the pressure transducer is marginalised to a range of 0 – 250 bar, and has a relative measurement range of 0.75 – 187.5 bar. The transducer can also withstand process temperatures up to 200 °C. However, any temperature variability can lead to a pressure shift at an estimated rate of 100 Pa for each 10 K. These transducers are positioned above both vessels, shown in Figure 3.03b.

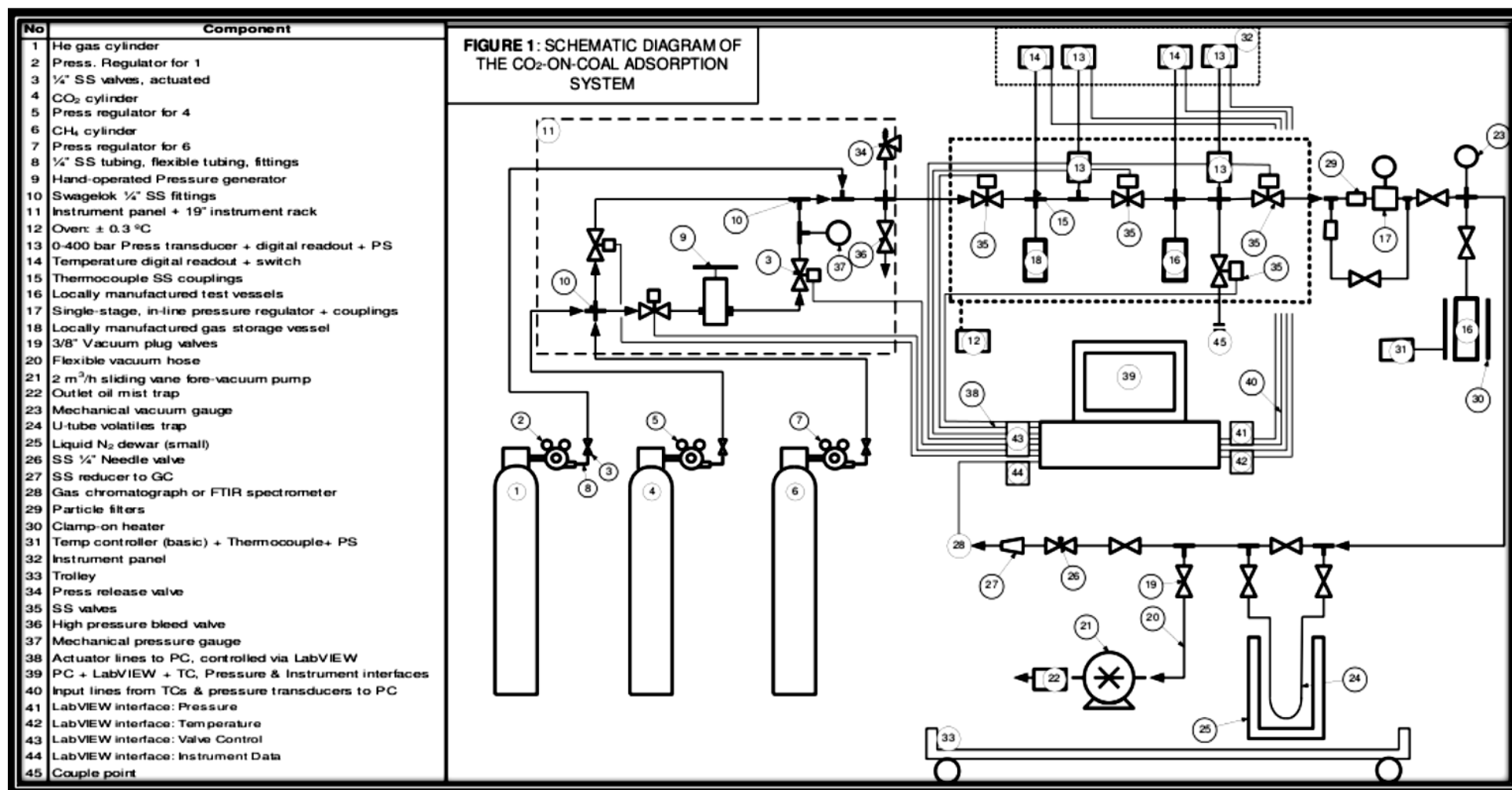


Figure 3.02: The Schematic Diagram of the CO<sub>2</sub>-on-Coal VAS



*a. Teledyne Isco 260D automatic pump*



*d. Zeolite packed bed to trap degassed volatiles*



*g. Swift Heaters degassing heater*



*b. Labcon air heated oven with piping and vessels*



*e. LabVIEW integrated pc controlling and acquiring data*



*h. Overall system excl. the pc*



*c. Display and control panel with a cRIO and Pycnometer*



*f. Vacuum pump*

*The two silver vessels pointed by the white arrow are: the gas (left) and sample (right) cell*

Figure 3.03: The Images of the Experimental Setup. a) The Teledyne Isco Pump, b) Labcon Oven incubating the Reference and Sample Cell, c) The Control Panel and Stereopycnometer, d) Volatile Trapping Zeolites Bed, e) The PC for LabView Control and f) Vacuum Pump

#### 3.1.1.4 Valves, Electro-valve and piping equipment

High-pressure electro-valves with special solenoids are used as they can withstand high temperatures. The electro-valve can operate at maximum and absolute pressures of 2000 bar and temperatures between -20 °C and 150 °C. These units are all located inside the oven shown in Figure 3.03b.

#### 3.1.1.5 Oven

As shown in Figure 3.03b, the oven is a ventilated and insulated incubator that keeps the temperature constant for the gas vessel, adsorption vessel, and tube circuit. The temperature limits of the oven range between 0 to 60 °C. The oven should have a regulatory accuracy of 0.3 K and maximum temperature gradient of 1 K. In order to allow the gas (in the supply gas cylinders) access into the oven a hole was bored on the walls.

#### 3.1.2 Data acquisition and control system

The experimental procedure is automated using National Instruments (NI) hardware and LabView. LabView is utilised to determine the inputs, throughputs, and output algorithm for the software procedure. In order to obtain the reliability of the equipment, the experiment is reproduced more than once with an expectation of consistency. A proper understanding of LabView is vital since it is used during automation of the experiment and in the data acquisition process.

The major portion of the experimental procedure and equipment is automated in order to acquire, analyse, and present information for further data processing. A process of this nature is called data acquisition. Data acquisition is PC-based and utilises a combination of hardware, software, and a computer to automate measurements and make data available (NI, 2011).

System integration with the NI hardware was implemented with the assistance of a JAD System programmer. The algorithm includes the inputs, throughputs, and outputs which describes the adsorption, desorption, and Helium leak detection experiments. The inputs, throughputs, and outputs involve the application of equation of states (EOS) in the algorithm so that the program can display the results with model predictions.

Table 3.01: Summary of the specification of the various items of the VAS per segmentation

Segment	Item	Description	Supplier
<b>1. Adsorption Equipment</b>	<b>Vacuum Pump</b>	Vacuating the system under 100 Pa, or preferably under 30 Pa	Edward
	<b>Vessels</b>	Interchangeable cells, stainless steel ¼" piping, electropolished inside 0 - 160 bar, 253 K - 333 K	Manufacturer (in collaboration with Swagelok)
	<b>Valves</b>	High press electro-valve, 0 - 200 bar, 253 K - 423 K, 24 V DC voltage Filter: + 7 µm retained, 0 - 41300 kPa and 273 K - 755 K	Fittings: Swagelok Valves and Asco
	<b>Temperature measurement</b>	Has a 4wire Pt100 with ¼" NPT, output: 4 - 20 mA DC with an absolute accuracy of 0.1 K. It operates between 233 K - 493 K. Located in both reference and sample cell	Thermocouple Products
	<b>Pressure transducers</b>	Operate on the piezoresistive principle using a polysilicon sensor and pressure limits are 0 - 250 bar (absolute and gauge), 0.075 % accuracy, up to 473 K	Endress and Hauser
	<b>Oven</b>	The oven need to be able to maintain a stable temperature, ideal less than ± 0.3 °C, and has to have an internal height sufficient for the sample cylinders to be used and a hole for fitting, piping and tubing	JP Selecta (or other manufacturer in collaboration with swagelok)
<b>2. Data Acquisition</b>	<b>Data Acquisition</b>	Data acquisition system specification: I/O - NI 9203 8-Channel ± 20 mA, 200 kS/s, 16 Bit analog input module. Control system specs: CPU - cRIO-9073 8-slot integrated 266 MHz, 17999.00 Real Time Controller	National Instruments
<b>3. Measurement display and control</b>	<b>Software and Peripherals</b>	LabView	JAD System (algorithm and system integration and National Instrument)

## 3.2 Material and Sample preparation

### 3.2.1 Materials

Materials that were used during the experiment are liquid CO<sub>2</sub> and coal. Liquid CO<sub>2</sub> was supplied by Afrox in a dip tube cylinder. The coal sample was a low rank bituminous coal from a South African Witbank coal field.

### 3.2.2 Sample Preparation

A large initial sample is required to obtain a number of representative subsamples which were homogeneously prepared to ensure a single population of samples throughout the research. The homogeneity of the sample is very important for the reliability studies using of a VAS and during the inter-laboratory studies (Gensterblum et al., 2009).

A 20 kg initial sample, with particle distribution between 1 and 10 cm, was coned and quartered in a well-ventilated area away from contaminants. A quarter was crushed to particle sizes less than 1 mm using crushers at the Department of Metallurgical Engineering of the University of Johannesburg, Doornfontein Campus. A quarter of the - 1 mm coal sample was crushed and sized to 212 µm using an in-house mill (Retsch ZM 200) in a well-ventilated area. The product from the Retsch ZM 200 was coned and quartered,

and split with an 8 test tube splitter into representative subsamples. The subsamples were then stored inside a 25 ml airtight container under an N<sub>2</sub> medium to prevent any form of reaction with the environment and stored in the lab refrigerator. The mass of each sample was 2 g.

### 3.2.3 Characterisation

Before commencing with the actual experiment with the VAS, the proximate and BET analysis and the volume determination of the sample and reference cell was performed. This enables the determination of the properties of the adsorbent and potential storage capacity of the adsorbent.

BET analysis for pore volume and surface area determination was undertaken at North West University (NWU), Potchefstroom Campus. The proximate analysis is the determination of the moisture, volatile matter, fixed carbon, and ash content of the sample (Bhebehe 2008). The proximate analysis was carried out using a Thermo Gravimetric Analyser (TGA) positioned in the coal laboratory at Wits.

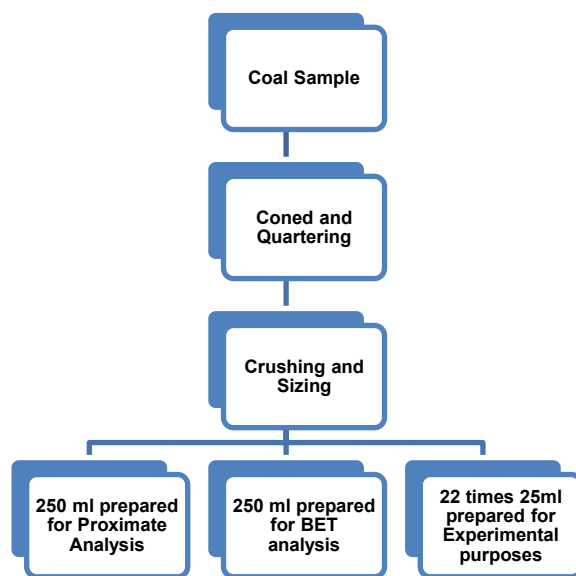


Figure 3.04: The overall structure displaying the sample preparation procedure

### 3.2.4 BET and proximate analysis

Standard characterisation of coal was undertaken by conducting BET and proximate analysis. BET analysis was performed to determine the surface area and pore volume of the adsorbent's mass. Proximate analysis was conducted to estimate the moisture, ash and carbon content of the coal sample. Please see Appendix 3 for the elaboration of the methodology used when conducting BET and proximate analysis.

## 3.3 Experimental Procedure for the VAS

In order to operate a VAS , a number of steps are required, namely: vessels volume determination, and the execution of both manual and automatic runs. The volume determination was done in order to size the reference and sample cell. To test the manual capabilities of the VAS, the manual runs were conducted through the manual opening and closing of the valves at each pressure step. The automatic runs executed through the control and monitorship of the LabVIEW system in order to enhance the operating capabilities of an automated VAS.

### 3.3.1 Volume determination of the cells

The determination of the total volume of the reference and sample cell section was performed using the following simple steps; first, definitions of volumes were established. Based on Figure 3.05, let the section of the reference cell including the tubes which the gas can access between  $V_1$  and  $V_2$  be  $V_{ref}$ , and the volume of sample cell section plus the tubes which the gas can access between  $V_2$  and  $V_3$  be  $V_{sam}$ .

Since the volume of the  $V_{ref}$  and  $V_{sam}$  were initially unknown, the first phase was to determine the ratio  $V_{sam}:V_{ref}$ . The following steps were performed without a known mass object inside the sample cells.

1.  $V_1$ ,  $V_2$  and  $V_3$  were initially closed and both the reference cell and sample cells were evacuated of pre-adsorbed gases present by a vacuum pump.



2.  $V_1$  was open and close to introduce  $\text{CO}_2$  into the reference cell such that the desired pressure can be reached and then the pressure  $P_1$  was recorded with its corresponding temperature.
3. Then  $V_2$  was open in order to allow the gas to expand into  $V_{\text{sam}}$ . However, the gas was allowed to equilibrate such that the temperature can be similar to the one recorded in step 2. Hence, since the temperature and the number of moles are constant and the ratio of the compressibility factors at both stages were assumed equal to 1. The complete gas equation state between initial and final stage was depicted as equation 3.01a:

$$P_1 V_A = P_2 (V_{\text{ref}} + V_{\text{sam}}) \dots \dots \dots 3.01a$$

Where:  $P_1$  is the initial pressure of the gas in the reference cell only and  $P_2$  is the pressure of the gas after the opening of  $V_2$ .

Rearranging equation 3.01a such that the  $V_{\text{sam}}:V_{\text{ref}}$  can be the subject of the formulae, equation 3.02b is

$$\frac{V_{\text{sam}}}{V_{\text{ref}}} = \frac{P_1}{P_2} - 1 \dots \dots \dots 3.01b$$

Table 3.02 shows three repetitions of the above steps. However, the value of interest is the average  $V_{\text{sam}}:V_{\text{ref}}$  ratio.

Without a known volume object in the sample cell					
Runs	$P_1$ (bar)	$P_2$ (bar)	$T_1$ ( $^{\circ}\text{C}$ )	$T_2$ ( $^{\circ}\text{C}$ )	$V_{\text{sam}}:V_{\text{ref}}$
1	5.1900	1.8400	28.6000	28.6000	1.8207
2	5.0600	1.7600	28.6000	28.6000	1.8750
3	5.1800	1.8450	28.6000	28.6000	1.8076
Mean	5.1433	1.8150	28.6000	28.6000	1.8344

The following experiment runs include the known volume object ( $V_x$ ) in the sample cell.

1. Repeat step 1-3 with a known volume.
2. Next, consider equation 3.01a with a known volume object by using the following equation 3.01c:

$$P_1 V_A = P_2 (V_{\text{ref}} + V_{\text{sam}} + V_x) \dots \dots \dots 3.01c$$

Where:  $P_3$  and  $P_4$  are the same forms of pressure as  $P_1$  and  $P_2$  respectively in equation 3.01a. Rearranging, equation 3.01c result in equation 3.01d:

$$V_{\text{ref}} = V_x \left[ \frac{P_3}{P_4} - \left( 1 + \frac{V_{\text{sam}}}{V_{\text{ref}}} \right) \right]^{-1} \dots\dots\dots 3.01d$$

Equation 3.01d is easy to solve since  $V_{\text{sam}}:V_{\text{ref}}$ ,  $V_x$  and  $P_3:P_4$  are known.

Table 3.03: Determination of the average  $V_x$  (1.8344) using  $\text{CO}_2$  gas with a known volume  $x$  ( $V_x$ ) object. The unit of the volume is ml.

With a known volume object in the sample cell					
Runs	$P_1$ (bar)	$P_2$ (bar)	$T_1$ ( $^{\circ}\text{C}$ )	$T_2$ ( $^{\circ}\text{C}$ )	$V_{\text{ref}}$
1	5.3063	1.9950	28.6000	28.6000	14.5292
2	5.1465	1.9312	28.6000	28.6000	14.9696
3	5.0700	1.8824	28.6000	28.6000	17.9883
Mean	5.1743	1.9362	28.6000	28.6000	15.8290

Table 3.02 shows the reference cell volume to be 15.8290 ml.

Hence, using equation 3.01e below, the volume of the sample cell was found 29.0370 ml.

Solving equation 3.01e was possible since  $V_{\text{sam}}:V_{\text{ref}}$  and  $V_{\text{ref}}$  are known

$$V_{\text{sam}} = \left( \frac{V_{\text{sam}}}{V_{\text{ref}}} \right) V_{\text{ref}} \dots\dots\dots 3.01e$$

### 3.3.2 Degassing procedure

Before commencing with each run, samples were preheated in order to remove pre-adsorbed matters. The used heater was purchased at Swift Heaters<sup>3</sup>. The heater is able to incubate a 90 mm diameter vessel with a height equivalent to its diameter. The degassing process is important because it helps to unlock the pores in the samples by vaporising volatiles, which are pre-adsorbed gases and water. The volatiles are drawn out by a suction vacuum pump installed in the system.

<sup>3</sup> Swift Heaters are the manufactures of the degassing heater used when removing volatiles from adsorbent when conducting sample preparation before the adsorption experiment

### 3.3.3 Manual Operation

In order to generate adsorption isotherms, the following experimental procedure was performed using a manual technique. The experimental conditions were set at 10, 20, 30, 40 and 50 bar. The experiment was performed at a temperature of 27 °C. Each point of the isotherm was run until pressure equilibrium was reached; hence, each isotherm consists of six points including the zero point. The collection of these points was carried out over 8 hours. Projects looking at adsorption potential should run longer, but the intention of this research is to determine the reliability and reproducibility of data on a single sample set.

Initially, the system is completely flushed with liquid CO<sub>2</sub> so that compression to high pressures can be achieved. The adsorption process for the experiment is run in a batch manner. Before commencing with the experiment, valve V<sub>1</sub>, V<sub>2</sub> and V<sub>3</sub> (Figure 3.05) are closed and the sample cell is filled with a degassed sample and vacuumed to almost absolute vacuum. A perfect vacuum is impossible with the used vacuum pump, but it yields values close to the acceptable pressures for this research. Carbon dioxide gas is pumped from the supply gas cylinders (top left corner of Figure 3.01) to the gas vessel via V<sub>1</sub>. The system gas pumping was performed using an installed Teledyne Isco 260D automatic and LabVIEW-compatible pump.

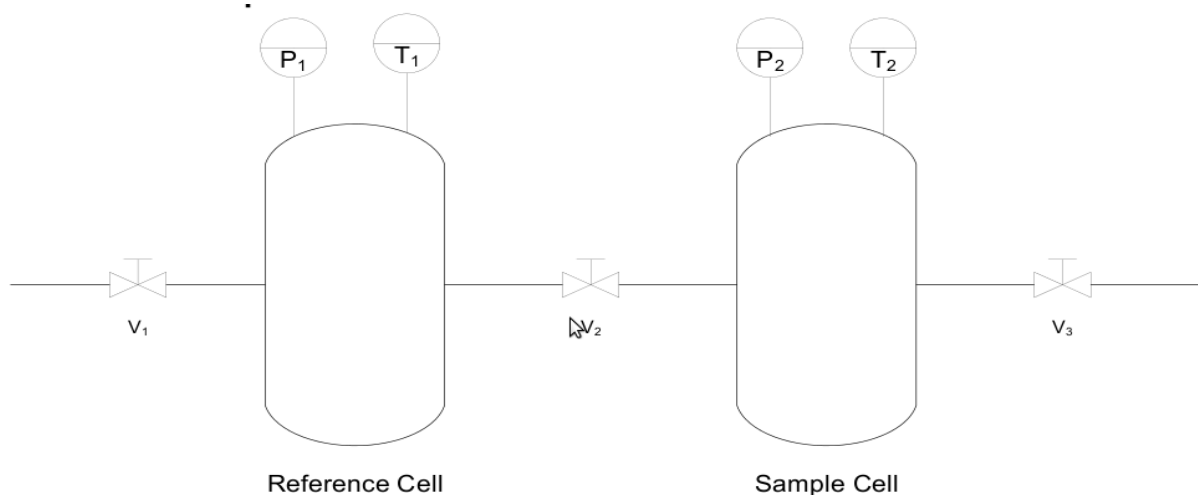


Figure 3.05: The Simplified Version of Section Number 12 in Figure 3.02

As soon as the gas vessel is filled to the desired pressure, V<sub>1</sub> is closed. Since the process is batch, this scenario is considered as the initial condition, t<sub>1</sub>. Carbon dioxide gas in the gas vessel (at the initial stage of the process) is considered as the system boundary. In the

initial stage, a record of the pressure ( $P_1$ ), temperature ( $T_1$ ), and volume ( $V_1$ ) of the gas vessel are conducted for both reference and sample cells. The mass balance for estimating the amount of  $\text{CO}_2$  adsorbed should be based on the difference of the number of moles between the initial and final stages. However, the difference in the number of moles for this project was adjusted such that excess adsorption isotherms can be generated.

After recording the conditions in the gas vessel,  $V_2$  is opened in order to allow the gas through the pipe into the adsorbent vessel. Then,  $V_2$  is closed and held for at least 30 minutes until pressure equilibrium is attained. The established equilibrium is still valid when the tolerance is less or equals to  $10^{-3}$ . At the established equilibrium, another record of the pressure ( $P_2$ ) and temperature ( $T_2$ ) readings is taken. The same steps are run for each pressure (0, 20, 30, 40, 50 and 60 bar) until the last experimental point is achieved. After the final step of the run, the gas vessel is emptied to the atmospheric pressure through a manual venting valve after the sample vessel.

After an experimental data collection, the sample cell is removed from the system and cleaned and filled with another degassed fresh sample for the next isotherm generation experiment.

#### 3.3.4 Automated Operation

The automated operation enables the equipment to function with less human intervention. The VAS is supported by a PC (with LabVIEW) and a control panel in order to perform control and data acquisition.

The NI cRIO used in this project is labelled NI-cRIO9073-0142A90D with the IP Address 192.168.0.191 in the network of the University of the Witwatersrand. The cRIO can only connect to the designated desktop PC in order to avoid possible data corruption due to external interference.

LabVIEW (PC App)	Control Panel	Volumetric Adsorption Equipment
LabVIEW Project Main app	Valves ( $V_1$ , $V_2$ & $V_3$ ) Controller NI Temperature Modules NI Pressure Modules NI cRIO Vessel's Pressure Display Vessel's Temperature Display	Valves ( $V_1$ , $V_2$ & $V_3$ ) Tubes Temperature Transducers Pressure Transducers Oven Vessels

Figure 3.06: Systematic View of the Controlled Experimental Setup

In order to operate the system automatically, switch the control panel key on so that the compact RIO (NI cRIO) can be turned on. Connect the PC and the cRIO using a network cable to enable the linking of the two devices, and then launch the LabVIEW software. Open the project file labelled abspro.lvproj in the desktop of LabVIEW.

### 3.3.4.1 Main virtual interface.vi

The virtual interface (vi) is a window where codes are created and run on the LabVIEW platform. The automatic procedure is essentially a repetition of the manual one, and includes computer software elements. The procedure for conducting an automated run is as follows:

- Launch LabVIEW from the start menu. The operating system utilised to run LabVIEW is Microsoft Windows XP.
- Open the LabVIEW desktop interface from the start menu.
- Open adspro.lvproj project from the launched LabVIEW desktop. If the recent file link is not available on the open links positioned on the desktop, the project file should be browsed. The directory link when browsing is C:\.....\Desktop\abspro.lvproj.
- Connect cRIO in the folder of the opened project. The connection is done by right clicking the NI-cRIO9073-0142A90D line, and then click the connect or deploy all option. In order to access the VIs, the thread of cRIO should be dropped and then open rt\_app thread which contains all the supporting VIs.
- Open the VI labelled main.vi in the same folder referred to above. The link of the main.vi is abspro.lvproj/NI-cRIO9073-0142A90D/rt\_app.lvlib:main. Figure 3.06 shows the interface of main.vi. Main.vi is the main LabVIEW window for operating the machine automatically, and it is dependent on other small 'vis'. Main.vi displays all the contents fed from the cRIO. cRIO acquires the pressures and temperatures of the reference and sample cell using the installed modules.
- While all the valves' control buttons on the control panel are off, switch the mode trigger from manual to LabVIEW to enable the PC automatic control VAS.
- Press the run white arrow on the top left corner of the main.vi to initiate the VI and press the "initialise script" button in the script tab to operate and acquire data (pressure-temperature and time) for the a certain set pressure.

The running script automatically performs all that is done in the manual operation. All this computer-programming commands run with less manual interventions, which can easily lead to errors in data acquisition.

The script tab has the ability to:

- open or close the pneumatic valves  $V_1$ ,  $V_2$  and  $V_3$ .
- set the desired pressure in the reference cell.
- start and stop logging data into cRIO

Appendix 4 contains an example of the script code which shows the data acquisition of adsorption in a single pressure step.

Running the script enables data acquisition as long as the exit button is not pressed. Normally, some data acquisition can take many hours before reaching equilibrium. The data recorded is stored in the cRIO. The cRIO stores files in the MS Excel csv format.

Filezilla is used to move the file from the cRIO to the desktop of the PC. FileZilla is a free cross-platform FTP software, consisting of FileZilla Client and FileZilla Server. Figure 3.09 shows the interface of Filezilla as viewed in the desktop of the XP OS.

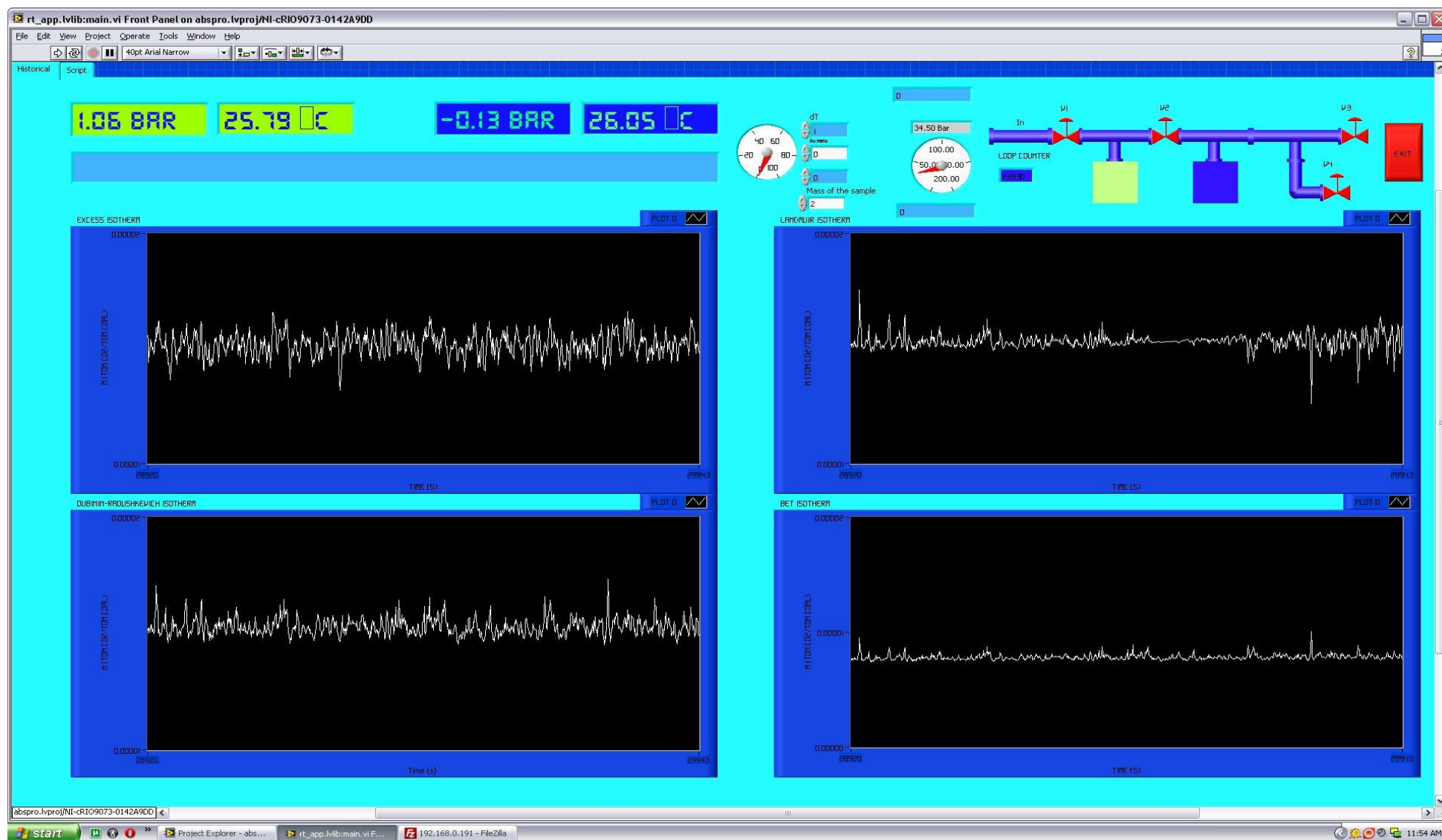


Figure 3.07: The interface of Main.vi. This tab displays the real-time adsorption isotherms



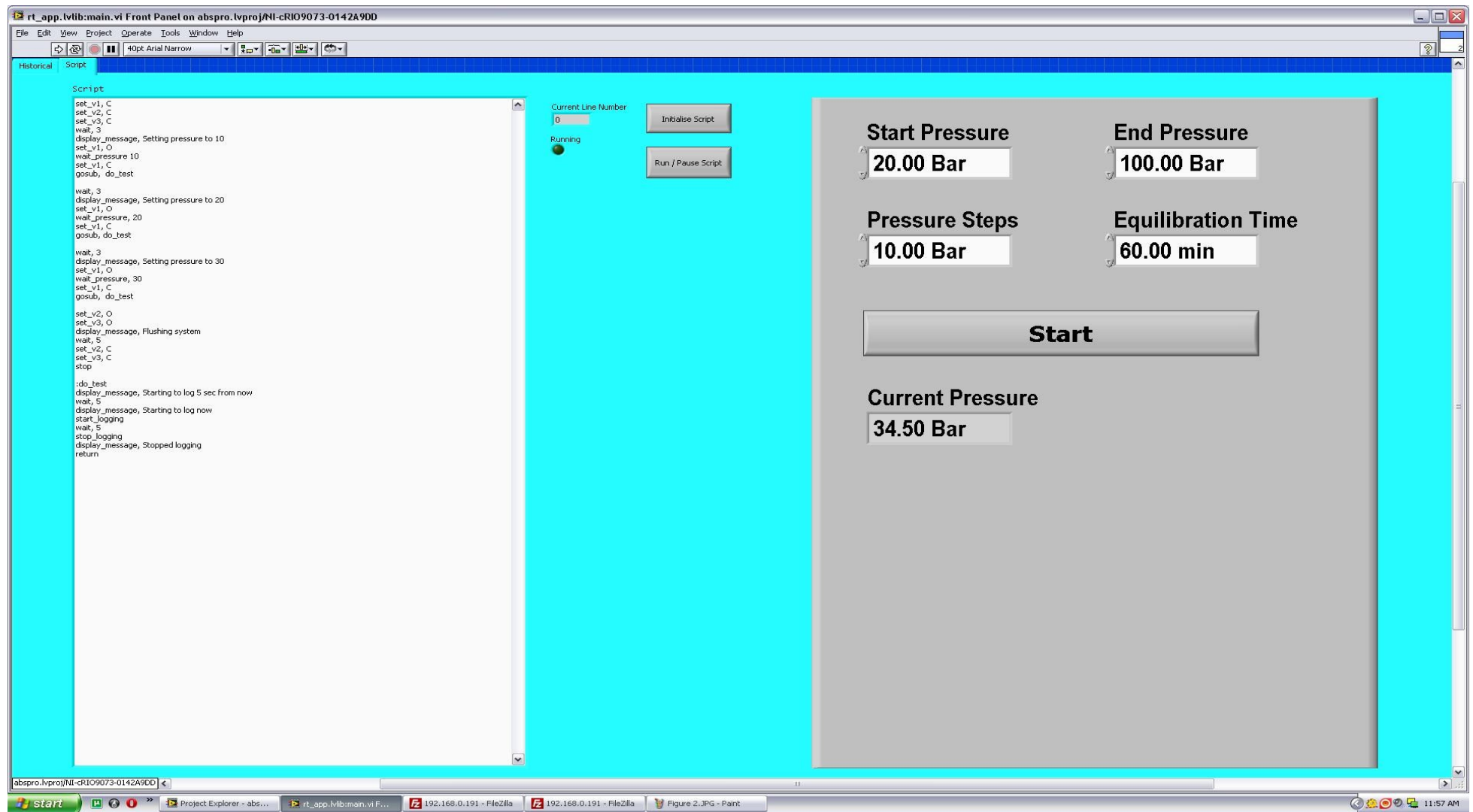


Figure 3.08: The interface of Main.vi. The Tab of the Script Code. The Script Execute the Desired Commands

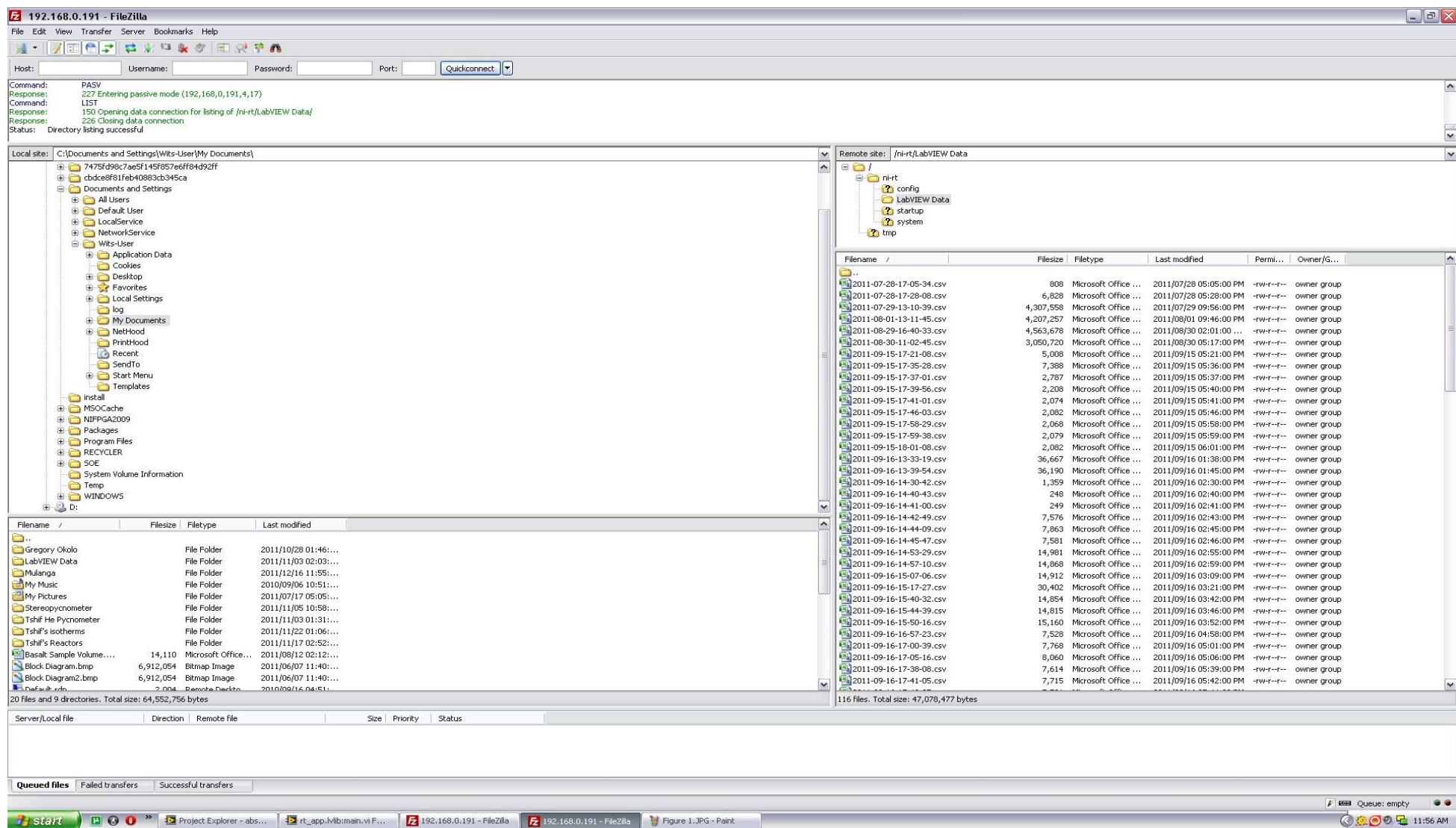


Figure 3.09: The interface of Filezilla showing the csv files in the cRIO and the desktop

### 3.4 Safety Precautions

Improper utilisation of the VAS is very dangerous and could cause harm due to the types of gases used and high operating pressures. Hence, it is necessary that the following precautions are seriously adhered to in ensuring safety:

1. Ensure the fastening nuts linking the vessels to the system are tightly tightened before commencing with the experimental run. When assembling the vessel to the system in the oven, ensure that the nuts are well tightened by hand, or using a spanner. Under tightening the nuts leads to leaks, while over tightening quickly wears the nuts and the vessel.
2. Ensure no CO<sub>2</sub> from the gas cell enters the sample cell when emptying the fresh sample vessel containing the virgin sample. This is done by a vacuum pump connected to the sample cell and is shown in Figure 3.03f
3. Before disassembling the sample vessel from the system, ensure that the gas in the pressure of the system is atmospheric by venting the gas before hand.
4. Be aware of the atmospheric temperature. The oven cannot cool, so if the atmospheric temperature is higher than the temperature of your experiment, it is recommended that you increase your experimental temperature, or cool the lab. During the experiment always ensure that the oven door is closed.
5. Ensure the pump does not suck pressures greater than atmospheric by flushing the system venting the gas before hand. Failure to do leads to the spill of the oil in the suction pump.
6. Wear a laboratory coat and safety goggles, as per laboratory rules

### 3.5 Tips on Avoiding Leaks

Before commencing with the experiment, ensure that all nuts (for both the vessel and the line) are well tightened. In order to tighten and unfasten the screws of the vessel when inserting a new sample, a 10 mm sized allen key is used. However, the nuts assembling the vessel to the system tighten and unfasten by a shaft and 13 mm spanner.

Ensure the seals in both gas and sample cells are not worn out. If they are worn out, replace them with fresh ones. The recommended usage period of the seals is at most five times, but when the tightened vessel leak at the seal interface, replace them. When seals are damaged, they display an uneven profile on the top view. Since these seals are expensive, it is important to determine the exact cause of leakage so that they can be replaced at the appropriate time.

The vacuum pump at the end of the VAS can be used to observe major leaks. If the reading on the  $P_2$  in Figure 3.06 (top right pressure box) is greater than -1.1 bar, that means there is a leak. Should this be the case, check whether the cause is worn seals or partially tightened nuts and screws, and then respond accordingly.

Another way of checking the leaks is by using the bubble solution method or a gas leak detector. Bubble solutions unfortunately are not useful for very low leaks, and advanced He gas sniffers are extremely expensive. Frequently the system was leak tested below 50 bar, but above 50 bar leaks developed.

### 3.6 Data analysis

The results were recorded and used to determine adsorption isotherm in both LabVIEW and MS Excel. As discussed in the Procedure Section (Section 3.3.3), different isotherm models are compared with the experimental results. The models help in understanding which theoretical model best predicts sequestration capacity of  $\text{CO}_2$  in the coal sample used. Some interest is also invested in analysing kinetic data for adsorption rates and thermodynamic data.

#### 3.6.1 Isotherm Calculations

The mass balance of the process was based on the calculation of the number of moles. In order to get the number of moles, a website of NIST<sup>4</sup> was used to obtain the density of the free phase. The site generates the isothermal density (mol/l) at 27 °C as the following function of pressure (NIST, 2011):

$$\rho_{\text{free}} = 0.0007P^2 + 0.0241P + 0.0787 \dots \dots \dots 3.01$$

<sup>4</sup> NIST is the National Institute for Standards and Technology. The website is <http://webbook.nist.gov/chemistry/fluid/> and is reliable in providing the density of both sub- and supercritical conditions.

Where:  $\rho$  is the density;  $T$  and  $P$  are temperature and pressure respectively. The subscript free is the  $\text{CO}_2$  in the free (bulk) phase instead of the adsorbed. See Appendix 5 for further details.

The general equation of representing the number of moles adsorbed is in terms of the density and the volume (Recall Equation 2.02):

$$N_{\text{ads}} = N_t - \rho_g V_g \dots \dots \dots 2.02$$

The volume of the gas ( $V_g$ ) phase can be described Equation 3.02 below:

$$V_g = V_{\text{sam,vessel}} - V_{\text{sam}} \dots \dots \dots 3.02$$

Where:  $V_{\text{sam,vessel}}$  and  $V_{\text{sam}}$  are the volumes of the gas vessel and sample respectively. And the initial total number of moles ( $N_t$ ) is:

$$N_t = \rho_0 V_g \dots \dots \dots 3.03$$

Where:  $\rho_0$  is the density of the gas in the sample vessel at the initial time

Equation 2.02, divided by the mass of the sample (adsorbent),  $m_{\text{sam}}$ , is the mostly used representation of isotherms (Belmabkhout, Frère, and De Weireld, 2004).

### 3.6.2 Standard Deviation

According to Pakseresht et al. (2002), the standard deviation (S.D.),  $\sigma$ , is:

$$\sigma = \sqrt{\sum \frac{(N_i - N_{\text{calc}})^2}{n}} \dots \dots \dots 3.04$$

Where,  $i$  is the number of experimental points per run;  $N_{\text{calc}}$  is the adsorbed amount based on the models, and  $N_i$  is the experimental adsorbed amount at each experimental point.

The more consistent the Standard Deviation (S.D.) of each run, the more reliable are the generated isotherms, and hence the equipment itself; the smaller S.D. is, the better (Weisstein, 2011).

### 3.6.3 Correlation Coefficient

The correlation coefficient,  $r$ , is used to confirm the uniformity of the generated isotherms. The  $r$  of each consecutive run should be as close to 1 as possible, in order for the

experimental results to be considered to be consistent (Pakseresht et al., 2002). Following Pakseresht et al. (2002), the correlation coefficient is expressed:

$$r^2 = \frac{n \sum N_i P_i - (\sum P_i)^2}{n \sum N_i^2 - (\sum N_i)^2} \dots \dots \dots 3.05$$

### 3.6.4 Reliability Measurement

For this project, the desired reliability of the VAS is 70 % with a confidence limit of 95 %. Since reliability is based on the reproducibility and consistency of the experiment, the above expectations were combined with the success testing expression below in order to determine the number of runs necessary (Dhillon and Anude, 1992):

$$m = \frac{\ln(1 - CL)}{\ln(1 - R_t)} \dots \dots \dots 3.06$$

Where: CL is the confidence limit of the values,  $R_t$  is the true reliability, and m is the number of machines required in the test. Success testing is normally used in receiving inspection and in engineering test laboratories where a no-failure test is specified. In the case of this project, m was equated to the number of runs in order to affirm the specified reliability. The result of the test with Equation 3.06 was 8 runs at the same conditions. The conditions of evaluation are in the range between 0 and 50 bar.

The other equation that can be used to measure reliability is equation 3.07. Where:  $\sigma_{true}$  is the true adsorbed amounts variance, and  $\sigma_{variance}$  is the observed adsorbed amount variance.  $R_t$  ranges before 0 and 1, and reliability is attained when it is close to 1.

$$R_t = \frac{\sigma_{true}^2}{\sigma_{observer}^2} \dots \dots \dots 3.07$$

### 3.6.5 T-TEST

The T-TEST is an inference statistical methods used to determine the difference in the two means of sample different sample. There are three types of T-TEST:

**One-sample T-TEST:** Used to compare a sample mean with a known population mean or any other meaningful, fixed value

**Independent samples T-TEST:** Used to compare two means from independent groups

**Paired samples T-TEST:** Used to compare two means that are repeated measures for the same participants - scores might be repeated across different measures or across time. Used also to compare paired samples, as in a two treatment randomized block design.

The T-TEST used in this research is the one-sample T-TEST.

The assumptions of the T-TEST are that the dependent variable must be:

- measured at an interval or ratio level of measurement - i.e., needs to be continuous.
- normally distributed in all groups of the independent variable.
  - Robust to violations of this assumption if sample sizes are large and approximately equal (> 15 cases per group)
- has approximately equal variance across all groups of the IV (homogeneity of variance e.g., tested by Levene's test).
  - If not the p-values for significance tests are inaccurate.
  - If the variances are different SPSS has post-hoc tests to adjust for this.
- the cases represent random samples from the populations and the scores of the test variable are independent of each other.
  - Inaccurate p-values if the independence assumption is violated.

According to the Choudhury (2009), the independent two-sample T-TEST is utilised to test whether population means are significantly different from each other, using the means from randomly drawn samples. Although the samples are randomly selected, there is no requirement that the two samples should be of equal size (Choudhury, 2009). The independent two-sample T-TEST is a test for small sample and can be used if the sum of the size of the two samples does not exceed 30 (Choudhury, 2009). However, for this case, the samples are each run, and participating candidates are the experimental relative pressures (which were 5 experimental data points per run), and the results required are moles adsorbed. The runs can be considered independent as they were operated discreetly. For more information and assumptions see Appendix 6. Equation 3.08 shows a general form of the T-TEST.

$$t - \text{test} = \frac{N_{\text{mean}}(\text{test 1}) - N_{\text{mean}}(\text{test 2})}{\sqrt{\frac{\sigma_{\text{test1}}^2}{k_{\text{test1}}} + \frac{\sigma_{\text{test2}}^2}{k_{\text{test2}}}}} \dots\dots\dots 3.07$$

Where: T-TEST is the measure of the difference in the means of two compared runs,  $N_{\text{mean}}$  is the average in number of moles,  $k$  is the count of observed relative pressures,  $\sigma$  is the variance.

#### **‘Hypothesis’ statement to reliability T-TEST**

- Hypothesis H0 (Null hypothesis):  $N_{\text{mean}}(\text{test 1}) = N_{\text{mean}}(\text{test 2})$ : at same conditions, the VAS yields means different results without statistics significance. The VAS can generate consistent results.
- Hypothesis H1 (Alternative hypothesis):  $N_{\text{mean}}(\text{test 1}) \neq N_{\text{mean}}(\text{test 2})$ : at same conditions, the VAS yields different results with statistic significance.



The T-TEST is testing H1, which is where the statistical significant difference between the two means occurs.

### **Formulate an analysis plan**

For this analysis, the significance level is 0.05. The test method is a one-sample T-TEST. The 'true' results were assumed to be the average isotherm (see Section 4.3.2)

### **Analyse sample data and interpretation of results**

If the sample findings are unlikely, given the H1, the researcher rejects the null hypothesis (StatTrek, 2012). Typically, this entails comparing the p-value to the significance level (alpha), and rejecting the null hypothesis when the p-value is less than the significance level (StatTrek, 2012). In statistical hypothesis testing, the p-value is the probability of obtaining a T-TEST at least as extreme as the one that was actually observed, assuming that the null hypothesis is true.

The above T-TEST is done at degree of freedom (df) of 10 (10 relative pressures count for the two runs – 2) and alpha-value of 0.05. When alpha = 0.05, there is a 95 % chance that the findings are true (Creative-Research-System, 2010). The implication of alpha = 0.05 and df = 10 is that if T-TEST > T-TEST critical and p-value < alpha, H1 is not true, and hence there is a significant difference in the observed data (KnowWare International Inc., 2012). Alternatively, if T-TEST < T-TEST critical and p-value > alpha, the null hypothesis is true, and hence there is a significant difference in the observed data (KnowWare International Inc., 2012). These analyses were performed using MS excel add-in Data Analysis function. However, if H1 is true, then there is a statistical significant difference in the observed findings which implies the data is reliable for the difference in means is small.

## **3.7 Chapter Summary**

In this chapter, the volumetric adsorption equipment is described, the operating procedure documented, and the verification technique determined. In order to determine the reliability, the inference statics methods T-TEST will be used.

## 4 RESULTS AND DISCUSSION

The results discussed in this chapter are based on a single coal sample from the South African Witbank coal field and liquid CO<sub>2</sub>, utilised as the adsorbent and adsorbate respectively. This chapter aims to discuss the coal characterisation, and the results of the commissioning and verification phases of the VAS.

### 4.1 Analysis

#### 4.1.1 Proximate analysis

Table 4.01: Proximate Analysis of the coal adsorbent

<b>Moisture</b>	<b>Volatile</b>	<b>Fixed Carbon</b>	<b>Ash</b>
9.14%	17.50%	46.04%	27.32%

The coal sample has ash content of 27.32 %, volatile content of 17.50 %, moisture content of 9.14 % and fixed carbon of 46.04 %. The coal sample is typical of the Witbank coalfield. See Appendix 7 for the proximate analysis figure displaying the mass % vs time.

#### 4.1.2 BET analysis

The BET results were generated by at NWU. The results show the surface area of the coal available to adsorb the CO<sub>2</sub>. The Langmuir and BET surface area are close in magnitude. The kinetic diameter of adsorptive molecule (CO<sub>2</sub>) is 3.230 Å – this is kinetic diameter. The pore width is 3.893 Å, which implies pore adsorption in the adsorbent is possible.

##### 4.1.2.1 Surface Area

The single point surface area at  $P/P_o = 0.032964681$  is 74.3723 m<sup>2</sup>/g;  $P/P_o$  is the relative pressure defined as the absolute pressure of N<sub>2</sub> relative to the vapour pressure the respective pressure. The BET Surface Area is 84.6001 ± 2.9023 m<sup>2</sup>/g. The Langmuir Surface Area is 89.7928 m<sup>2</sup>/g.

##### 4.1.2.2 Pore Volume

The Single point adsorption total pore volume of pores the diameter is less than 5.218 Å at  $P/P_o = 0.000003721$  is 0.000041 cm<sup>3</sup>/g.

According to the IUPAC (1984) porosity classification, solids with porosity between 2 Å and 50 Å are mesoporous (Groen, 2011). Hence, the Witbank coal used in this research is mesoporous and can adsorb CO<sub>2</sub> in the pores.

## 4.2 Commissioning of the VAS

The following experiences were encountered during the commissioning phase of the project, which were taken as learning's to improve the equipment and the analytical procedure.

### 4.2.1 Leaks and Pressure

V<sub>1</sub> leaked the gas into the reference cell at pressures greater than 100 bar and constant temperature of 27 °C; below 90 bar the leak rate was more stable. However, leaks were stopped by changing the seal in the sample vessel regularly (after three runs), and

ensuring the nuts of the vessel and line were tightened. Leaks were tested by the use of the soap solution test method.

#### 4.2.2 Oven

The oven is dependent on the room temperature air and is therefore unable to cool to operate at temperatures below the room temperature. Hence, it is recommended that the experiments should be performed at temperatures greater than room temperature, which may be seasonal. The operational temperature was 27 °C in the winter period and was kept constant by frequently venting the 'hot' air with a compressed air hose.

#### 4.2.3 LabVIEW

If LabVIEW is frozen, the solution is to reboot cRIO (compact RIO), but if the dilemma persists restart cRIO and the PC. When cRIO and the script in the main.vi are running, the indicator turns light green.

#### 4.2.4 Inequality of pressures between the reference and sample cells

The pressures read by the pressure transducers in the reference and sample cells are unequal due to the fact that the volume between  $V_1$  and  $V_2$  and between  $V_2$  and  $V_3$  are not equal. However, the pressure magnitudes are not greatly different when the vessels are empty. The pressure set-up in the reference cell filling has magnitudes approximately equals to the desired whole numbers. This is due to the system not being fully automated, but the values are not greater than 1 % from the desired.

It is recommendable that the ratio of the reference cell to the sample cell should be greater than 1; hence the system will be modified to the ratio of 2. The actual volume of the cells will also be reduced  $\pm 10$  ml. The inequality of pressures dilemma resulted in longer pressurisation of the sample cell by the reference cell.

#### 4.2.5 Pump

A syringe pump is strongly not recommended when it comes pressurising the reference cell, for it requires a lot of manual work to control the syringe. Due to this dilemma an automatic pump D260 ISOC pump from Teledyne was purchased towards the end of the project, thus enabling an automatic control of the pump, and far less physical exertion to achieve high pressures

### 4.3 Verification of the VAS

Presented are the results of the repeatability tests as explained in Section 2.5, 3.3.4 and 3.6. Three isotherm models were selected due to their frequent appearance in literature, namely Langmuir, BET, and D-R. (Section 2.5). Nine isotherms are presented as Equation 3.06 shows that, in order to achieve 70 % reliability and 95 % confidence limit, at least 8 runs should be conducted; 9 runs were selected. The mass of the adsorbent was 2g while the adsorbate pressure ranged between 10 and 50 bar in five steps; the experiments were performed at 27 °C. Manual operation is discussed first, followed by ....

#### 4.3.1 Adsorption Isotherms for manual operation

Table 4.02: The comparison of relative pressures for all 9 runs at different experimental points of each run5.

Run		Relative Pressure (P/P <sub>VAP</sub> )						STDEV	N <sub>exc,max</sub>	Mean
		0.0000	0.0043	0.0045	0.0096	0.0085	0.0161			
1	NEXC (g CO <sub>2</sub> per g coal)	0.0000	0.0019	0.0024	0.0015	0.0046	0.0062	0.0023	0.0062	0.0028
2		0.0000	0.0059	0.0077	0.0063	0.0128	0.0139	0.0051	0.0139	0.0078
3		0.0000	0.0068	0.0056	0.0104	0.0237	0.0249	0.0102	0.0249	0.0119
4		0.0000	0.0052	0.0061	0.0088	0.0153	0.0165	0.0063	0.0165	0.0087
5		0.0000	0.0063	0.0013	0.0021	0.0055	0.0087	0.0034	0.0087	0.0040
6		0.0000	0.0023	0.0080	0.0136	0.0058	0.0143	0.0058	0.0143	0.0073
7		0.0000	0.0026	0.0030	0.0088	0.0115	0.0108	0.0049	0.0115	0.0061
8		0.0000	0.0036	0.0045	0.0167	0.0123	0.0411	0.0150	0.0411	0.0130
9		0.0000	0.0023	0.0015	0.0019	0.0034	0.0045	0.0016	0.0045	0.0023
MEAN		0.0000	0.0041	0.0045	0.0078	0.0105	0.0157	0.0048	0.0157	0.0071

Table 4.03: The comparison of excess mass (adsorbed mass) of all the runs at the average relative pressure. N<sub>exc,max</sub> is the maximum value of adsorption.

Run		Relative Pressure (P/P <sub>VAP</sub> )						STDEV	N <sub>exc,max</sub>	Mean	r <sub>average</sub>
		0.0000	0.0043	0.0045	0.0096	0.0085	0.0161				
1	NEXC (g CO <sub>2</sub> per g coal)	0.0000	0.0019	0.0024	0.0015	0.0046	0.0062	0.0023	0.0062	0.0028	0.9372
2		0.0000	0.0059	0.0077	0.0063	0.0128	0.0139	0.0051	0.0139	0.0078	0.9254
3		0.0000	0.0068	0.0056	0.0104	0.0237	0.0249	0.0102	0.0249	0.0119	0.9528
4		0.0000	0.0052	0.0061	0.0088	0.0153	0.0165	0.0063	0.0165	0.0087	0.9696
5		0.0000	0.0063	0.0013	0.0021	0.0055	0.0087	0.0034	0.0087	0.0040	0.7820
6		0.0000	0.0023	0.0080	0.0136	0.0058	0.0143	0.0058	0.0143	0.0073	0.7725
7		0.0000	0.0026	0.0030	0.0088	0.0115	0.0108	0.0049	0.0115	0.0061	0.9170
8		0.0000	0.0036	0.0045	0.0167	0.0123	0.0411	0.0150	0.0411	0.0130	0.9241
9		0.0000	0.0023	0.0015	0.0019	0.0034	0.0045	0.0016	0.0045	0.0023	0.9513
MEAN		0.0000	0.0041	0.0045	0.0078	0.0105	0.0157	0.0048	0.0157	0.0071	0.9035

r<sub>average</sub> - Pearson coefficients (r) based on the comparison of each run to the MEAN of all the runs

The excess mass is the amount of the adsorbed gas on the surface of coal.

Table 4.04: The population D-R adsorption capacities for all the runs at the average relative pressure. N<sub>exc,max</sub> is the maximum value of adsorption. STDEV is the standard deviation.

5 Please note EXC = Excess isotherm

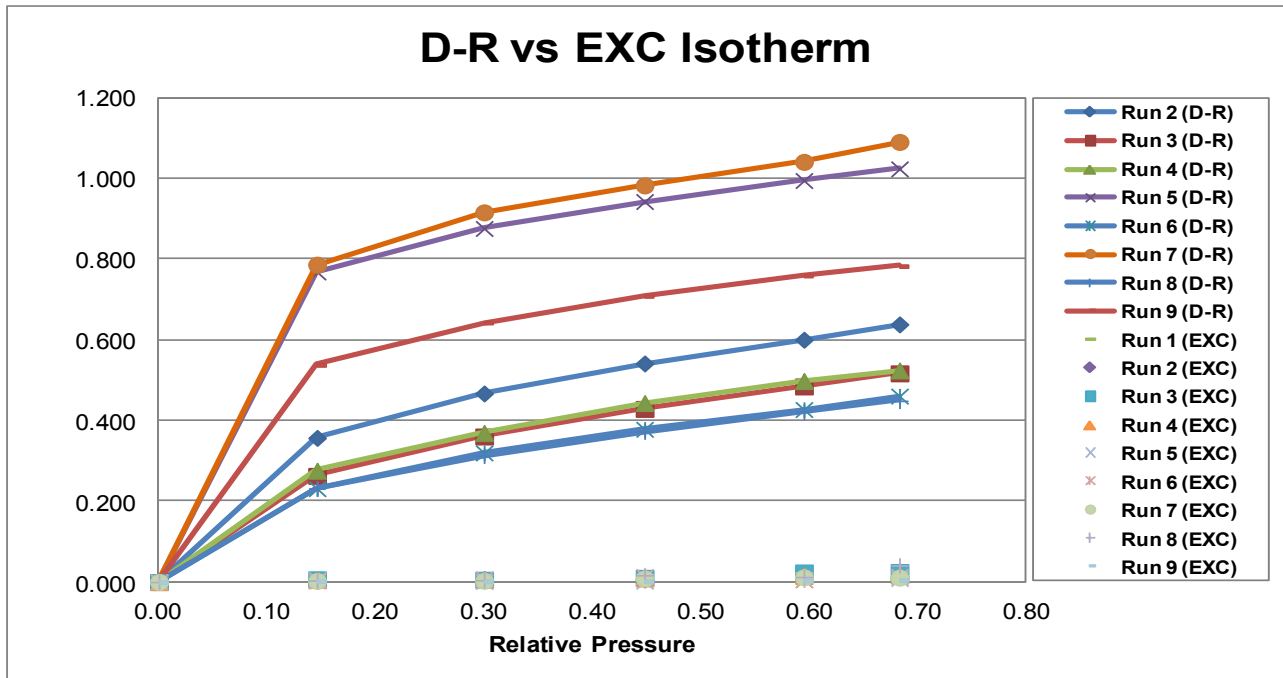


Figure 4.01: Comparison of D-R adsorption capacities and EXC isotherm adsorption capacity for all the run

Figure 4.01 shows that D-R isotherm over-predicts the EXC adsorption for all the 9 runs; hence this model cannot be used to estimate adsorption capacity of the Witbank coal utilised in these experiment. (Recall, D-R is Dubinin-Radushkevich isotherm and EXC is the excess isotherm).



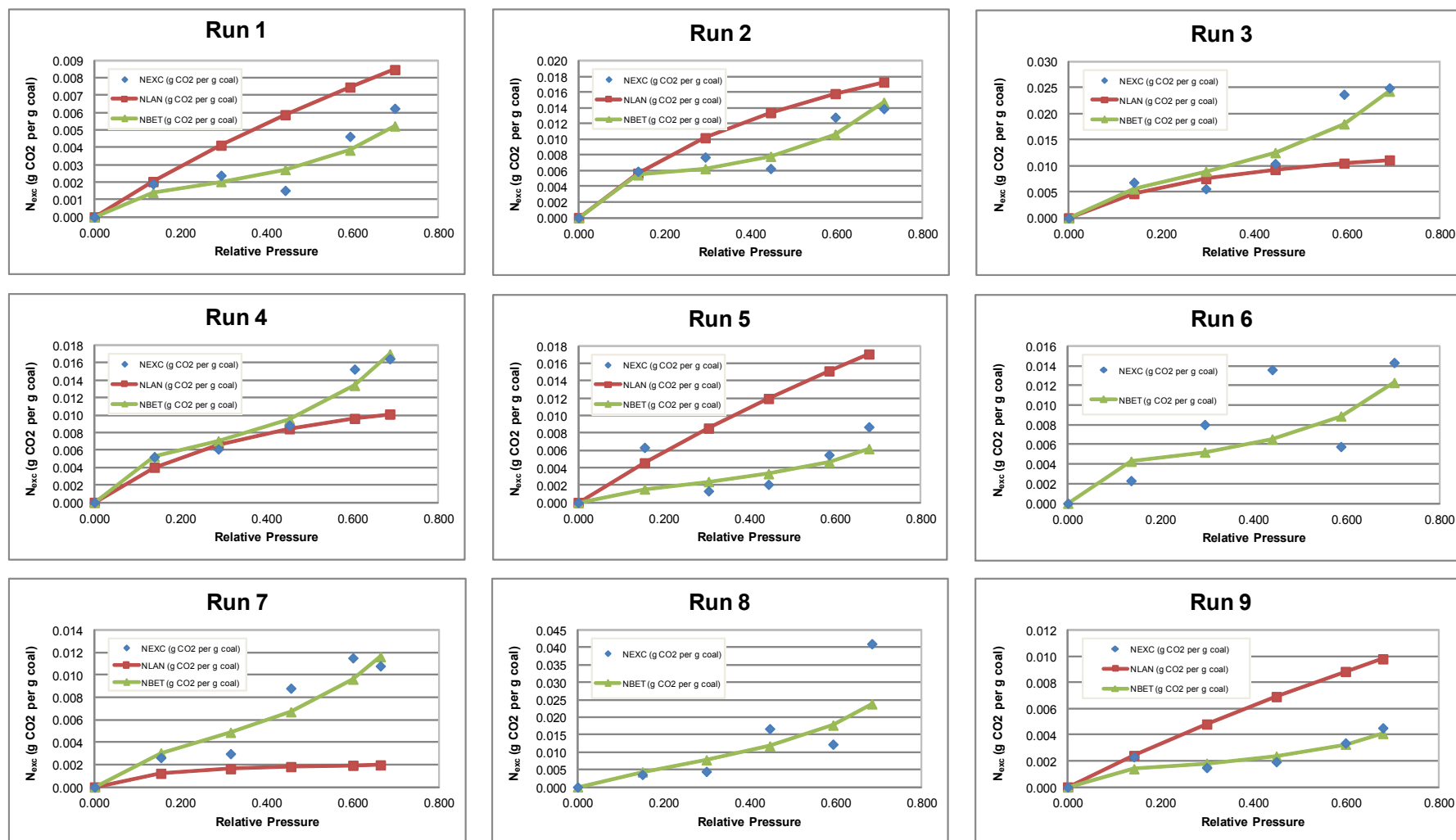


Figure 4.02: Nine comparisons of the excess adsorption isotherms (adsorption amount) and Langmuir and BET adsorption isotherm models with respect to the relative pressure. The vapour pressure is 68 bar.

#### 4.3.1.1 Run I

According to Figure 4.01 (Run I), the excess isotherm demonstrates an increasing trend, as the relative pressure ( $x$ ) increases with a drop  $x = 0.44$  (0.00239 g of CO<sub>2</sub> per g of coal). This drop can be attributed to the slight temperature increase in the oven, which can be attributed to gas interaction in the vessel (Day et al, 2008; Mantell, 1951). The oven was at times cooled by air in order to avoid spontaneous heating of the vessel. However, the Langmuir isotherm predicts the excess isotherm at  $x = 0.14$  (0.00191 g of CO<sub>2</sub> per g of Coal) and over-predicts at  $x = 0.29, 0.44, 0.59$  and  $0.70$ . The maximum capacity of this isotherm is 0.00624 g CO<sub>2</sub> per g of coal. The BET isotherm predicts the adsorption capacity of  $x = 0.7$ , which is closer to the excess isotherm than the other two isotherms. Although the BET model does not show exact capacities, it has the closest mean compared to the rest, with 8.84% deviation.

#### 4.3.1.2 Run II

According to Figure 4.02 (Run II), the excess isotherm shows an increase with a drop at  $x = 0.45$ . The maximum adsorption capacity of this run is 0.01389 g CO<sub>2</sub> per g coal. The Langmuir isotherm predicts the adsorption capacity of the excess well at  $x = 0.14$ . Run II excess isotherm follows the profile of the BET isotherm. The BET average of the run is 0.57 % deviant from the excess isotherm.

#### 4.3.1.3 Run III

Figure 4.02 (Run III) shows an increasing trend of the excess isotherm with a drop between  $x = 0.13$  and  $0.30$ . This drop can be attributed to the noise of the pressure output in LabVIEW. The BET isotherm accurately predicts the maximum capacity of the excess isotherm (0.02493 g CO<sub>2</sub> per g coal) at  $x = 0.69$ . The Langmuir isotherm under-predicts this excess isotherm, while the D-R over-predicts.

#### 4.3.1.4 Run IV

Figure 4.02 (Run IV) has the same pattern as Figure 4.02 (Run III), although there is a drop at  $x = 0.30$  for Figure 4.02 (Run IV). The mean of the excess isotherm is 0.60% deviant to the BET isotherm. The Langmuir isotherm is under-predicting the excess isotherm. The maximum capacity of the isotherm is 0.017 g CO<sub>2</sub> per g coal.

#### 4.3.1.5 Run V

In Figure 4.05, the maximum adsorption capacity of the excess isotherm is 0.00871 g CO<sub>2</sub> per g coal. However, the BET isotherm has a good resemblance of the adsorption capacity at  $x = 0.68$ . The divergence of the excess isotherm at  $x = 0.2$  can be attributed to noise of the pressure data displayed on LabVIEW and possible slow undetectable leak. The mean of the excess isotherm is 24.35 % deviant relative to the BET isotherm. The Langmuir isotherms overestimate the excess isotherm.

#### 4.3.1.6 Run VI

Figure 4.02 (Run VI) excess isotherm displayed an unexpected drop between at  $x = 0.59$  for the excess isotherm. The maximum adsorption capacity is 0.0143 g CO<sub>2</sub> per g coal. The BET isotherm shows a 15.56 % deviation relative to the mean of the excess isotherm. The drop in at  $x = 0.6$  can be attributed to the noise of the pressure data displayed in LabVIEW.

#### 4.3.1.7 Run VII

Figure 4.02 (Run VII) excess isotherm shows a sharply increasing trend compared to Figure 4.02 (Run VI). The maximum adsorption capacity is 0.0115 g CO<sub>2</sub> per g coal. The BET graph shows better resemblances of the excess isotherm. The decrease at the last point is due to the addition of less pressure into the reference before the generation of the last point.

#### 4.3.1.8 Run VIII

Although the BET isotherm in Figure 4.02 (Run VIII) accurately resembles the excess isotherm between the relative pressure of 0.00 and 0.45, it underestimates the adsorption capacities of the relative pressure at 0.68. The increase at the last point can be attributed to leaks due to high pressure.

#### 4.3.1.9 Run IX

Figure 4.02 (Run IX) excess isotherm showed a decrease between the relative pressure of 0.14 and 0.30 for the excess isotherm. However, the maximum adsorption capacity was

0.00452 g CO<sub>2</sub> per g coal. The BET isotherm estimates the excess isotherm better than Langmuir.

### **Summary of the runs**

Out of all the 9 runs, the isotherm with the highest maximum capacity is Run 8 - where the adsorbed capacity was 0.0411 g CO<sub>2</sub> per coal (Approx 60 bar). This value is comparably close to a type I isotherm generated using dry Pocanhontas #3 coals that had an adsorption capacity of 0.0460 g CO<sub>2</sub> per g coal.

Although all these runs have different adsorption capacities, they all display an increasing type IV adsorption isotherm – where adsorption capacities increased with the increase in pressure. Since the system had leaks, some of the isotherms had ‘unexpected’ drops. Another cause of the drops is temperature increases in temperature (Arumugam, 2004). All were also fitted to the BET, Langmuir and D-R models.

#### **4.3.2 Average Isotherm**

The average excess isotherms were derived by taking an average of all the 9 experimental points. The average excess isotherm showed an increasing trend with a pattern similar to the BET isotherm (Figure 4.03). All the excess adsorption isotherm figures resemble an increasing trend, which implies adsorption increases as the gas pressure increases. The slight difference in the scattering of data may be attributed to undetectable leaks, uncontrolled humidity content of the laboratory, and the noise of the data output. The maximum adsorption capacity of the average isotherm is 0.0165 g CO<sub>2</sub> per g coal. The Langmuir isotherm is under-predicting the excess isotherm, while D-R overestimates. According to Sakurovs (2008), the D-R isotherm estimated the excess isotherm of gas in coal and charcoal accurately when assessing the temperature dependence, but in this case the BET isotherm estimates the excess isotherm more accurately than Langmuir and D-R isotherms.

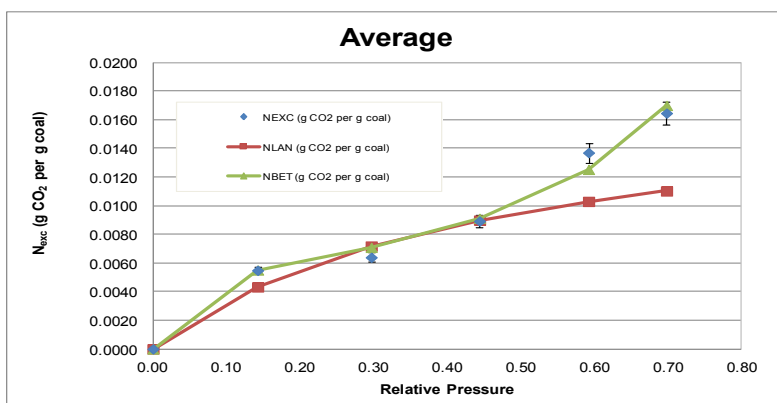


Figure 4.03: The average isotherm which was derived by averaging each pressure point for all the experimental runs. Please note,  $N_{\text{EXC}}$  = Excess Isotherm,  $N_{\text{LAN}}$  = Langmuir Isotherm and  $N_{\text{BET}}$  = BET Isotherm.

Further details on isotherm calculations are displayed in Appendix 8.

### 4.3.3 Automated Run

The automated operational procedure of the equipment enables the equipment to function with less human intervention (refer to Section 3.3.3). Figures 4.04 to 4.08 show the pressure-temperature profiles of each experimental point against time under automated conditions. Each experimental point of the run was set to operate for 30 minutes (1800 seconds). However, Figures 4.04 to 4.08 only show data in the first 150 seconds of the run. This was done to zoom the temperature and pressure profiles from the beginning and the other part of the period is not shown because the changes are small. The Figures 4.04 to 4.08 show that the reference cell pressure decreases while the sample cell temperature increases to a value almost equal to that of the reference cell. Note, T1 and P1 are the Temperature and Pressure of the reference cell respectively, while T2 and P2 are the Temperature and Pressure of sample cell respectively. The temperature difference is due to the expansion of the gas from the reference cell.

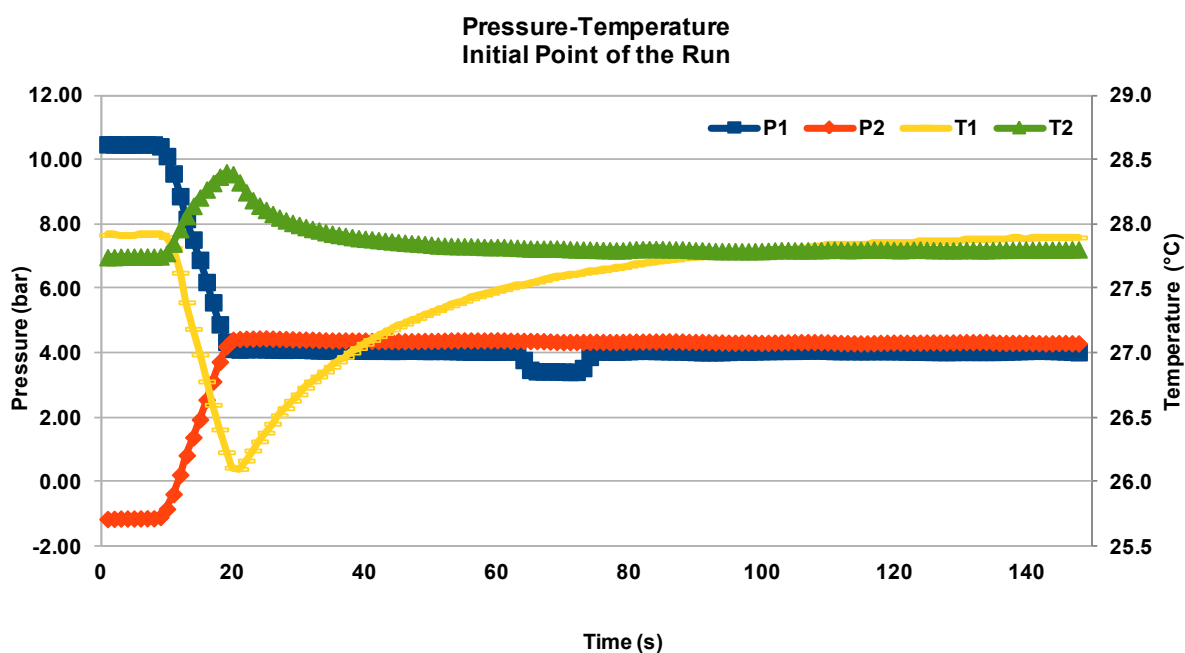


Figure 4.04: Pressure-Temperature profile of the first point at 28 °C and reference pressure of 10 bar (the 1<sup>st</sup> 150 seconds of this pressure step) and the equilibration pressure amounting to 4 bar.

The negative pressure ( $P2 = -1.1$  bar) is a gauge pressure and indicates the sample cell is approximately equals to 0 bar (vacuum = absolute pressure). The hook between the 60 and 80 seconds can be attributed to the beginning of the adsorption process.

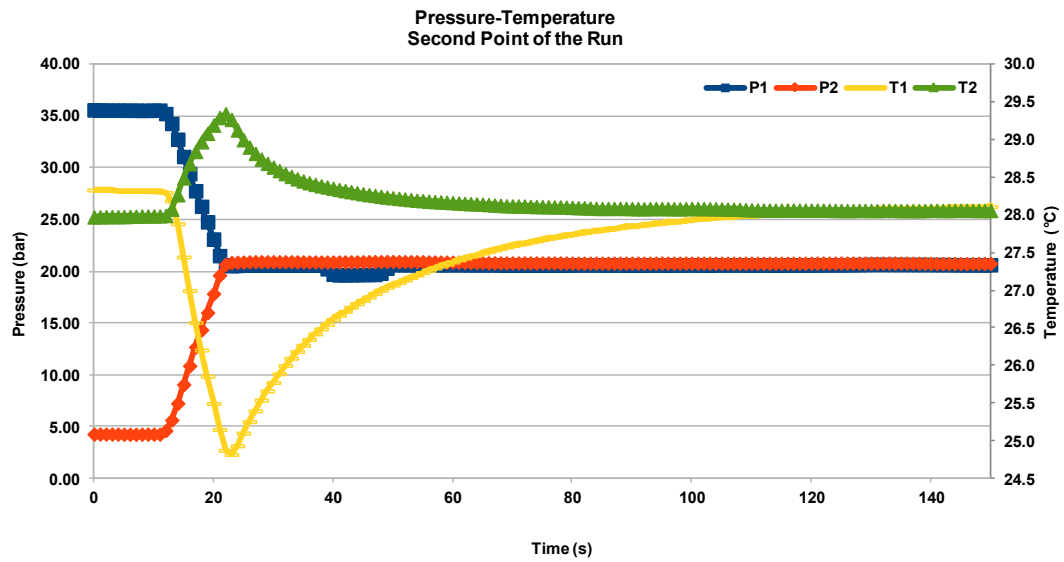


Figure 4.05: Pressure-Temperature profile of the second point at 28 °C and reference pressure of 35 bar (the 1st 150 seconds of this pressure step) and the equilibration pressure amounting to 20 bar.

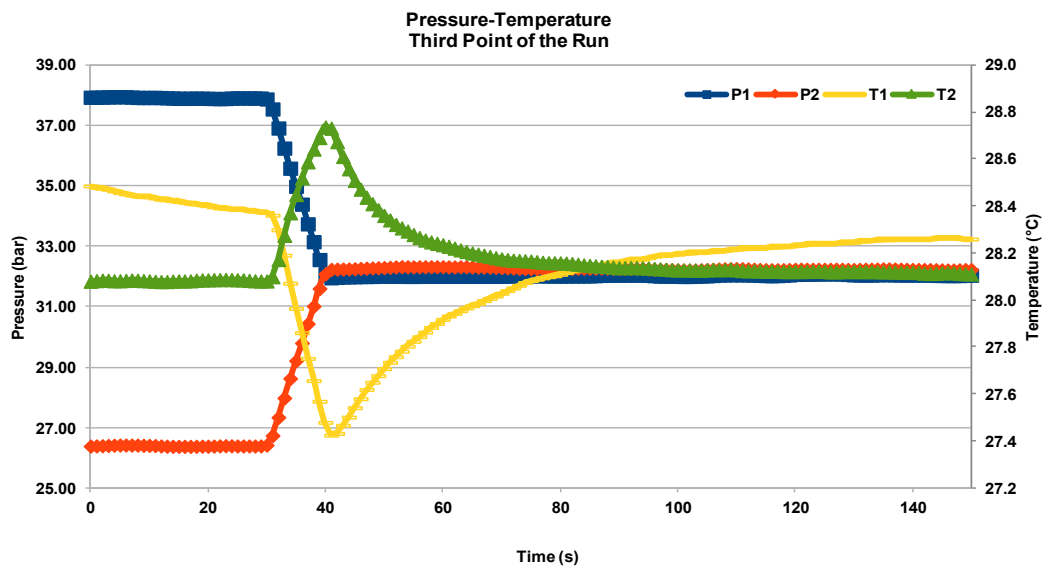


Figure 4.06: Pressure-Temperature profile of the third point at 28 °C and reference pressure of 38 bar (the 1st 150 seconds of this pressure step) and the equilibration pressure amounting to 32 bar.

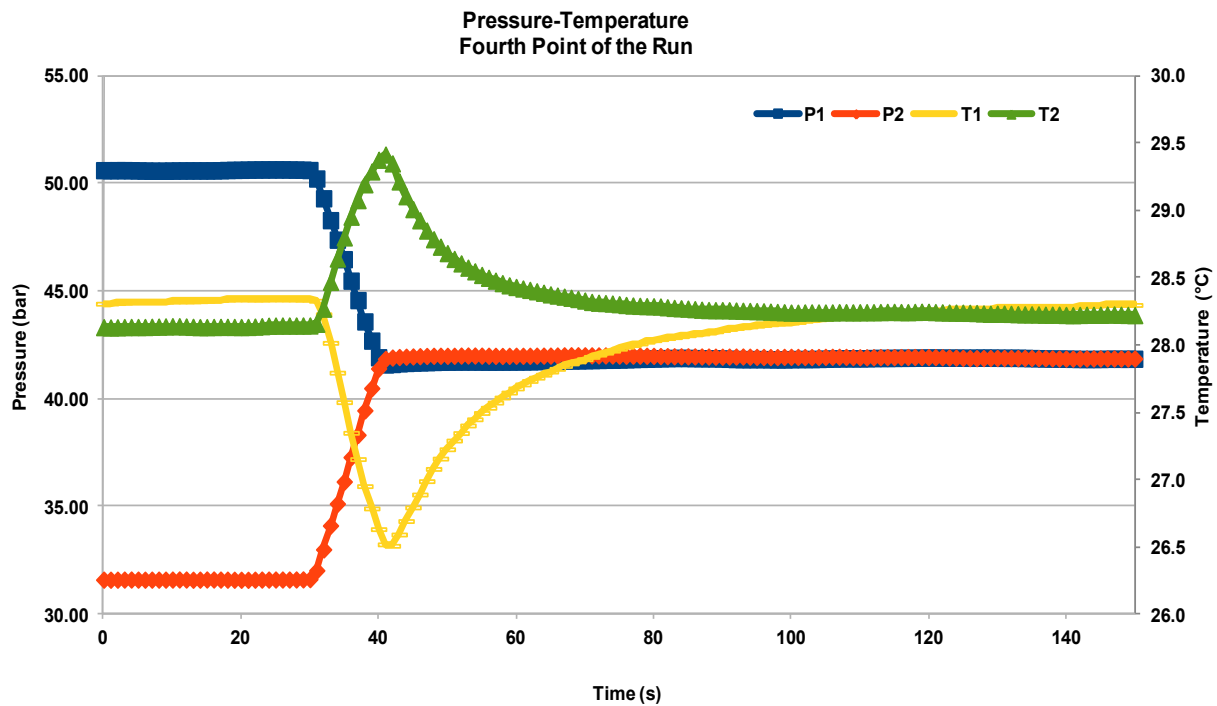


Figure 4.07: Pressure-Temperature profile of the fourth point at 28 °C and reference pressure of 50 bar (the 1st 150 seconds of this pressure step) and the equilibration pressure amounting to 41 bar.

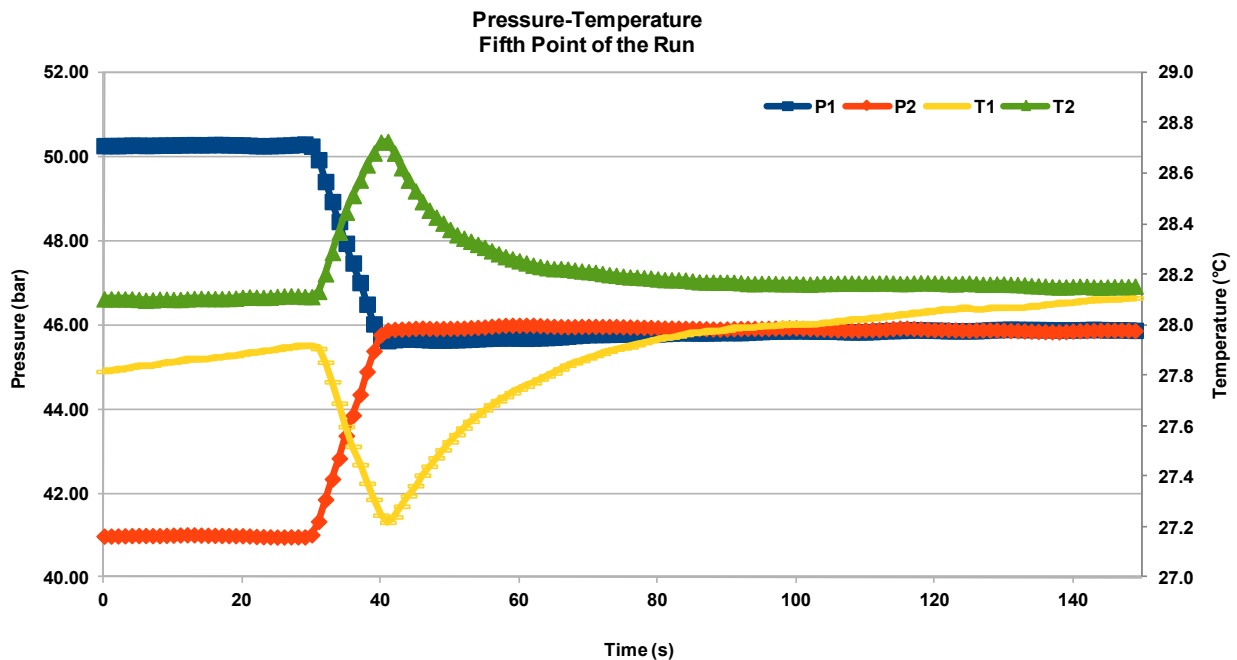


Figure 4.08: Pressure-Temperature profile of the fifth point at 27 °C and reference pressure of 50 bar (the 1st 150 seconds of this pressure step) and the equilibration pressure amounting to 45 bar.



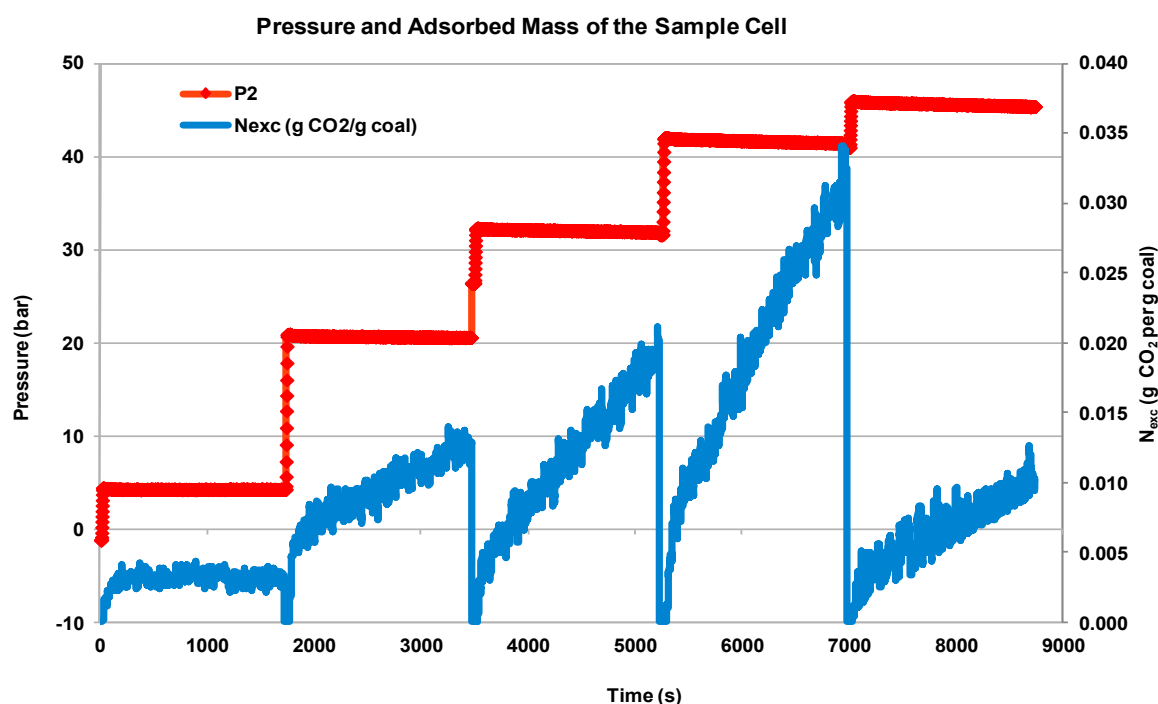


Figure 4.09: Pressure and Adsorbed amount profile as a function of time. Negative pressure means the sample sell was sucked to vacuum.  $P_2 = -1.1$  bar is a gauge pressure.  $P_2$  is the sample cell gas pressure.  $N_{\text{EXC}}$  (g  $\text{CO}_2$  per g coal) is the excess number of moles in the sample cell, which is the adsorbed amount.

Figure 4.09 shows the adsorbed amount change with respect to time and pressure at constant temperature of  $27^\circ\text{C}$ . The run shown in Figure 4.09 has five experimental steps which can also be viewed in the form of Figure 4.04 to 4.08 excess isotherms. The temperature-pressure data of the initial point are between 0 and 1723 seconds, the second point is between 1722 and 3470 seconds, the third point between 3469 and 5230 seconds, the fourth point between 5229 and 6980 seconds, and the fifth point is between 6979 and 8745 seconds. Each point of the run was operated for 30 minutes from the time adsorption is  $N_{\text{EXC}}$  greater than zero.

Figure 4.04 and Figures 4.08 until 4.09 show adsorption occurs when the pressure of the sample cell decreases with time. The pressure of the sample cell is dependent on the set pressurisation via the reference cell. According to Figure 4.09, the initial point equilibrated quicker compared to the other four points, which are still increasing at the screenshot of 30

minutes. The maximum adsorption capacity was 0.0341 g CO<sub>2</sub> per g coal, which is different from the average in Figure 4.02 (Run 9). The acquisition of data displayed in the form of Figure 4.09 is recommended compared to the Figures 4.02, since it displays the noise behind the data. The pressure-temperature conditions of isotherms in all the runs in Figure 4.02 were manually recorded from the continuous displayed data at a certain point of time of the run.

The adsorption capacity of point 5 of the run in Figure 4.09 is lower than point 4, because Figure 4.08 shows that only 5 bar was added into the sample cell while Figure 4.04 has an increase of 10 bar.

The automated experimental procedure is better than the manual operation since it takes into account more data points.

#### 4.3.4 Inter-laboratory results

The inter-laboratory results are based on the experiment performed using a VAS at AUT. Due to time constraints, it was impossible to perform more inter-laboratory studies as initially planned and hence the results are limited to one run shown in Figure 4.10. In an attempt to ensuring peer learning and generation of inter-laboratory results, AUT was visited in June 2011.

The simulated conditions of the isotherm were at 35 °C and 0 – 60 bar using the South African Witbank coal sample as an adsorbent. The isotherm displayed an increasing trend which resembles a Langmuir isotherm. The difference between inter-laboratory excess Wits isotherm and the average excess isotherm can be attributed to the generation of more than five experimental data points of the average isotherm and the different temperatures. Although there is a difference in the adsorption capacities displayed by the two excess isotherms in Figure 4.10, the displayed capacities imply the VAS at Wits is capable of generating comparable isotherm at isothermal temperatures.

In order to improve the Wits results and to align them with the AUT results, the Wits results have to be:

- generated without possible leaks;
- simulated in a moisture controlled environment;
- simulated at the same temperature of 35 °C; and
- generated with more data points as resembled in Figure 4.09

See Appendix 9 for the results.

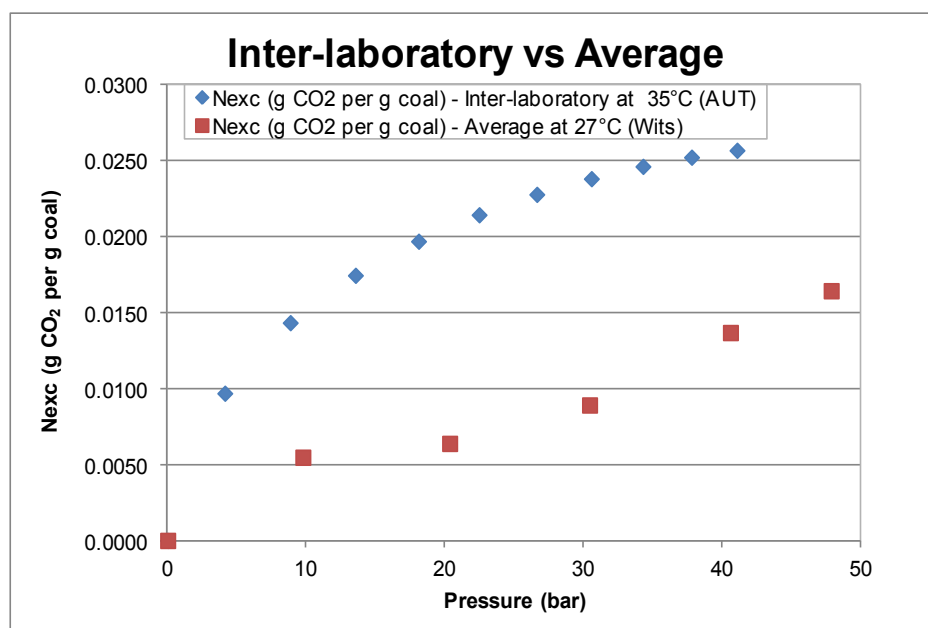


Figure 4.10: Comparison of the inter-laboratory results (35 °C) and the average isotherm in Figure 4.03 (27 °C)

#### 4.3.5 T-TEST

Table 4.05: The results of the T-TEST as displayed on the last column of the table. The T-TEST compared the averages of each run.

Runs	p-value	alpha	t-test	t-critical	df	Results interpretation	correlation coefficient
1	0.1069	0.0500	-1.7716	1.8125	10.0000	Accept the null hypothesis	0.9372
2	0.8314	0.0500	0.2186	1.8125	10.0000	Accept the null hypothesis	0.9254
3	0.1661	0.0500	1.0189	1.8125	10.0000	Accept the null hypothesis	0.9528
4	0.3291	0.0500	0.4559	1.8125	10.0000	Accept the null hypothesis	0.9696
5	0.1335	0.0500	-1.1753	1.8125	10.0000	Accept the null hypothesis	0.7820
6	0.4702	0.0500	0.0768	1.8125	10.0000	Accept the null hypothesis	0.7725
7	0.3756	0.0500	-0.3258	1.8125	10.0000	Accept the null hypothesis	0.9170
8	0.1935	0.0500	0.9045	1.8125	10.0000	Accept the null hypothesis	0.9241
9	0.0330	0.0500	-2.0638	1.8125	10.0000	Accept the null hypothesis	0.9513

Table 4.05 shows that the differences in the results generated by the VAS are not statistically different, since p-values are greater than the alpha (statistical significance) values of 0.05. This implies the VAS can reliably generate adsorption isotherms.

Additionally, the Pearson correlation coefficients for all the runs are close to each other (approximately equals to 0.90) with two outliers above 75%. All these coefficients are benchmarked against the average isotherm. This implies the runs are consistent since the results yield close correlation coefficients.

#### 4.4 Chapter Summary

The VAS was successfully designed, commissioned, and does generate adsorption excess isotherm. All the isotherms follow the pattern of the BET isotherm and they are under- and over-predicted by the Langmuir and D-R isotherm respectively. The results of all the excess isotherms were expected to display an increasing trend but all the runs, except Run 4 (Figure 4.02), had unexpected decreases. This can be attributed to anthropological errors associated with manually operating the system. As shown in the verification and commission phase, the decreases in pressures are due to undetectable leaks, uncontrollable laboratory air humidity content, pressure transducer output noise, and slightly increasing temperature. The average isotherm (Figure 4.03) showed that gas adsorption increases with the increase in pressure. The maximum adsorption capacity of the average isotherm is 0.01646 g CO<sub>2</sub> per g coal (at 50 bar and 27 °C). This adsorption capacity is lower than the 0.0400 g CO<sub>2</sub> per g coal (at 50 bar and 27 °C) conducted by Saghafi A. (2011) using the Bowen basin coal. The T-TEST result shows that the divergence of the results is not statistically significant.

## 5 SUMMARY AND CONCLUSIONS

The aim of this study was to commission and verify an automated VAS for the purposes of expanding the work on CO<sub>2</sub> adsorption in geological materials. A new piece of equipment, a VAS, was designed and commissioned during the research, and verified to determine the reliability of the results generated. The operating procedure, and lessons learnt has been documented in the dissertation for the benefit of future students using the equipment. Following are the conclusions based on the results of the research, thus addressing the aim, objectives and research questions posed in Chapter 1.

1. The success testing expression (*Section 3.64*) revealed that eight runs were required in order to attain the desired reliability of the equipment of 70 % with the confidence limit of 95 %. Each run was comprised of 6 experimental points which had the sample cell initial pressures were 0, 10, 20, 30, 40, 50 bar at 27 °C.
2. The VAS yielded the excess adsorption outputs greater than 0 when the relative pressures were greater than 0. Although this research was focused on determining the reliability – not validity – of the VAS, these greater than zero outputs are an indication that the system is expectedly yielding adsorption consistency results. For most of the runs, the maximum adsorption capacities difference occurred when the gas pressure was 47 bar, and excess isotherm values ranged between 0.0045 and 0.0411 g CO<sub>2</sub> per g coal. This revealed that adsorption increases with the increase in gas pressure in the void space.

The deviations in the excess isotherm results could be attributed to leaks (mainly), slight increases of temperature, manual recording of noisy pressure-temperature data and varying moisture content in the atmosphere.

3. The consistencies in the reproduced results (excess isotherms) were compared to the fixed average isotherm (*Section 4.3.2*) using the Pearson's correlation coefficients. The results revealed that there is a high linear consistency amongst the

runs since seven of the nine runs have a correlation coefficient ( $r$ ) values above 0.9000. Although runs five and six have  $r$ -values above 0.7500.

The excess isotherms results were also used to measure the statistical significance of the difference in the average of the mean of each run by performing an inference statistical test called the test-retest test (T-TEST). The T-TEST results (*Section 4.3.5*) revealed that the 'null hypothesis' on the difference amongst the means of the nine runs is acceptable – the difference amongst the means of the nine runs is not statistically significant – since T-TEST critical (1.8125) is greater than the T-TESTs outputs of the nine runs.

4. Of the three chosen commonly used isotherms – namely BET, Langmuir isotherms and Dubinin-Radushkevich (D-R) isotherms (*Section 2.5*) – the excess isotherm results matched the BET isotherm more than both Langmuir and D-R. D-R totally misfit the excess isotherms for each run with the magnitudes which are greater than ten times. The average deviation of the BET results is 8.900%, which is less than the 100% average deviation of the Langmuir isotherm variable from the excess adsorption isotherm.
5. The LabVIEW data acquisition and pressure-temperature monitoring software generated results which show that they can adequately and automatically monitor and acquire pressure-temperature data on the gas in the VAS. When relative pressures were greater than 0, the excess absorption amount greater than zero with noises. The automatic data acquisition resulted in the maximum excess adsorption capacity of 0.0350 g CO<sub>2</sub> per g coal, which is greater than the maximum excess adsorption capacities of eight (except run eight) of the nine runs. The maximum operating pressure was 45 bar. Hence, the data acquisition pressure-temperature data of the VAS should be automatically done.
6. The inter-laboratory comparison included in this project was not a satisfactory as anticipated, due to time constraints (lengthy delays from AUT); only one isotherm was generated. The excess adsorption isotherm of the Wits and AUT adsorption systems were different, since the Wits system resembled BET isotherm, while AUT's resembled the Langmuir isotherm, between 0 and 50 bar. The maximum

adsorption capacities of both Wits (average isotherm) and AUT systems were 0.0165 g CO<sub>2</sub> per g coal and 0.0251 g CO<sub>2</sub> per g coal respectively.

In view of the above conclusions, the designed VAS is reliable, and can be consistently and can be automatically utilised to perform adsorption isotherm studies under simulated pressure-temperature conditions comparable to geo-storage of CO<sub>2</sub>, bearing in mind certain limitations discussed above. The output isotherms of the VAS can be used to estimate the storage capacity of geological material.

## 6 RECOMMENDATIONS

- i. Studies should be performed to understand:
  - a. The effect of compressing the gas after equilibrium is reached. This is to observe whether compression increases or decreases adsorption. Current CCS operation are storing compressed CO<sub>2</sub>, so this study will help understand this phenomenon in the South African context.
  - b. The impact of inherent moisture. This study will help understand the decrease in gas adsorption capacity due to inherent moisture. Moisture may take up pore space, preventing adsorption.
  - c. Coal permeability studies using globally recommended instruments. This study will aid in clarifying the adsorption capacity of a storage site.
  - d. Flow rate effect. First install a variable valve in the place of V<sub>2</sub>. This study will help understand the impact of gas injection rate on adsorption.
- ii. A validity study should be done using activated carbon with enough known data such as adsorption capacity at STP. The commissioning and verifying study (as conducted here) focuses on measuring consistency, while a validity study will help determine the accurate adsorption capacity.
- iii. Perform a detailed sorption (desorption and adsorption) study which only focuses on coal under subcritical and supercritical conditions. In the study, detailed thermodynamics should be investigated in order to understand equilibrium achievement.
- iv. Modify the system to increase the volume. However, the ratio of the reference cell to the sample cell is bigger than 2. Replace the each reactor with two cut and welded Swagelok VCR connection. The sealing discs should have continental threads with 0.5 µm pore width. The above two recommendations should be resolved as soon as possible. Install at least two buffer vessels to pressurise the reference cell, but ensure they are at least 4 times bigger than the reference cell. These arrangement is cheap and will help add a buffer necessary to efficiently pressurise the reference cell.



- v. Look into the possibility of obtaining a gravimetric system. This will help understanding the difference between the volumetric and gravimetric method. Please note the volume ratio stated in iv since this simplifies pressurisation.
- vi. Ensure there are spare parts always available.  $\frac{1}{4}$  inch nuts, 10 mm allen keys,  $\frac{1}{4}$  inch tubes, reactors and seals.
- vii. It is recommended that a PhD student working on this project next year, spends some time at Aachen University of Technology with Dr Dirk Prinz as soon as possible. This will enable student new to the concept of CO<sub>2</sub> adsorption to understand the basics of the technology of CO<sub>2</sub> sequestration and where it is going in the future.

## **7 ACKNOWLEDGEMENTS**

1. Nicola Wagner from the University of Witwatersrand supervised the project
2. Tshifhiwa Maphala, a PhD candidate from the University of Witwatersrand CCRG who was my mentor.
3. Warren Hodgkinson from JAD System assisted with the LabVIEW coding and automation.
4. Willie Augustyn from Chem Vac built the equipment.
5. Reghana Daniels from the University of Witwatersrand helped with administration.
6. Sibongile Maswanganye from the University of Witwatersrand helped with administration.
7. Bruce Mothibeli from the University of Witwatersrand helped provision of lab accessories.

## REFERENCES

- Adiraju, B. (2010). Adsorption of CO<sub>2</sub> on Indian coals. National Institute of Technology (p. 71). Orissa
- Airgas. (2011). MSDS Library of Pure Gases. World Wide Web. Retrieved May 9, 2011, from <http://www.airgas.com/msds/msds.aspx>
- Arumugam, A. (2004). High Pressure Adsorption of Pure Coalbed Gases on Dry Coals (p. 1-127). Oklahoma.
- Asia University. (2012). Adsorption of Gases in multimolecular layers. World Wide Web. Retrieved September 26, 2012, from <http://dns2.asia.edu.tw/~ysho/YSHO-English/1000 WC/PDF/J Ame Che Soc60, 309.pdf>
- Bahadori, A., & Vuthaluru, H. (2009). New Method Accurately Predicts Carbon Dioxide Equilibrium Adsorption Isotherms. International Journal of Greenhouse Gas Control, 3(6), 768-772. Elsevier Ltd.
- Bellert, T., Knight, A., Hauser, R., & Oshier, J. (1996). Gas Adsorption. University of Florida: Chemistry Department. Retrieved April 7, 2011, from [http://www.chem.ufl.edu/~itl/4411L\\_f00/ads/ads\\_1.html](http://www.chem.ufl.edu/~itl/4411L_f00/ads/ads_1.html)
- Belmabkhout, Y., Frère, M., & De Weireld, G. (2004). High-Pressure Adsorption Measurements. A Comparative Study of the Volumetric and Gravimetric Methods. Measurement Science and Technology, 15(5), 848-858.
- Bhebhe, S. (2008). The Effect of Coal Compostion on Carbon Dioxide Adsorption. University of Witwatersrand (p. 151). Johannesburg.
- Brunauer, S. (1943). The Adsorption of Gases and Vapors (1st:Vol 1 ed., p. 528). Oxford: Oxford University Press. Retrieved December 14, 2012,from <http://www.archive.org/details/adsorptionofgase031704mbp>

- Brunauer, S., Emmett, P., & Teller, E. (1938). Adsorption of Gases in Multimolecular Layers. *Journal of American Chemical Society*, 60(2), 309–319.
- Busch, A., Gensterblum, Y., Krooss, B., & Siemons, N. (2006). Investigation of High-Pressure Selective Adsorption-Desorption Behaviour of CO<sub>2</sub> and CH<sub>4</sub> on Coals : An Experimental Study. *International Journal of Coal Geology*, 66, 53 - 68
- Choudhury, A. (2009). Independent samples T-TEST. World Wide Web. Retrieved June 3, 2011, from <http://www.medcalc.org/manual/ttest.php>
- Cloete, M. (2010). Atlas on Geological Storage of Carbon Dioxide in South Africa. The Council for Geoscience of South Africa (p. 62).
- Coal Fillers Incorporated (2009), MSDS of Bituminous Coal, World Wide Web, Retrieved December 14, 2012 from <http://www.rubberworld.com/coalfillers/msds%20sheet%20austin%20black%20325.pdf>
- Creative-Research-System. (2010). Significance in Statistics & Survey. World Wide Web. Retrieved June 3, 2011, from <http://www.surveysystem.com/signif.htm>
- Czepirski, L., Balys, M. R., & Komorowska-czepirska, E. (2000). Some generalization of Langmuir adsorption isotherm Some generalization of Langmuir adsorption isotherm. *Adsorption Journal Of The International Adsorption Society*.
- Day, S., Duffy, G., Sakurovs, R., & Weir, S. (2008). Effect of Coal Properties on CO<sub>2</sub> Sorption Capacity under Supercritical Conditions. *International Journal of Greenhouse Gas Control*, 2(3), 342-352.

Dubinin, M. (1969). The Potential Theory of Adsorption of Gases and Vapors for Adsorbents with Energetically Nonuniform Surfaces. *Journal of the American Chemical Society*, 60(2), 235–241.

Emmett, P. (1977). Citation Classics: Adsorption of Gases in Multimolecular Layers. *Journal of the American Chemical Society*, 35, 211. *Journal of the American Chemical Society*

Engelbrecht, A., Golding, A., & Scholes, B. (2008). The Potential for Sequestration of Carbon Dioxide in South Africa. CSIR website. Johannesburg. Retrieved January 4, 2012, from [http://playpen.meraka.csir.co.za/~acdc/education/CSIR conference 2008/Proceedings/CPO-0027.pdf](http://playpen.meraka.csir.co.za/~acdc/education/CSIR%20conference%202008/Proceedings/CPO-0027.pdf)

Everett, D. H., Koopal, L. H., Drakos, N., & Moore, R. (2002). Chemisorption and Physisorption. International Union of Pure and Applied Chemistry. Retrieved April 7, 2011, from [http://old.iupac.org/reports/2001/colloid\\_2001/manual\\_of\\_s\\_and\\_t/node16.html](http://old.iupac.org/reports/2001/colloid_2001/manual_of_s_and_t/node16.html)

Fujii, T., Sugai, Y., Sasaki, K., & Hashida, T. (2009). Measurements of CO<sub>2</sub> Sorption on Rocks Using a Volumetric Technique for CO<sub>2</sub> Geological Storage. *Energy Procedia*, 1(1), 3715-3722. Elsevier

Gensterblum, Y., Hemert, P., Billemon, P., Busch, A., Charrière, D., Li, D., Krooss, B., et al. (2009). European Inter-laboratory Comparison of High Pressure CO<sub>2</sub> Sorption Isotherms. I: Activated Carbon. *Carbon*, 47(13), 2958-2969

Gertenbach, R. M. (2009). Methane and Carbon Dioxide Sorption Studies on South African Coals. *Carbon* (p. 175). University of Witwatersrand. Johannesburg.

Goodman, A., Busch, A., Bustin, R., Chikamarla, L., Day, S., Duffy, G., Fitzgerald, J., et al. (2007). Inter-laboratory Comparison II: CO<sub>2</sub> Isotherms

Measured on Moisture-Equilibrated Argonne Premium Coals at 55 °C and Up to 15 MPa. *International Journal of Coal Geology*, 72(3-4), 153-164

Groen, J. (2011). Porosity and Surface Area. Van Bokhoven website. Retrieved January 5, 2012, from [http://www.vanbokhoven.ethz.ch/education/Porosity\\_and\\_Surface\\_Area\\_-\\_J.\\_C.\\_Groen](http://www.vanbokhoven.ethz.ch/education/Porosity_and_Surface_Area_-_J._C._Groen)

Hemert, P., Bruining, H., Rudolph, E., Wolf, K., & Maas, J. (2009). Improved Manometric Setup for the Accurate Determination of Supercritical Carbon Dioxide Sorption. *Review of Scientific Instruments*, 80, 1-11

Herold, M. (2002). Langmuir-Adsorption. Thuis Experimenteren Website. Retrieved April 7, 2011, from <http://www.thuisexperimenteren.nl/infopages/langmuir/langmuir.htm>

Karr, C. (1978). *Analytical Methods for Coal and Coal Products Volume I*. New York: Academic Press.

Keller, J. U., & Robens, E. (2003). A Note on Sorption Measuring Instruments. *Journal of Thermal Analysis*, 71, 37-45.

Keller, J. U., & Staudt, R. (2005). *Gas Adsorption Equilibria: Experimental Methods and Adsorptive Isotherms* (p. 422). Springer. Retrieved December 14, 2012, from <http://books.google.com/books?id=ZxrHRZc4SDcC&pgis=1>

Kiefer, S., & Robens, E. (2008). Some Intriguing Items in the History of Volumetric and Gravimetric Adsorption Measurements. *Journal of Thermal Analysis*, 94, 613-618.

KnowWare International Inc. (2012). t test - one sample in Excel using the QI Macros. World Wide Web. Retrieved September 9, 2012, from <http://www.qimacros.com/hypothesis-test/T-TEST-one-sample/>

- Kobulnicky, C. (2008). Phase Diagram of CO<sub>2</sub>. University of Wyoming: Physics Department. Retrieved April 7, 2011, from [http://www.google.co.za/imgres?q=Phase+diagram+of+co2&hl=en&client=firefox-a&sa=X&rls=org.mozilla:en-US:official&tbm=isch&tbnid=zffWx\\_ndhPxEM:&imgrefurl=http://physics.uwyo.edu/~chip/Courses/PHYS1210/Slides/Day39/&ei=idmdTf7kHpGmvgP28t27BA&zoom=1&iact=hc&vpx=932&vpy=134&dur=125&hovh=192&hovw=263&tx=108&ty=96&oei=n9idTer6MlqOuQPpyozJBA&page=2&tbnh=118&tbnw=173&start=21&ndsp=22&ved=1t:429,r:12,s:21&biw=1366&bih=548](http://www.google.co.za/imgres?q=Phase+diagram+of+co2&hl=en&client=firefox-a&sa=X&rls=org.mozilla:en-US:official&tbm=isch&tbnid=zffWx_ndhPxEM:&imgrefurl=http://physics.uwyo.edu/~chip/Courses/PHYS1210/Slides/Day39/&ei=idmdTf7kHpGmvgP28t27BA&zoom=1&iact=hc&vpx=932&vpy=134&dur=125&hovh=192&hovw=263&tx=108&ty=96&oei=n9idTer6MlqOuQPpyozJBA&page=2&tbnh=118&tbnw=173&start=21&ndsp=22&ved=1t:429,r:12,s:21&biw=1366&bih=548)
- Lashof, D. A., & Ahuja, D. R. (1990). Relative Contributions of Greenhouse Gas Emissions to Global Warming. *Nature*, 344(6266), 529-531
- Li, D., Liu, Q., Weniger, P., Gensterblum, Y., Busch, A., & Krooss, B. (2010). High-Pressure Sorption Isotherms and Sorption Kinetics of CH<sub>4</sub> and CO<sub>2</sub> on Coals. *Fuel*, 89(3), 569-580. Elsevier Ltd
- Lin W. (2009), Gas Sorption and the Consequent Volumetric and Permeability Change of Coal, 2009, PhD Thesis, Stanford University
- Mantell, C. L. (1951). Adsorption. McGraw-Hill (2nd ed., p. 643). New York: McGraw-Hill. Retrieved from <http://hdl.handle.net/2027/mdp.39015000970346>
- Menon, V. C., Leon, C. A., Kyotani, L. T., & Radovic, L. R. (1991). Effects of Moisture on the Sorption of CO<sub>2</sub> by Coal. New York: Journal of the American Chemical Society National Meeting
- Metz, B., Davidson, O., de Coninck, H., Loos, M., & Meyer, L. (2005). Carbon Dioxide Capture and Storage (1st ed., p. 443). New York: Cambridge University Press
- Mugge, J., Bosch, H., & Reith, T. (2000). Gas Adsorption Kinetics in Activated Carbon. Adsorption Science and Technology - Proceedings of the Second

Pacific Basin Conference, 451-455. Singapore: World Scientific Publishing Co. Pte. Ltd

Myers, A. (2002). Thermodynamics of Adsorption in Porous Materials. *AIChE Journal*, 48(1).

NI. (2011). National Instruments - Data Acquisition (DAQ). World Wide Web. Retrieved May 11, 2011, from <http://www.ni.com/dataacquisition/>

NIST. (2011). NIST Webbook for Fluid Data. National Institute of Standards and Technology. Retrieved January 27, 2011, from <http://webbook.nist.gov/chemistry/fluid/>

Nicholson, D., & Sing, W. (1976). Adsorption at the Gas-Solid Interface. *Journal of Colloid Interface Science*, 282, 1-62.

Nix, R. M. (2003). 2.3 Adsorption Kinetics - The Rate of Adsorption. University of London : Biological and Chemical Science Department. Retrieved April 7, 2011, from [http://www.chem.qmul.ac.uk/surfaces/scc/scat2\\_3.htm](http://www.chem.qmul.ac.uk/surfaces/scc/scat2_3.htm)

Pakseresht, S., Kazemeini, M., & Arkbarnejad, M. (2002). Equilibrium Isotherms for CO, CO<sub>2</sub>, CH<sub>4</sub> and C<sub>2</sub>H<sub>4</sub> on the 5A Molecular Sieve by a Simple Volumetric Apparatus. *Separation and Purification Technology*, 28(1), 53-60

Qing-ling. (2008). Adsorption Mechanism of Different Coal Ranks under Variable Temperature and Pressure Conditions. *J China Univ Mining & Technol*, 18(3), 395-400.

Saghafi, A., Faiz, M., & Roberts, D. (2007). CO<sub>2</sub> Storage and Gas Diffusivity Properties of Coals from Sydney Basin, Australia. *International Journal of Coal Geology*, 70(1-3), 240-254

Saghafi, A. (2011). Enhanced Coal Bed Methane (ECBM) and CO<sub>2</sub> storage in Australian coals (p. 43)



- Sakurovs, R., Day, S., Weir, S., & Duffy, G. (2008). Temperature dependence of sorption of gases by coals and charcoals. *International Journal of Coal Geology*, 73(3-4), 250-258
- Schneider, S. (1990). The Global Warming Debate: Science or Politics? *Environmental Science & Technology*, 24(4), 432-435
- Shi, J., Mazumder, S., Wolf, K., & Durucan, S. (2008). Competitive Methane Desorption by Supercritical CO<sub>2</sub> Injection in Coal. *Transport in Porous Media*, 75(1), 35-54
- StatTrek. (2012). Hypothesis Test for a Mean. World Wide Web. Retrieved September 9, 2012, from <http://stattrek.com/hypothesis-test/mean.aspx>
- UIG. (2008). Carbon Dioxide (CO<sub>2</sub>) Properties, Uses, Applications CO<sub>2</sub> Gas and Liquid Carbon Dioxide. Universal Industrial Gases, Inc. Retrieved April 7, 2011, from <http://www.uigi.com/carbondioxide.html>
- Viljoen, J., Stapelberg, F., & Cloete, M. (2010). Technical Report on the Geological Storage of Carbon Dioxide in South Africa. The Council for Geoscience of South Africa (p. 236)
- De Weireld, G., Frere, M., & Jadot, R. (1999). Automated Determination of High-Temperature and High-Pressure Gas Adsorption Isotherms Using a Magnetic Suspension Balance. *Meas. Sci. Technol*, 10, 117–126. Retrieved from <http://iopscience.iop.org/0957-0233/10/2/010>
- Weisstein, E. W. (2011). Standard Deviation -- from Wolfram MathWorld. World Wide Web. Wolfram Research, Inc. Retrieved May 12, 2011, from <http://mathworld.wolfram.com/StandardDeviation.html>
- Yu, H., Guo, W., Cheng, J., & Hu, Q. (2008). Impact of Experimental Parameters for Manometric Equipment on CO<sub>2</sub> Isotherms Measured: Comment on “Inter-laboratory Comparison II: CO<sub>2</sub> Isotherms Measured on Moisture-Equilibrated

Argonne Premium Coals at 55°C and up to 15 MPa” by Goodman et al.  
(2007). International Journal of Coal Geology, 74(3-4), 250-258

## **APPENDICES**

### **Appendix 1: MSDS**

MSDS of Coal

The MSDS data was retrieved from the Coal Fillers Incorporated (2009)

# MATERIAL SAFETY DATA SHEET (MSDS)

(In compliance with CFR 1910.1200 and WHMIS)

HMIS Rating	
2	Health
1	Flammability
0	Reactivity

## Section 1 – Identification of Substance/Preparation & Company

**Trade Name:** Austin Black® 325 is a ground coal product. Austin Black is a registered trade name of Coal Fillers Incorporated.

**Product type:** Bituminous Coal

**Product Chemical Name:** Bituminous Coal, a naturally occurring mineral

**Chemical Family:** Carbon

**Product Trivial Name:** Ground coal filler

**Manufacturer:** Coal Fillers Incorporated  
271 St Clairs Crossing  
Bluefield, VA. 24605

**Emergency Telephone No.**  
(276) – 322 - 4675

**Prepared by:** Health, Safety, and Environmental

**Issue Number:** 5

**Date Revised:** October 7, 2011

**Previous Revision Date:** November 10, 2009

**Reason for Revision:** Section 1: Change Coal Fillers Inc. street address

Section 14: Changed the description of Schedule B Number from "Bituminous coal, not metallurgical not agglomerated" to "Bituminous –Other".

## Section 2 - Composition/Information on Ingredients

Substance Name	C.A.S. Number	% by Weight
Bituminous Coal	Not Applicable	90 - 100
Silica (Quartz)	14808-60-7	0.1 – 1.0

## Section 3 - Hazards Identification

**Classification:** Ground bituminous has been evaluated by IARC as a Group 3: *Unclassifiable as to carcinogenicity to humans*. Ground bituminous coal may contain up to 1.0% Silica (Quartz) which has been evaluated by IARC as a Group 1: *Carcinogenic to humans*. The USA, National Toxicology Program (NTP) has not classified bituminous coal as to its carcinogenicity, but has classified Silica (Quartz) as a NTP-K: *Known to be a human carcinogen*. See Section 11 for further information.

**Physical Hazards:** Combustible black powder. Releases COx SOx and Methane when burning. Not easily extinguished when burning.

**Health Risks:** Long term inhalation of coal dust may lead to pneumoconiosis.

## Section 4 – First Aid Measures

**Inhalation:** Temporary discomfort to upper respiratory tract may occur due to inhalation of high dust levels well above the 8 hour occupational exposure limit. Long term inhalation of coal dust may lead to pneumoconiosis.

**Skin Contact:** No adverse affects expected.

**Ingestion:** No adverse affects expected.

**Eyes:** Not identified as an irritant. High dust concentrations may cause mechanical irritation.

## Section 5 - Fire Fighting Measures

**Extinguishing Media:** Water spray (fog), foam, or carbon dioxide (CO<sub>2</sub>), are the best extinguishing medium for fires.

**Unsuitable Media:** Water stream

**Lower Explosive Limit:** Unknown

**Upper Explosive Limit:** Unknown

**Flash Point:** Not applicable

**Flammability Classification:** Combustible Solid

**Flame Propagation in Air:** Slow burning solid

**Ignition in Air<sup>1</sup>:** Above 1300° F, ( 704° C )

**Fire Fighting Instructions:** Normal fog nozzle water application and/or exclusion of air.

**Combustion Hazards:** COx SOx and Methane.

**Protective Equipment:** Normal fire fighting equipment with appropriate respirator for COx, SOx, and Methane

**Unusual Fire Hazards:** It may not be noticed that the product is burning unless it is stirred and sparks are and sparks are apparent. Material that has been on fire should be watched closely to insure that no smoldering material is present.

**Dust Explosion Potential<sup>2</sup>:** When high dust concentrations exist and a significant energy source is applied tests have determined that dust clouds and layers of 200 mesh (0.075mm) coal dust and an air mixture can explode.  
Minimum Ignition Temperature cloud > 1200° F (649° C)  
Minimum Ignition Temperature layer > 350° F (177° C)

**Sensitivity to Impact:** Not Applicable.

**Sensitive to Static Charge:** Not Applicable.

<sup>1</sup> Anon., Steam, It's Generation and Use, The Babcock and Wilcox Co., New York, 1955, pp. 2-15.

<sup>2</sup> Schrecengost, H.A. and Childers, " Fire and Explosion Hazards in Fluidized-Bed Thermal Coal Dryers," Circular No. 8258, US Bureau of Mines 1965.

## Section 6 - Accidental Release Measures/Spills and Leaks

**Personal Precautions:** Wear appropriate respiratory protection for the dust levels anticipated, see Section 10.

**Spill Cleanup Measures:** In order to minimize dust, spills should be removed by vacuuming, or by lightly spraying with water and sweeping the mixture into a suitable container  
Do not dry sweep.

**Environmental Precautions:** Ground coal is not a hazardous waste. Dispose in a landfill, or by incineration in accordance with national and local laws and regulations.

## Section 7 - Handling and Storage

**Handling and Storage Precautions:**

- Store in a dry clean area.
- Prevent exposure to high temperature and flames.
- Prevent exposure to strong oxidizers.

**Hygienic Practices:** Avoid creating dust. Clean up all spills promptly. Wash exposed skin daily.  
Wash work clothes daily.

## Section 8 – Exposure Controls/ Personal Protection

**Inhalation:** In case of discomfort, remove the exposed individual to fresh air.

**Respiratory Protection:** Not required if dust levels are maintained below the PEL or TWA listed.

For levels above the listed PEL and TWA an appropriate NIOSH/MSHA approved respirator should be used. Like any nuisance dust, Austin Black may aggravate certain pre-existing upper respiratory disorders, such as bronchitis or asthma.

**Skin:** Not hazardous. Wash exposed skin for hygienic purposes.

**Ingestion:** Not hazardous. Symptomatic treatment is recommended.

**Eyes:** Treat symptomatically for irritation. Flush lightly with water to remove the dust.

Section 9 - Physical and Chemical Properties		
<b>PHYSICAL STATE</b> Solid Powder	<b>COLOR</b> Brownish Black	<b>ODOR</b> None
<b>ODOR THRESHOLD</b> Not Applicable	<b>pH</b> 7	<b>BOILING POINT</b> Not Applicable
<b>EVAPORATION RATE</b> Not Applicable	<b>MELTING/FREEZING POINT</b> Not Applicable	<b>% VOLATILE BY VOLUME</b> 20% Max. when heated to 950°C
<b>SOLUBILITY IN WATER</b> Insoluble	<b>SPECIFIC GRAVITY</b> 1.31	<b>VAPOR DENSITY</b> Not Applicable
<b>VAPOR PRESSURE</b> Not Applicable	<b>RAPID VAPOR PRESSURE</b> Not Applicable	<b>WATER/OIL DISTRIBUTION</b> Not Applicable
<b>VISCOSITY</b> Not Applicable	<b>POUR POINT</b> Not Applicable	<b>INTENTIONALLY LEFT BLANK</b>

## Section 10 - Stability and Reactivity

**Chemical Stability:** Stable

**Conditions to Avoid:** Contact with strong oxidizers, especially when heated.  
High temperatures or flames.

**Incompatible Materials:** Strong oxidizers.

**Reactivity:** May react exothermically upon contact with strong oxidizers.

**Hazard Decomposition:** Releases carbon monoxide (CO), carbon dioxide (CO<sub>2</sub>), sulfur monoxide (SO), sulfur dioxide (SO<sub>2</sub>), and Methane.

**Hazard polymerization:** Not applicable.

## Section 11 – Toxicological Information

INHALATION STANDARDS	EXPOSURE LIMITS		AMOUNT
<u>C.A.S.No.</u>	<u>PEL</u>	<u>TLV</u>	<u>%</u>
<b>Coal, bituminous</b>	* 2.4mg/m <sup>3</sup>	* 0.9mg./m <sup>3</sup>	90 - 100
C.A.S. No. Not Applicable			
Naturally Occurring Mineral			
<b>Silica (Quartz)</b>	10mg/m <sup>3</sup>	* 0.05mg/m <sup>3</sup>	0.1 – 1.0
C.A.S. No. 14808-60-7	% SiO <sub>2</sub> +2		

\* Respirable fraction <5% SiO<sub>2</sub>

### Personal Protective Equipment:

**Gloves.** None required.

**Protective Clothing:** None required. Confine work clothing to the workplace and wash daily.

**Eye/Face Protection:** None required.

**Engineering Controls:** Use sufficient ventilation in volume and pattern to maintain dust exposures below the TWA.

**Other Protective Measures:** Wash exposed skin before eating, drinking and smoking. Wash clothing daily.

### Acute Effects:

**Inhalation:** None expected. Based on experience, temporary discomfort or mechanical irritation to upper respiratory tract may occur due to inhalation of dust concentrations well above the 8 hour TWA.

**Ingestion:** No adverse effects expected.

**Eye:** No adverse effects expected. High dust concentrations may cause mechanical irritation.

**Skin:** No adverse effects expected.

**Chronic Effects:**

**Inhalation:** Long term inhalation of coal dust may lead to the development of pneumoconiosis.

**Carcinogenicity:** Coal contains a small amount of Crystalline Silica (Quartz).

IARC has classified Silica (Quartz) as a Group 1, "*carcinogenic to humans*"

The National Toxicology Program, (NTP) has listed Silica (Quartz) as a (NTP-K),  
*known to be human carcinogen*

The Occupational Safety and Health Administration, (OSHA) has not classified  
Silica (Quartz) as to its carcinogenicity.

**Ingestion:** No adverse effects expected.

**Eye:** No adverse effects expected.

**Skin:** No adverse effects known.

**OECD Test Values:**

**Irritancy:** Not Available.

**Sensitization:** Not Available.

**Mutagenicity:** Not Available.

**Reproductive Toxicity:** Not Available.

**Teratogenicity:** Not Available.

**Synergistic Materials:** None expected.

**Section 12 – Ecological Information**

Austin Black is ground bituminous coal, which is a naturally occurring mineral. Keep product away from drains, sewers, streams, and rivers.

**Section 13 – Disposal Considerations**

The product may be disposed of by incineration, or deposited in a solid waste land fill, provided that these methods and facilities comply with local and national regulations.

**Section 14 – Transport Information**

**Domestic:** The U. S. Department of Transportation classifies this product as aerated coal, a non-hazardous product.

**International:** US Customs, Harmonized Tariff System, Schedule B Number: 2701.12.0050 - Bituminous coal: Other

**Section 15 – Regulatory Information**

**Resource Conservation and Recovery Act, (RCRA) :** All metals are below the TCLP listed levels.

**UN Classification:** Not classified

**SARA TITLE III :** This product does not contain any toxic chemicals subject to the reporting requirements of Section 313 of the Emergency Planning and Community Right-to-Know Act of 1986 and of CFR 372.

**TSCA & DSL Inventories:** This product is listed as a naturally occurring substance.

**REACH, EU Legislation:** Austin Black 325 is 100 % bituminous coal. No chemicals are used in the grinding process and no chemicals are added to the finished product. Austin Black 325 is classified as a naturally occurring mineral, and therefore exempt from this regulation.

**Section 16 – Other Health and Safety Information**

There is no additional health and safety information available. It is the customers responsibility to ensure that a suitable and sufficient assessment of the risks created by a work activity using this product is under taken before this product is used.

**Disclaimer:** The information contained in this Safety Data Sheet is based on information which Coal Fillers Incorporated believes to be accurate. No warranty, expressed or implied, is intended. The information is provided solely for your information and consideration. Coal Fillers Incorporated assumes no responsibility for its use or reliance thereon.





## MSDS of CO<sub>2</sub>

The following MSDS is adopted for the (Airgas, 2011):

# Material Safety Data Sheet



Carbon Dioxide

## Section 1. Chemical product and company identification

<b>Product name</b>	: Carbon Dioxide
<b>Supplier</b>	: AIRGAS INC., on behalf of its subsidiaries 259 North Radnor-Chester Road Suite 100 Radnor, PA 19087-5283 1-610-687-5253
<b>Product use</b>	: Synthetic/Analytical chemistry.
<b>Synonym</b>	: Carbonic Acid, Carbon Dioxide Liquid, Carbon Dioxide, Refrigerated Liquid, Carbonic Anhydride
<b>MSDS #</b>	: 001013
<b>Date of Preparation/Revision</b>	: 2/25/2009.
<b>In case of emergency</b>	: 1-866-734-3438

## Section 2. Hazards identification

<b>Physical state</b>	: Gas or Liquid.
<b>Emergency overview</b>	: WARNING! GAS: CONTENTS UNDER PRESURE. MAY CAUSE RESPIRATORY TRACT, EYE, AND SKIN IRRITATION. CAN CAUSE TARGET ORGAN DAMAGE. Do not puncture or incinerate container. Can cause rapid suffocation. LIQUID: MAY CAUSE RESPIRATORY TRACT, EYE, AND SKIN IRRITATION. CAN CAUSE TARGET ORGAN DAMAGE. Extremely cold liquid and gas under pressure. Can cause rapid suffocation. May cause severe frostbite.  Do not puncture or incinerate container. Avoid contact with eyes, skin and clothing. May cause target organ damage, based on animal data. Wash thoroughly after handling. Keep container closed. Avoid breathing gas. Use with adequate ventilation. Contact with rapidly expanding gas, liquid, or solid can cause frostbite.
<b>Target organs</b>	: May cause damage to the following organs: lungs, cardiovascular system, skin, eyes, central nervous system (CNS).
<b>Routes of entry</b>	: Inhalation Dermal Eyes
<b>Potential acute health effects</b>	
<b>Eyes</b>	: Moderately irritating to eyes. Contact with rapidly expanding gas may cause burns or frostbite. Contact with cryogenic liquid can cause frostbite and cryogenic burns.
<b>Skin</b>	: Moderately irritating to the skin. Contact with rapidly expanding gas may cause burns or frostbite. Contact with cryogenic liquid can cause frostbite and cryogenic burns.
<b>Inhalation</b>	: Moderately irritating to the respiratory system.
<b>Ingestion</b>	: Ingestion is not a normal route of exposure for gases. Contact with cryogenic liquid can cause frostbite and cryogenic burns.
<b>Potential chronic health effects</b>	: <b>CARCINOGENIC EFFECTS:</b> Not available. <b>MUTAGENIC EFFECTS:</b> Not available. <b>TERATOGENIC EFFECTS:</b> Not available.
<b>Medical conditions aggravated by over-exposure</b>	: Pre-existing disorders involving any target organs mentioned in this MSDS as being at risk may be aggravated by over-exposure to this product.

See toxicological information (section 11)

## Carbon Dioxide

### Section 3. Composition, Information on Ingredients

Name	CAS number	% Volume	Exposure limits
Carbon Dioxide	124-38-9	100	<b>ACGIH TLV (United States, 1/2008).</b> STEL: 54000 mg/m <sup>3</sup> 15 minute(s). STEL: 30000 ppm 15 minute(s). TWA: 9000 mg/m <sup>3</sup> 8 hour(s). TWA: 5000 ppm 8 hour(s). <b>NIOSH REL (United States, 6/2008).</b> STEL: 54000 mg/m <sup>3</sup> 15 minute(s). STEL: 30000 ppm 15 minute(s). TWA: 9000 mg/m <sup>3</sup> 10 hour(s). TWA: 5000 ppm 10 hour(s). <b>OSHA PEL (United States, 11/2006).</b> TWA: 9000 mg/m <sup>3</sup> 8 hour(s). TWA: 5000 ppm 8 hour(s). <b>OSHA PEL 1989 (United States, 3/1989).</b> STEL: 54000 mg/m <sup>3</sup> 15 minute(s). STEL: 30000 ppm 15 minute(s). TWA: 18000 mg/m <sup>3</sup> 8 hour(s). TWA: 10000 ppm 8 hour(s).

### Section 4. First aid measures

No action shall be taken involving any personal risk or without suitable training. If it is suspected that fumes are still present, the rescuer should wear an appropriate mask or self-contained breathing apparatus. It may be dangerous to the person providing aid to give mouth-to-mouth resuscitation.

<b>Eye contact</b>	: Check for and remove any contact lenses. Immediately flush eyes with plenty of water for at least 15 minutes, occasionally lifting the upper and lower eyelids. Get medical attention immediately.
<b>Skin contact</b>	: In case of contact, immediately flush skin with plenty of water for at least 15 minutes while removing contaminated clothing and shoes. Wash clothing before reuse. Clean shoes thoroughly before reuse. Get medical attention immediately.
<b>Frostbite</b>	: Try to warm up the frozen tissues and seek medical attention.
<b>Inhalation</b>	: Move exposed person to fresh air. If not breathing, if breathing is irregular or if respiratory arrest occurs, provide artificial respiration or oxygen by trained personnel. Loosen tight clothing such as a collar, tie, belt or waistband. Get medical attention immediately.
<b>Ingestion</b>	: As this product is a gas, refer to the inhalation section.

### Section 5. Fire-fighting measures

<b>Flammability of the product</b>	: Non-flammable.
<b>Products of combustion</b>	: Decomposition products may include the following materials: carbon dioxide carbon monoxide
<b>Fire-fighting media and instructions</b>	: Use an extinguishing agent suitable for the surrounding fire.  Apply water from a safe distance to cool container and protect surrounding area. If involved in fire, shut off flow immediately if it can be done without risk. Contains gas under pressure. In a fire or if heated, a pressure increase will occur and the container may burst or explode.
<b>Special protective equipment for fire-fighters</b>	: Fire-fighters should wear appropriate protective equipment and self-contained breathing apparatus (SCBA) with a full face-piece operated in positive pressure mode.

## Carbon Dioxide

### Section 6. Accidental release measures

- Personal precautions** : Immediately contact emergency personnel. Keep unnecessary personnel away. Use suitable protective equipment (section 8). Shut off gas supply if this can be done safely. Isolate area until gas has dispersed.
- Environmental precautions** : Avoid dispersal of spilled material and runoff and contact with soil, waterways, drains and sewers.
- Methods for cleaning up** : Immediately contact emergency personnel. Stop leak if without risk. Note: see section 1 for emergency contact information and section 13 for waste disposal.

### Section 7. Handling and storage

- Handling** : Wash thoroughly after handling. High pressure gas. Do not puncture or incinerate container. Use equipment rated for cylinder pressure. Close valve after each use and when empty. Keep container closed. Avoid contact with skin and clothing. Use with adequate ventilation. Avoid contact with eyes. Protect cylinders from physical damage; do not drag, roll, slide, or drop. Use a suitable hand truck for cylinder movement. Never allow any unprotected part of the body to touch uninsulated pipes or vessels that contain cryogenic liquids. Prevent entrapment of liquid in closed systems or piping without pressure relief devices. Some materials may become brittle at low temperatures and will easily fracture.
- Storage** : Cylinders should be stored upright, with valve protection cap in place, and firmly secured to prevent falling or being knocked over. Cylinder temperatures should not exceed 52 °C (125 °F). For additional information concerning storage and handling refer to Compressed Gas Association pamphlets P-1 Safe Handling of Compressed Gases in Containers and P-12 Safe Handling of Cryogenic Liquids available from the Compressed Gas Association, Inc.

### Section 8. Exposure controls/personal protection

- Engineering controls** : Use only with adequate ventilation. Use process enclosures, local exhaust ventilation or other engineering controls to keep worker exposure to airborne contaminants below any recommended or statutory limits.
- Personal protection**
- Eyes** : Safety eyewear complying with an approved standard should be used when a risk assessment indicates this is necessary to avoid exposure to liquid splashes, mists or dusts. When working with cryogenic liquids, wear a full face shield.
- Skin** : Personal protective equipment for the body should be selected based on the task being performed and the risks involved and should be approved by a specialist before handling this product.
- Respiratory** : Use a properly fitted, air-purifying or air-fed respirator complying with an approved standard if a risk assessment indicates this is necessary. Respirator selection must be based on known or anticipated exposure levels, the hazards of the product and the safe working limits of the selected respirator. The applicable standards are (US) 29 CFR 1910.134 and (Canada) Z94.4-93
- Hands** : Chemical-resistant, impervious gloves complying with an approved standard should be worn at all times when handling chemical products if a risk assessment indicates this is necessary. Insulated gloves suitable for low temperatures
- Personal protection in case of a large spill** : Self-contained breathing apparatus (SCBA) should be used to avoid inhalation of the product. Full chemical-resistant suit and self-contained breathing apparatus should be worn only by trained and authorized persons.

#### Product name

## Carbon Dioxide

carbon dioxide

### ACGIH TLV (United States, 1/2008).

STEL: 54000 mg/m<sup>3</sup> 15 minute(s).

STEL: 30000 ppm 15 minute(s).

TWA: 9000 mg/m<sup>3</sup> 8 hour(s).

TWA: 5000 ppm 8 hour(s).

### NIOSH REL (United States, 6/2008).

STEL: 54000 mg/m<sup>3</sup> 15 minute(s).

STEL: 30000 ppm 15 minute(s).

TWA: 9000 mg/m<sup>3</sup> 10 hour(s).

TWA: 5000 ppm 10 hour(s).

### OSHA PEL (United States, 11/2006).

TWA: 9000 mg/m<sup>3</sup> 8 hour(s).

TWA: 5000 ppm 8 hour(s).

### OSHA PEL 1989 (United States, 3/1989).

STEL: 54000 mg/m<sup>3</sup> 15 minute(s).

STEL: 30000 ppm 15 minute(s).

TWA: 18000 mg/m<sup>3</sup> 8 hour(s).

TWA: 10000 ppm 8 hour(s).

Consult local authorities for acceptable exposure limits.

## Section 9. Physical and chemical properties

Molecular weight	: 44.01 g/mole	
Molecular formula	: C-O <sub>2</sub>	
Boiling/condensation point	: -78.6°C (-109.5°F)	
Melting/freezing point	: Sublimation temperature: -78.5°C (-109.3°F)	
Critical temperature	: 30.9°C (87.6°F)	
Vapor pressure	: 830 (psig)	
Vapor density	: 1.53 (Air = 1)	Liquid Density@BP: Solid density = 97.5 lb/ft <sup>3</sup> (1562 kg/m <sup>3</sup> )
Specific Volume (ft <sup>3</sup> /lb)	: 8.7719	
Gas Density (lb/ft <sup>3</sup> )	: 0.114	

## Section 10. Stability and reactivity

Stability and reactivity	: The product is stable.
Hazardous decomposition products	: Under normal conditions of storage and use, hazardous decomposition products should not be produced.
Hazardous polymerization	: Under normal conditions of storage and use, hazardous polymerization will not occur.

## Section 11. Toxicological information

### Toxicity data

Product/ingredient name	Result	Species	Dose	Exposure
carbon dioxide	LC50 Inhalation Gas.	Rat	470000 ppm	30 minutes

IDLH : 40000 ppm

Chronic effects on humans : May cause damage to the following organs: lungs, cardiovascular system, skin, eyes, central nervous system (CNS).

Other toxic effects on humans : No specific information is available in our database regarding the other toxic effects of this material to humans.

### Specific effects

Carcinogenic effects : No known significant effects or critical hazards.

Mutagenic effects : No known significant effects or critical hazards.

Reproduction toxicity : No known significant effects or critical hazards.

## Carbon Dioxide

### Section 12. Ecological information

#### Aquatic ecotoxicity

Not available.

**Toxicity of the products of biodegradation** : not available

**Environmental fate** : Not available.




**Environmental hazards** : No known significant effects or critical hazards.

**Toxicity to the environment** : Not available.

### Section 13. Disposal considerations

Product removed from the cylinder must be disposed of in accordance with appropriate Federal, State, local regulation. Return cylinders with residual product to Airgas, Inc. Do not dispose of locally.

### Section 14. Transport information

Regulatory information	UN number	Proper shipping name	Class	Packing group	Label	Additional information
<b>DOT Classification</b>	UN1013	CARBON DIOXIDE	2.2	Not applicable (gas).		<b>Limited quantity</b> Yes.
	UN2187	Carbon dioxide, refrigerated liquid				<b>Packaging instruction</b> <b>Passenger aircraft</b> Quantity limitation: 75 kg  <b>Cargo aircraft</b> Quantity limitation: 150 kg
<b>TDG Classification</b>	UN1013	CARBON DIOXIDE	2.2	Not applicable (gas).		<b>Explosive Limit and Limited Quantity Index</b> 0.125
	UN2187	Carbon dioxide, refrigerated liquid				<b>Passenger Carrying Road or Rail Index</b> 75
<b>Mexico Classification</b>	UN1013	CARBON DIOXIDE	2.2	Not applicable (gas).		-
	UN2187	Carbon dioxide, refrigerated liquid				

"Refer to CFR 49 (or authority having jurisdiction) to determine the information required for shipment of the product."



## Section 15. Regulatory information

### United States

#### U.S. Federal regulations

- : **United States inventory (TSCA 8b):** This material is listed or exempted.  
**SARA 302/304/311/312 extremely hazardous substances:** No products were found.  
**SARA 302/304 emergency planning and notification:** No products were found.  
**SARA 302/304/311/312 hazardous chemicals:** carbon dioxide  
**SARA 311/312 MSDS distribution - chemical inventory - hazard identification:**  
carbon dioxide: Sudden release of pressure, Immediate (acute) health hazard, Delayed (chronic) health hazard  
**Clean Water Act (CWA) 307:** No products were found.  
**Clean Water Act (CWA) 311:** No products were found.  
**Clean Air Act (CAA) 112 accidental release prevention:** No products were found.  
**Clean Air Act (CAA) 112 regulated flammable substances:** No products were found.  
**Clean Air Act (CAA) 112 regulated toxic substances:** No products were found.

#### State regulations

- : **Connecticut Carcinogen Reporting:** This material is not listed.  
**Connecticut Hazardous Material Survey:** This material is not listed.  
**Florida substances:** This material is not listed.  
**Illinois Chemical Safety Act:** This material is not listed.  
**Illinois Toxic Substances Disclosure to Employee Act:** This material is not listed.  
**Louisiana Reporting:** This material is not listed.  
**Louisiana Spill:** This material is not listed.  
**Massachusetts Spill:** This material is not listed.  
**Massachusetts Substances:** This material is listed.  
**Michigan Critical Material:** This material is not listed.  
**Minnesota Hazardous Substances:** This material is not listed.  
**New Jersey Hazardous Substances:** This material is listed.  
**New Jersey Spill:** This material is not listed.  
**New Jersey Toxic Catastrophe Prevention Act:** This material is not listed.  
**New York Acutely Hazardous Substances:** This material is not listed.  
**New York Toxic Chemical Release Reporting:** This material is not listed.  
**Pennsylvania RTK Hazardous Substances:** This material is listed.  
**Rhode Island Hazardous Substances:** This material is not listed.

### Canada

#### WHMIS (Canada)

- : **Class A:** Compressed gas.  
**CEPA Toxic substances:** This material is listed.  
**Canadian ARET:** This material is not listed.  
**Canadian NPRI:** This material is not listed.  
**Alberta Designated Substances:** This material is not listed.  
**Ontario Designated Substances:** This material is not listed.  
**Quebec Designated Substances:** This material is not listed.

## Section 16. Other information

### United States

#### Label requirements

- : **GAS:**  
CONTENTS UNDER PRESURE.  
MAY CAUSE RESPIRATORY TRACT, EYE, AND SKIN IRRITATION.  
CAN CAUSE TARGET ORGAN DAMAGE.  
Do not puncture or incinerate container.  
Can cause rapid suffocation.  
**LIQUID:**  
MAY CAUSE RESPIRATORY TRACT, EYE, AND SKIN IRRITATION.  
CAN CAUSE TARGET ORGAN DAMAGE.  
Extremely cold liquid and gas under pressure.  
Can cause rapid suffocation.  
May cause severe frostbite.

### Canada

## Carbon Dioxide

**Label requirements** : Class A: Compressed gas.

**Hazardous Material Information System (U.S.A.)** :

Health	*	1
Flammability		0
Physical hazards		0

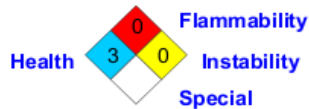
liquid:

Health		3
Fire hazard		0
Reactivity		0
Personal protection		

**National Fire Protection Association (U.S.A.)** :



liquid:



### Notice to reader

To the best of our knowledge, the information contained herein is accurate. However, neither the above-named supplier, nor any of its subsidiaries, assumes any liability whatsoever for the accuracy or completeness of the information contained herein.

Final determination of suitability of any material is the sole responsibility of the user. All materials may present unknown hazards and should be used with caution. Although certain hazards are described herein, we cannot guarantee that these are the only hazards that exist.

## Appendix 2: Derivation of Isotherms

### Langmuir Derivation

#### Thermodynamics Derivation

As shown in Figure A-1, the process of adsorption between gas phase molecules (A) vacant surface sites (S) and occupied surface sites (SA) can be expressed by the equation A-01 below (Fairbrother, 2011);

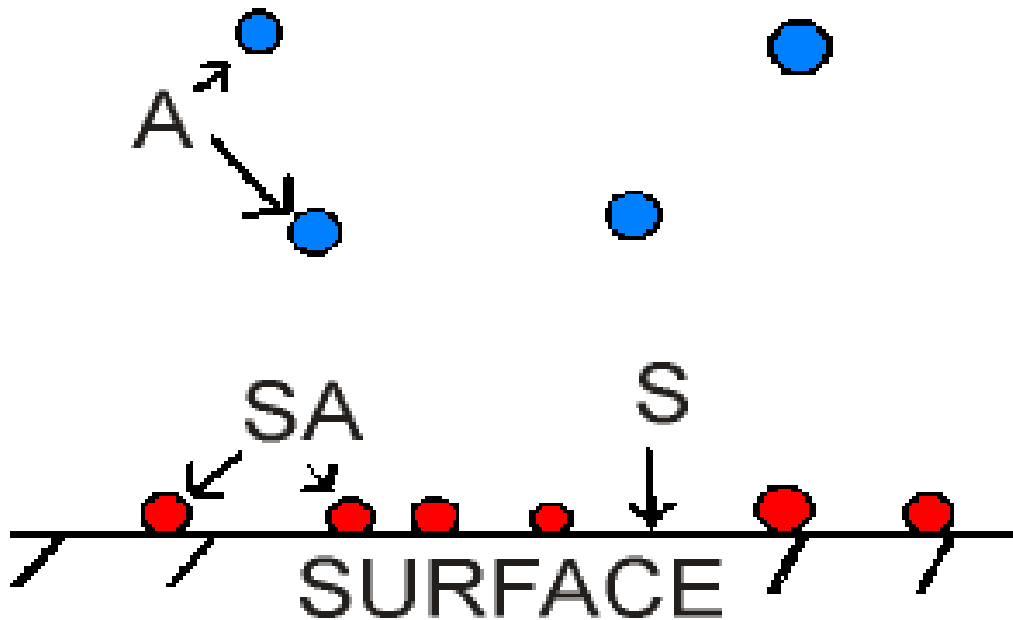
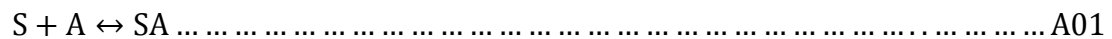


Figure A1.1: Schematic Picture of the Adsorption Process



Hence, assuming there is a fixed number of surface sites available on the surface, the equilibrium constant (K) can be presented as:



$$K = \frac{[SA]}{[S][A]} \dots\dots\dots A02$$

The ratio of surface sites occupied to the number of vacant sites is  $\theta$  and ranges from 0 to 1.

However,

$$SA \propto \theta \dots\dots\dots A03$$

$$SA \propto 1 - \theta \dots\dots\dots A04$$

$$A \propto P \dots\dots\dots A05$$

Where, P is the pressure of gas

Therefore K can be expressed as shown below:

$$K = \frac{\theta}{(1 - \theta)P} \dots\dots\dots A06$$

Rearranging Equation A-06 such that  $\theta$  is the subject of the formula generates Equation A-07:

$$\theta = \frac{KP}{KP + 1} \dots\dots\dots A07$$

However,

$$\theta = \frac{[SA]}{[S]} = \frac{N}{N_s} \dots\dots\dots A08$$

Where,  $N:N_s$  is an ratio of amount adsorbed and the saturated limit adsorbed respectively.

Therefore,

$$\frac{N}{N_s} = \frac{KP}{KP + 1} \dots\dots\dots A09$$

### **BET isotherm derivation**

Although the derivation of the BET isotherm is not here, it can be redirected to the original article by Stephen Brunauer, Paul Hugh Emmett, and Edward Teller - BET, which was published in 1938 in the Journal of the American Chemical Society (ACS Publications). To view the article, please click [here](#) (Asia University, 2012).

### **Dubinin-Radushkevich isotherm derivation**

The derivation of the Dubinin-Radushkevich isotherm can be retrieved from the article by Dubinin (1960). The name of the article is the potential theory of adsorption of gases and vapors for adsorbents with energetically nonuniform surfaces, and was published in the ACS Publications.

### Appendix 3: BET and proximate analysis methodology

#### BET Analysis Methodology

The BET analysis entails determining the surface area and the micropore volume of the coal sample. This is required for determining storage potential of an adsorbate. The geometry of the sample can be characterised by determining specific surface area, pore size distribution, specific pore volume, particle size distribution and density (Keller and Robens, 2003). The determination of the surface area was conducted at the North-West University (Potchefstroom Campus), using a Micromeritics ASAP2020 BET analyser. The equipment consists of a sample tube which is maintained at 273.15 K (0°C) for the adsorption tests. Carbon dioxide gas was introduced into the adsorption system and the isotherm plotted by the software. The isotherm was then used to determine the micropore surface area.

The surface area of coal particles is a product of the monolayer capacity and the area occupied by a single adsorbed molecule. The monolayer capacity is the number of molecules necessary to cover the surface of the adsorbent with a complete monolayer (Karr, 1978). The monolayer capacity was determined by the Dubin-Radushkevich (D-B) equation. This equation was found to be more appropriate compared with the BET equation because it is based on the adsorption of CO<sub>2</sub>; therefore it is expected to yield results which relate well with the adsorption measurements since the adsorbate is the same. The D-B surface area was determined from CO<sub>2</sub> adsorption isotherms measured at 273 K.

$$\begin{aligned} \log V & \\ &= \log V_0 \\ &- 0.434 \frac{BT^2}{\beta^2} \left[ \log \left( \frac{P_{VAP}}{P} \right) \right]^2 \dots \dots \dots 3.01 \end{aligned}$$

Where:  $V$  is volume of gas adsorbed at equilibrium pressure  $p$ ,  $V_o$  is micropore capacity,  $P_{VAP}$  is saturation vapor pressure of the adsorbate,  $\beta$  is affinity coefficient of the adsorbate relative to  $CO_2$ , and  $B$  – constant which is a measure of the micropore size.

A plot of  $\log V$  and  $[\log (P_{VAP}/P)]^2$  results in the micropore capacity  $V_o$  at the intercept, which is multiplied by the cross-sectional area of an adsorbed molecule to give the micropore surface area. The cross sectional area of the adsorbed molecule is calculated by using the Emmet-Brunauer equation. This equation assumes hexagonal packing of close-packed spheres;

$$\sigma_m = 3.494 \times 10^{16} \left[ \sqrt{2} \frac{MN_A \rho_s}{4} \right]^{2/3} \dots \dots \dots 3.02$$

Where:  $M$  is molecular weight,  $N_A$  is Avogadro's number and  $\rho_s$  – density of adsorbed phase

#### Proximate Analysis

The proximate analysis for a coal sample is the determination of the moisture, volatile matter, fixed carbon and ash content of the sample. These properties are the mostly utilised in the coal trading industry and are described as follows:

- moisture analysis involves the determination of the surface and inherent moisture,
- the volatile matter content involves determination of the volatile gases in coal,
- fixed carbon indicates the approximate carbon content,

- ash content indicates the amount of non-combustible material in coal.

To this end, a Perkin Elmer STA600 thermogravimetric analyzer (TGA) was used for the proximate analysis. The used TGA is installed with Pyris software and housed in the coal lab at Wits.

Thermogravimetric analysis is an analytical technique which is utilised to determine a material's fraction of volatile and combustible components by monitoring its weight change, as the sample is heated in an inert or oxidizing atmosphere. This method relies heavily upon high degree of precision for mass and temperature change measurements. The Perkin Elmer ST600 analyser that was used consists of a high-precision balance with a platinum weighing pan. The pan is placed in a small electrically heated oven with a thermocouple to accurately measure the temperature. The equipment has a built-in mass flow controller, with inputs for two different gases which allows for automatic switching between nitrogen and oxygen. The following in-house procedure was loaded onto the computer for the determination of moisture, volatile matter, fixed carbon and ash.

A 15 mg sample with particle size of +300  $\mu\text{m}$  to -600  $\mu\text{m}$  was placed in the sample cup, at a temperature of 30 °C under an inert atmosphere; nitrogen was used as the inert gas.

#### **Appendix 4: Adsorption Experiment Script for a Single Pressure Set**

display\_message, Initialising

set\_v1, O //close v1

set\_v2, O //close v2

set\_v3, O //close v3

wait, 20 // 20 seconds

display\_message, Filling the Reference Cell

set\_v1, C //open v1

wait, 60

set\_v1, C //open v1

wait, 30

start\_logging

wait, 30

display\_message, Expansion of the Gas

wait, 30

set\_v2, C

wait, 60

set\_v2, 0

display\_message, Run in Progress for 30 min

wait, 1800

stop\_logging

display\_message, Stopped logging

wait, 30

display\_message, Run is complete move to the next one

**\*\*Note: removing // and all after it and copying this code will make the code**

## Appendix 5: Density of the Bulk Gas at 27 °C

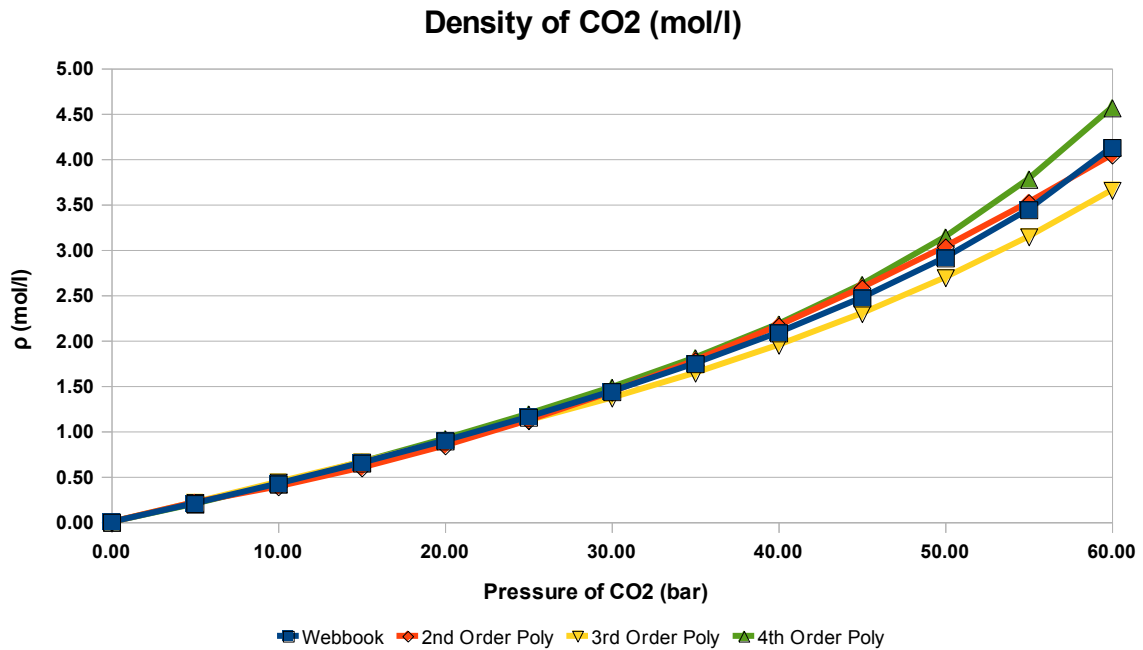


Figure A5.1: Density of CO<sub>2</sub>

Table A5.2: Density of CO<sub>2</sub>

Pressure - Density				
P (bar)	$\rho$ (mol/l)			
	Webbook	2 <sup>nd</sup> Order Poly	3 <sup>rd</sup> Order Poly	4 <sup>th</sup> Order Poly
0	0	0	0	0
5	0.20542	0.2167	0.21615	0.1992875
10	0.42191	0.3897	0.4414	0.4206
15	0.65111	0.5977	0.66165	0.6612875
20	0.89507	0.8407	0.8844	0.9176
25	1.1564	1.1187	1.11715	1.1902875
30	1.4387	1.4317	1.3674	1.4846
35	1.7467	1.7797	1.64265	1.8102875
40	2.0872	2.1627	1.9504	2.1816
45	2.4702	2.5807	2.29815	2.6172875
50	2.9124	3.0337	2.6934	3.1406
55	3.4436	3.5217	3.14365	3.7792875
60	4.1289	4.0447	3.6564	4.5656
Average	1.6582776923	1.6706461538	1.5440615385	1.7667942308
Deviation	0.00%	0.75%	6.89%	6.54%



## Appendix 6: Example of the independent two-sample T-TEST

Note the symbol  $\mu$  is the mean in this case. This case is quoted exactly from (Choudhury, 2009).

### Hypothesis Testing

Generally speaking, this test includes testing the null hypothesis  $H_0: \mu(x) = \mu(y)$  against the alternative research hypothesis,  $H_1: \mu(x) \neq \mu(y)$  where  $\mu(x)$  and  $\mu(y)$  are respectively the population mean of the two populations from which the two samples have been drawn. Hypothesis testing is frequently used for the scientific method.

### An Example

Imagine that a school has two buildings – one for girls and the other for boys. Suppose that the principal want to know if the pupils of the two buildings are working equally hard, in the sense that they put in equal number of hours in studies on the average.

Statistically speaking, the principle is interested in testing whether the average number of hours studied by boys is significantly different from the average for girls.

### Steps

To calculate, we begin by specifying the hypothesis to be tested.

In this case, the null hypothesis would be  $H_0: \mu(\text{boys}) = \mu(\text{girls})$ , which essentially states that mean study hours for boys and girls are no different.

The alternative research hypothesis is  $H_1: \mu(\text{boys}) \neq \mu(\text{girls})$ .

In the second step, we take a sample of say 10 students from the boy's building and 15 from girl's building and collect data on how long they study daily. These 10 and 15 different study hours are our two samples.

It is not difficult to see that the two samples have been drawn independent of each other – an essential requirement of the independent two-sample T-TEST.

Suppose that the sample mean turns out to be 7.25 hours for boys and 8.5 for girls. We cannot infer anything directly from these sample means - specifically as to whether boys and girls were equally hard working as it could very well have happened by sheer luck (even though the samples were drawn randomly) that boys included in the boy's sample were those who studied fewer hours.

On the other hand, it could also be the case that girls were indeed working harder than boys.

The third step would involve performing the independent two-sample T-TEST which helps us to either accept or reject the null hypothesis.

If the null hypothesis is rejected, it means that two buildings were significantly different in terms of number of hours of hard work.

On the other hand if the null hypothesis is accepted, one can conclude that there is no evidence to suggest that the two buildings differed significantly and that boys and girls can be said to be at par.

Assumption

Along with the independent single sample T-TEST, this test is one of the most widely tests. However, this test can be used only if the background assumptions are satisfied.

The populations from which the samples have been drawn should be normal – appropriate statistical methods exist for testing this assumption (For example, the Kolmogorov Smirnov non-parametric test). One needs to note that the normality assumption has to be tested individually and separately for the two samples. It has however been shown that minor departures from normality do not affect this test – this is indeed an advantage.

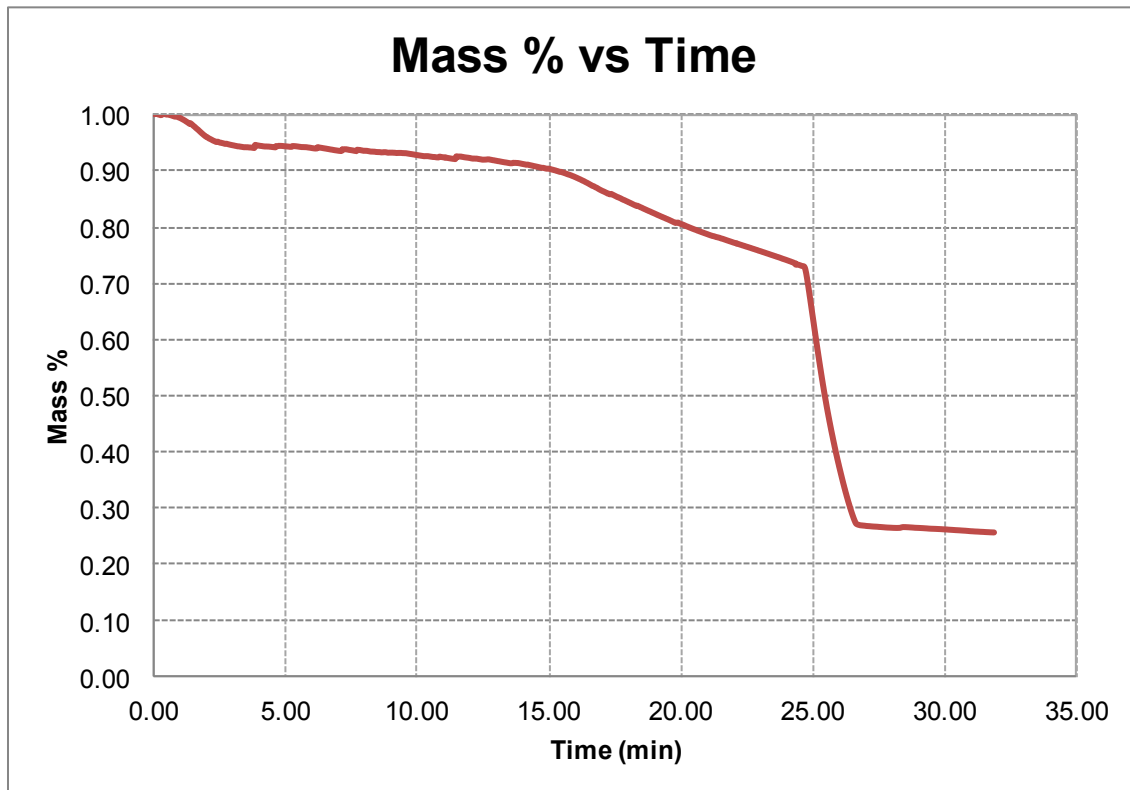
The standard deviation of the populations should be equal i.e.  $\sigma_X^2 = \sigma_Y^2 = \sigma^2$ , where  $\sigma^2$  is unknown. This assumption can be tested by the F-test.

Table A6.1: Student t-table

dfp	0.4	0.25	0.1	0.05	0.025	0.01	0.005	0.0005
1	0.32492		3.077684	6.313752	12.7062	31.82052	63.65674	636.6192
2	0.288675	0.816497	1.885618	2.919986	4.30265	6.96456	9.92484	31.5991
3	0.276671	0.764892	1.637744	2.353363	3.18245	4.5407	5.84091	12.924
4	0.270722	0.740697	1.533206	2.131847	2.77645	3.74695	4.60409	8.6103
5	0.267181	0.726687	1.475884	2.015048	2.57058	3.36493	4.03214	6.8688
6	0.264835	0.717558	1.439756	1.94318	2.44691	3.14267	3.70743	5.9588
7	0.263167	0.711142	1.414924	1.894579	2.36462	2.99795	3.49948	5.4079
8	0.261921	0.706387	1.396815	1.859548	2.306	2.89646	3.35539	5.0413
9	0.260955	0.702722	1.383029	1.833113	2.26216	2.82144	3.24984	4.7809
10	0.260185	0.699812	1.372184	1.812461	2.22814	2.76377	3.16927	4.5869
11	0.259556	0.697445	1.36343	1.795885	2.20099	2.71808	3.10581	4.437
12	0.259033	0.695483	1.356217	1.782288	2.17881	2.681	3.05454	4.3178
13	0.258591	0.693829	1.350171	1.770933	2.16037	2.65031	3.01228	4.2208
14	0.258213	0.692417	1.34503	1.76131	2.14479	2.62449	2.97684	4.1405
15	0.257885	0.691197	1.340606	1.75305	2.13145	2.60248	2.94671	4.0728
16	0.257599	0.690132	1.336757	1.745884	2.11991	2.58349	2.92078	4.015
17	0.257347	0.689195	1.333379	1.739607	2.10982	2.56693	2.89823	3.9651
18	0.257123	0.688364	1.330391	1.734064	2.10092	2.55238	2.87844	3.9216
19	0.256923	0.687621	1.327728	1.729133	2.09302	2.53948	2.86093	3.8834
20	0.256743	0.686954	1.325341	1.724718	2.08596	2.52798	2.84534	3.8495
21	0.25658	0.686352	1.323188	1.720743	2.07961	2.51765	2.83136	3.8193
22	0.256432	0.685805	1.321237	1.717144	2.07387	2.50832	2.81876	3.7921
23	0.256297	0.685306	1.31946	1.713872	2.06866	2.49987	2.80734	3.7676
24	0.256173	0.68485	1.317836	1.710882	2.0639	2.49216	2.79694	3.7454
25	0.25606	0.68443	1.316345	1.708141	2.05954	2.48511	2.78744	3.7251
26	0.255955	0.684043	1.314972	1.705618	2.05553	2.47863	2.77871	3.7066
27	0.255858	0.683685	1.313703	1.703288	2.05183	2.47266	2.77068	3.6896
28	0.255768	0.683353	1.312527	1.701131	2.04841	2.46714	2.76326	3.6739
29	0.255684	0.683044	1.311434	1.699127	2.04523	2.46202	2.75639	3.6594
30	0.255605	0.682756	1.310415	1.697261	2.04227	2.45726	2.75	3.646
inf	0.253347	0.67449	1.281552	1.644854	1.95996	2.32635	2.57583	3.2905

## Appendix 7: Proximate Analysis

Table A7.1: Proximate analysis of coal



## Appendix 8: Results Data of the Generated Isotherms

### Isotherms

Run	Isotherm	1	2	3	4	5	Deviations	MIN	MAX
1 20110222	P (bar)/P <sub>VAP</sub> (bar)	0.136	0.294	0.444	0.594	0.698		0.136	0.698
	N <sub>EXC</sub> (mmol/g)	0.095	0.119	0.076	0.230	0.310	0.00%	0.076	0.310
	N <sub>LAN</sub> (mmol/g)	0.059	0.073	0.078	0.081	0.083	54.86%	0.059	0.083
	N <sub>BET</sub> (mmol/g)	0.056	0.094	0.132	0.193	0.267	10.52%	0.056	0.267
	N <sub>D-R</sub> (mmol/g)	0.011	0.034	0.063	0.097	0.123	60.56%	0.011	0.123
2 20110225	P (bar)/P <sub>VAP</sub> (bar)	0.143	0.291	0.443	0.600	0.698		0.143	0.698
	N <sub>EXC</sub> (mmol/g)	0.279	0.742	1.036	1.803	1.874	0.00%	0.279	1.874
	N <sub>LAN</sub> (mmol/g)	-0.010	-0.009	-0.009	-0.009	-0.009	100.82%	-0.010	-0.009
	N <sub>BET</sub> (mmol/g)	0.342	0.636	0.988	1.542	2.153	1.27%	0.342	2.153
	N <sub>D-R</sub> (mmol/g)	0.079	0.305	0.677	1.201	1.603	32.59%	0.079	1.603
3 20110228	P (bar)/P <sub>VAP</sub> (bar)	0.138	0.294	0.446	0.597	0.710		0.138	0.710
	N <sub>EXC</sub> (mmol/g)	0.293	0.383	0.311	0.635	0.689	0.00%	0.293	0.689
	N <sub>LAN</sub> (mmol/g)	0.072	0.077	0.079	0.080	0.081	83.14%	0.072	0.081
	N <sub>BET</sub> (mmol/g)	0.301	0.318	0.390	0.525	0.723	2.31%	0.301	0.723
	N <sub>D-R</sub> (mmol/g)	0.001	0.012	0.038	0.085	0.137	88.15%	0.001	0.137
4 20110301	P (bar)/P <sub>VAP</sub> (bar)	0.141	0.296	0.445	0.593	0.691		0.141	0.691
	N <sub>EXC</sub> (mmol/g)	0.338	0.278	0.517	1.175	1.236	0.00%	0.278	1.236
	N <sub>LAN</sub> (mmol/g)	0.032	0.033	0.034	0.034	0.034	95.31%	0.032	0.034
	N <sub>BET</sub> (mmol/g)	0.199	0.386	0.598	0.916	1.272	4.84%	0.199	1.272
	N <sub>D-R</sub> (mmol/g)	0.069	0.224	0.429	0.677	0.863	36.14%	0.069	0.863
5 20110302	P (bar)/P <sub>VAP</sub> (bar)	0.139	0.288	0.453	0.605	0.687		0.139	0.687
	N <sub>EXC</sub> (mmol/g)	0.259	0.303	0.439	0.758	0.816	0.00%	0.259	0.816
	N <sub>LAN</sub> (mmol/g)	0.029	0.031	0.032	0.032	0.032	93.95%	0.029	0.032
	N <sub>BET</sub> (mmol/g)	0.225	0.332	0.467	0.670	0.857	0.92%	0.225	0.857
	N <sub>D-R</sub> (mmol/g)	0.004	0.022	0.070	0.145	0.200	82.85%	0.004	0.200
6 20110308	P (bar)/P <sub>VAP</sub> (bar)	0.155	0.304	0.444	0.586	0.679		0.155	0.679
	N <sub>EXC</sub> (mmol/g)	0.315	0.066	0.104	0.272	0.432	0.00%	0.066	0.432
	N <sub>LAN</sub> (mmol/g)	-0.731	-0.908	-0.986	-1.032	-1.054	496.10%	-1.054	-0.731
	N <sub>BET</sub> (mmol/g)	0.055	0.104	0.158	0.240	0.328	25.67%	0.055	0.328
	N <sub>D-R</sub> (mmol/g)	3.604	3.546	3.514	3.491	3.478	1383.00%	3.478	3.604
7 20110310	P (bar)/P <sub>VAP</sub> (bar)	0.136	0.294	0.439	0.587	0.702		0.136	0.702
	N <sub>EXC</sub> (mmol/g)	0.115	0.398	0.675	0.287	0.711	0.00%	0.115	0.711
	N <sub>LAN</sub> (mmol/g)	-0.003	-0.003	-0.003	-0.003	-0.003	100.58%	-0.003	-0.003
	N <sub>BET</sub> (mmol/g)	0.213	0.259	0.325	0.441	0.610	15.49%	0.213	0.610
	N <sub>D-R</sub> (mmol/g)	0.017	0.066	0.137	0.230	0.317	64.93%	0.017	0.317
8 20110311	P (bar)/P <sub>VAP</sub> (bar)	0.149	0.311	0.435	0.575	0.718		0.149	0.718
	N <sub>EXC</sub> (mmol/g)	0.491	0.232	0.375	0.276	0.435	0.00%	0.232	0.491
	N <sub>LAN</sub> (mmol/g)	-0.251	-0.288	-0.299	-0.307	-0.312	180.46%	-0.312	-0.251
	N <sub>BET</sub> (mmol/g)	1.169	0.256	0.257	0.308	0.438	34.25%	0.256	1.169
	N <sub>D-R</sub> (mmol/g)	624.243	171.192	94.284	57.816	39.025	54426.67%	39.025	624.243
9 20110314	P (bar)/P <sub>VAP</sub> (bar)	0.154	0.315	0.455	0.599	0.663		0.154	0.663
	N <sub>EXC</sub> (mmol/g)	0.130	0.147	0.437	0.571	0.535	0.00%	0.130	0.571
	N <sub>LAN</sub> (mmol/g)	0.004	0.004	0.004	0.004	0.004	98.83%	0.004	0.004
	N <sub>BET</sub> (mmol/g)	0.106	0.211	0.321	0.494	0.612	4.13%	0.106	0.612
	N <sub>D-R</sub> (mmol/g)	0.021	0.069	0.126	0.197	0.233	64.51%	0.021	0.233
10 20110315	P (bar)/P <sub>VAP</sub> (bar)	0.151	0.299	0.447	0.594	0.684		0.151	0.684
	N <sub>EXC</sub> (mmol/g)	0.178	0.221	0.829	0.608	2.036	0.00%	0.178	2.036
	N <sub>LAN</sub> (mmol/g)	-0.004	-0.004	-0.004	-0.004	-0.004	100.48%	-0.004	-0.004
	N <sub>BET</sub> (mmol/g)	0.136	0.307	0.545	0.931	1.332	16.03%	0.136	1.332
	N <sub>D-R</sub> (mmol/g)	0.179	0.398	0.632	0.880	1.037	19.26%	0.179	1.037
11 20110316	P (bar)/P <sub>VAP</sub> (bar)	0.143	0.300	0.449	0.599	0.679		0.143	0.679
	N <sub>EXC</sub> (mmol/g)	0.115	0.074	0.096	0.167	0.224	0.00%	0.074	0.224
	N <sub>LAN</sub> (mmol/g)	0.118	0.152	0.166	0.174	0.177	16.75%	0.118	0.177
	N <sub>BET</sub> (mmol/g)	0.062	0.087	0.116	0.162	0.205	6.35%	0.062	0.205
	N <sub>D-R</sub> (mmol/g)	0.013	0.036	0.063	0.094	0.112	52.84%	0.013	0.112

## Parameters

Table A8.3: Parameters of the Langmuir, BET and D-R Model

Runs	1	2	3	4	5	6	7	8	9	10	11
Date	20110222	20110225	20110228	20110301	20110302	20110308	20110310	20110311	20110314	20110315	20110316
<b>Langmuir Isotherm</b>											
Intercept	5.2595	-0.3476	1.5741	0.8665	0.9794	7.0314	-0.5111	3.4378	0.3599	-0.2367	7.0453
Slope	57.2383	37.5383	18.8651	25.0803	30.1058	-5.8024	-1.7991	-10.3300	83.3198	64.7080	34.4404
$K_{LAN}$	0.1901	-2.8768	0.6353	1.1540	1.0210	0.1422	-1.9565	0.2909	2.7783	-4.2242	0.1419
$N_{mLAN}$	0.0919	-0.0093	0.0834	0.0345	0.0325	-1.2118	0.2841	-0.3328	0.0043	-0.0037	0.2046
<b>Dubinin-Radushkevich Isotherm</b>											
Intercept	-1.5682	1.1516	-1.0328	-0.5111	-0.6574	1.2372	-0.5111	3.0796	-0.7824	0.4767	-1.6459
Slope	-1.4791	-1.8935	-2.7761	-1.7991	-2.5290	0.0240	-1.7991	1.7643	-1.6416	-1.1597	-1.3955
$N_o$	-0.6377	0.8683	-0.9682	-1.9565	-1.5211	0.8083	-1.9565	0.3247	-1.2781	2.0979	-0.6076
$D_{D-R}$	1.0603	-0.6082	0.3720	0.2841	0.2600	51.5415	0.2841	1.7455	0.4766	-0.4110	1.1794
<b>BET Isotherm</b>											
Intercept	1.3835	0.3361	-0.1560	-0.0118	0.2517	2.4146	-0.0118	-1.3346	1.2540	1.2102	0.6430
Slope	10.4571	1.0587	4.9852	5.5149	3.3606	5.9532	5.5149	9.9522	2.9577	0.6060	14.2622
$C_{BET}$	8.5584	4.1500	-30.9542	-465.1888	14.3530	3.4655	-465.1888	-6.4573	3.3585	1.5008	23.1797
$N_{mBET}$	0.0845	0.7170	0.2071	0.1817	0.2768	0.1195	0.1817	0.1160	0.2374	0.5506	0.0671

## Appendix 9: The AUT isotherm results

Pressure	Absolute Isotherm	Excess Isotherm	Excess Isotherm
(bar)	(mmol/g)	(m <sup>3</sup> STP/g)	(g CO <sub>2</sub> per g coal)
0.0	0.0000	0.0	0.0000
4.1	0.2221	5.0	0.0098
8.8	0.3311	7.4	0.0146
13.6	0.4065	9.1	0.0179
18.1	0.4631	10.4	0.0204
22.5	0.5090	11.4	0.0224
26.6	0.5465	12.3	0.0241
30.6	0.5774	12.9	0.0254
34.3	0.6035	13.5	0.0266
37.8	0.6251	14.0	0.0275
41.1	0.6433	14.4	0.0283
58.0	0.6739	15.1	0.0297
68.4	0.6320	14.2	0.0278
74.2	0.5310	11.9	0.0234
77.3	0.3771	8.5	0.0166
79.2	0.8875	19.9	0.0391
80.0	1.5727	35.2	0.0692
80.6	2.1257	47.6	0.0936
81.5	1.6434	36.8	0.0723
83.1	1.1950	26.8	0.0526
85.9	0.9040	20.3	0.0398
90.6	0.7452	16.7	0.0328
99.2	0.6265	14.0	0.0276
108.2	0.5727	12.8	0.0252
137.1	0.4694	10.5	0.0207
169.5	0.4043	9.1	0.0178
199.2	0.3679	8.2	0.0162
224.0	0.3466	7.8	0.0153
243.3	0.3366	7.5	0.0148
257.9	0.3245	7.3	0.0143
268.8	0.3199	7.2	0.0141

## Appendix 10: Operational Procedure

1. Vacuum the sample cell
2. Set the oven to the desired isothermal conditions, noting that oven cannot cool and the minimum temperature is the atmospheric air temperature.
3. Load the sample cell with sample of desired.
4. Ensure that V1, V2 and V3 are closed.
5. The sample can also be degassed in order to unlock pores closed by pre-adsorbed material.
6. Vacuum the sample cell by opening V3 and other valve channelling the gas line to the vacuum pump. Then close V3. However, make sure that the sample is relieved to the atmosphere pressure of at most 1 bar before commencing the run. Note V1, V2 and V3 are valves are shown in Figure 3.05.
7. Fill the reference cell with the desired of gas by opening and closing V1 together with the manual valve position before in the line. Ensure that V1 is closed afterwards. Wait for at least 60 seconds. Record the condition in the LabVIEW display tab.
8. Then, open V2 or 30 seconds for the expansion of the gas. Then, close V2 and wait for 30 seconds. Record the condition in the LabVIEW display tab. Wait for whatever period of choice until pressure equilibrium is attained.
9. Then what? How do you depressurise and remove the sample?



## **Appendix 11: Documents about the VAS and Automatic Pump**

There are three files in the laboratory:

1. File 1 is a blue file bound by Chem Vac and contains the documents gathered during the construction of the VAS. One of the sections serve is operational manual
2. File 2 is thinner than File 1, it was bound by Teledyne Isco and contains the automatic pump's operational procedure.
3. File 3 contains LabVIEW graphical codes used to automatically operate the equipment

## Appendix 12: Runs

Isotherm Data

22. Feb. 2011

Experimental Data		
-------------------	--	--

(ton CO <sub>2</sub> /ton Coal)		
N <sub>ADS</sub>	P (bar)	N <sub>exc</sub>
0	0	0.00000
0.00194328	0.14	0.00191
0.00248553	0.29	0.00239
0.00162815	0.44	0.00152
0.00513121	0.59	0.00463
0.00712687	0.70	0.00624

Model Isotherms		
-----------------	--	--

LAN Isotherm (ton CO <sub>2</sub> /ton Coal)		
X <sub>LAN,LIN</sub>	Y <sub>LAN,LIN</sub>	N <sub>LAN</sub>
0	0	0
0.10729614	522.895837	0.00203336
0.04970179	417.826192	0.00412464
0.03299241	656.047308	0.0058788
0.02463054	215.808494	0.00746823
0.02095557	160.130517	0.0084753

LAN PARAMETERS	
Intercept	158.79855917
Slope	4329.4521795
K <sub>LAN</sub>	0.0062972864
N <sub>mLAN</sub>	0.0366786726

ρ (mol/l)	N <sub>bulk</sub>	N <sub>excess</sub>
		dP (bar)
0.3641	0.0095	0.0001
0.3608	0.0094	0.0900
0.8470	0.0221	0.0001
0.8428	0.0219	0.0800
1.4523	0.0378	0.0001
1.4496	0.0377	0.0400
2.2110	0.0576	0.0002
2.2029	0.0574	0.1000
2.8228	0.0735	0.0003
2.8119	0.0732	0.1200

D-R Isotherm (ton CO <sub>2</sub> /ton Coal)		
X <sub>D-R,LIN</sub>	Y <sub>D-R,LIN</sub>	N <sub>DR</sub>
0	0	0
-6.2593823	3.96876032	0.42431908
-6.0350655	1.49480713	0.52768838
-6.4862329	0.66074091	0.59264476
-5.3743914	0.27099243	0.64380982
-5.0759892	0.12887152	0.67396691

D-R PARAMETERS	
Intercept	-0.29287042
Slope	-0.283308045
N <sub>O</sub>	0.7461188168
D <sub>DR</sub>	0.2833080447

V <sub>REF</sub> (l)	0.0159746
V <sub>VOID</sub> (l)	0.0260389
P <sub>VAP</sub> (bar)	68.3292136
V <sub>SAMPLE</sub> (l)	0.0030941
V <sub>CELL</sub> (l)	0.029133
ρ <sub>ADS</sub> (mol/l)	22.7221086

BET Isotherm (ton CO <sub>2</sub> /ton Coal)		
X <sub>BET,LIN</sub>	Y <sub>BET,LIN</sub>	N <sub>BET</sub>
0	0	0
0.13639847	82.58692	0.00140467
0.29445678	174.378762	0.00203312
0.44358772	523.0196	0.00272217
0.59418216	315.978123	0.00383976
0.69838357	370.777285	0.0052325

BET PARAMETERS	
Intercept	32.327989485
Slope	587.34086147
C <sub>BET</sub>	19.168184005
N <sub>mBET</sub>	0.0016137652

## Experimental Data

(ton CO <sub>2</sub> /ton Coal)		
N <sub>ADS</sub>	P (bar)	N <sub>exc</sub>
0	0	0.00000
0.006007	0.14	0.00591
0.008014	0.29	0.00772
0.006692	0.45	0.00626
0.014176	0.60	0.01280
0.015901	0.71	0.01389

## Model Isotherms

LAN Isotherm (ton CO <sub>2</sub> /ton Coal)		
X <sub>LAN,LIN</sub>	Y <sub>LAN,LIN</sub>	N <sub>LAN</sub>
0	0	0
0.1058694	169.1537557	0.00567141
0.049619173	129.5514427	0.010183303
0.032725404	159.6814055	0.013380238
0.024477887	78.13796271	0.015802149
0.020587654	72.00264442	0.017277248

LAN PARAMETERS	
Intercept	47.42288698
Slope	1388.84842
K <sub>LAN</sub>	0.021086865
N <sub>mLAN</sub>	0.034145474

ρ (mol/l)	N <sub>bulk</sub>	N <sub>excess</sub>
		dP (bar)
0.3688	0.0096	0.0003
0.3585	0.0093	0.2779
0.8487	0.0221	0.0004
0.8352	0.0217	0.2584
1.4688	0.0382	0.0003
1.4578	0.0380	0.1637
2.2316	0.0581	0.0006
2.2092	0.0575	0.2754
2.9008	0.0755	0.0006
2.8766	0.0749	0.2637

D-R Isotherm (ton CO <sub>2</sub> /ton Coal)		
X <sub>D-R,LIN</sub>	Y <sub>D-R,LIN</sub>	N <sub>DR</sub>
0	0	0
-5.1308081	3.922554056	0.357242764
-4.86407804	1.495031807	0.467470242
-5.07318061	0.650424981	0.541875272
-4.35847602	0.266367209	0.600690289
-4.27670285	0.117669032	0.638739966

D-R PARAMETERS	
Intercept	-0.326531884
Slope	-0.354855977
N <sub>o</sub>	0.721421373
D <sub>DR</sub>	0.354855977

V <sub>REF</sub> (l)	0.015975
V <sub>VOID</sub> (l)	0.026039
P <sub>VAP</sub> (bar)	68.44927
V <sub>SAMPLE</sub> (l)	0.003094
V <sub>CELL</sub> (l)	0.029133
ρ <sub>ADS</sub> (mol/l)	22.72211

BET Isotherm (ton CO <sub>2</sub> /ton Coal)		
X <sub>BET,LIN</sub>	Y <sub>BET,LIN</sub>	N <sub>BET</sub>
0	0	0
0.137994165	27.07897126	0.00544611
0.294429724	54.06094447	0.006240223
0.446422577	128.7722034	0.007807882
0.59683908	115.6753729	0.010625926
0.70961749	175.9552802	0.014691392

BET PARAMETERS	
Intercept	-3.664806489
Slope	239.5693424
C <sub>BET</sub>	-64.37025709
N <sub>mBET</sub>	0.004239003

## Experimental Data

(ton CO <sub>2</sub> /ton Coal)		
N <sub>ADS</sub>	P (bar)	N <sub>exc</sub>
0.00000	0	0.00000
0.00693	0.14	0.00682
0.00581	0.30	0.00560
0.01112	0.45	0.01042
0.02620	0.59	0.02370
0.02834	0.69	0.02493

## Model Isotherms

LAN Isotherm (ton CO <sub>2</sub> /ton Coal)		
X <sub>LAN,LIN</sub>	Y <sub>LAN,LIN</sub>	N <sub>LAN</sub>
0	0	0
0.10400535	146.59158	0.00466053
0.04946259	178.634776	0.00754122
0.03285874	96.0051932	0.00928907
0.02464402	42.1942083	0.0104922
0.02115628	40.1188161	0.01110275

LAN PARAMETERS	
Intercept	25.78665552
Slope	1502.732032
K <sub>LAN</sub>	0.038779748
N <sub>mLAN</sub>	0.01715985

ρ (mol/l)	N <sub>bulk</sub>	N <sub>excess</sub>
		dP (bar)
0.3751	0.0098	0.0003
0.3632	0.0095	0.3189
0.8521	0.0222	0.0003
0.8423	0.0219	0.1869
1.4605	0.0380	0.0005
1.4423	0.0376	0.2733
2.2092	0.0575	0.0011
2.1679	0.0564	0.5135
2.7818	0.0724	0.0011
2.7383	0.0713	0.4837

D-R Isotherm (ton CO <sub>2</sub> /ton Coal)		
X <sub>D-R,LIN</sub>	Y <sub>D-R,LIN</sub>	N <sub>DR</sub>
0	0	0
-4.9876504	3.84900459	0.26316499
-5.1853434	1.48513776	0.36078206
-4.5644023	0.65555507	0.42918605
-3.742283	0.27246295	0.48493253
-3.6918455	0.13644323	0.51738441

D-R PARAMETERS	
Intercept	-0.50216957
Slope	-0.424491381
N <sub>O</sub>	0.605216175
D <sub>DR</sub>	0.424491381

V <sub>REF</sub> (l)	0.015975
V <sub>VOID</sub> (l)	0.026039
P <sub>VAP</sub> (bar)	68.38825
V <sub>SAMPLE</sub> (l)	0.003094
V <sub>CELL</sub> (l)	0.029133
ρ <sub>ADS</sub> (mol/l)	22.72211

BET Isotherm (ton CO <sub>2</sub> /ton Coal)		
X <sub>BET,LIN</sub>	Y <sub>BET,LIN</sub>	N <sub>BET</sub>
0	0	0
0.14059273	23.9813077	0.00555652
0.29562537	74.9728462	0.00891003
0.44500776	76.9795566	0.01250453
0.59334466	61.5649313	0.01800837
0.69116118	89.7832982	0.02428141

BET PARAMETERS	
Intercept	13.42416707
Slope	113.9277493
C <sub>BET</sub>	9.486764858
N <sub>mBET</sub>	0.007852257

## Experimental Data

(ton CO <sub>2</sub> /ton Coal)		
N <sub>ADS</sub>	P (bar)	N <sub>exc</sub>
0	0	0.00000
0.005301	0.14	0.00522
0.006334	0.29	0.00611
0.009453	0.45	0.00884
0.016926	0.60	0.01528
0.01867	0.69	0.01646

## Model Isotherms

LAN Isotherm (ton CO <sub>2</sub> /ton Coal)		
X <sub>LAN,LIN</sub>	Y <sub>LAN,LIN</sub>	N <sub>LAN</sub>
0	0	0
0.10590707	191.666861	0.00401826
0.05125839	163.664594	0.00659021
0.03256141	113.070212	0.00843801
0.02440632	65.4617777	0.00961373
0.02149484	60.7439966	0.010117

LAN PARAMETERS	
Intercept	29.3068902686
Slope	1777.23379976
K <sub>LAN</sub>	0.0341216687
N <sub>mLAN</sub>	0.0164901716

p (mol/l)	N <sub>bulk</sub>	N <sub>excess</sub>
		dP (bar)
0.3687	0.0096	0.0002
0.3596	0.0094	0.2451
0.8153	0.0212	0.0003
0.8046	0.0210	0.2080
1.4791	0.0385	0.0004
1.4636	0.0381	0.2306
2.2413	0.0584	0.0007
2.2146	0.0577	0.3282
2.7150	0.0707	0.0007
2.6862	0.0699	0.3228

D-R Isotherm (ton CO <sub>2</sub> /ton Coal)		
X <sub>D-R,LIN</sub>	Y <sub>D-R,LIN</sub>	N <sub>DR</sub>
0	0	0
-5.2557588	3.88274723	0.27594069
-5.0978192	1.5494925	0.36963914
-4.728009	0.62573576	0.44377649
-4.1814664	0.25275627	0.49842694
-4.1066683	0.14116515	0.5245972

D-R PARAMETERS	
Intercept	-0.4937659421
Slope	-0.4028500091
N <sub>0</sub>	0.6103236175
D <sub>DR</sub>	0.4028500091

V <sub>REF</sub> (l)	0.015975
V <sub>VOID</sub> (l)	0.026039
P <sub>VAP</sub> (bar)	67.739
V <sub>SAMPLE</sub> (l)	0.003094
V <sub>CELL</sub> (l)	0.029133
p <sub>ADS</sub> (mol/l)	22.72211

BET Isotherm (ton CO <sub>2</sub> /ton Coal)		
X <sub>BET,LIN</sub>	Y <sub>BET,LIN</sub>	N <sub>BET</sub>
0	0	0
0.1393915	31.0440002	0.00525428
0.2880025	66.2022152	0.0070393
0.45337548	93.781491	0.00952201
0.60486577	100.207944	0.01339769
0.68679495	133.199223	0.01700601

BET PARAMETERS	
Intercept	5.8415470524
Slope	179.239633192
C <sub>BET</sub>	31.6835897382
N <sub>mBET</sub>	0.0054030345

## Experimental Data

(ton CO <sub>2</sub> /ton Coal)		
N <sub>ADS</sub>	P (bar)	N <sub>exc</sub>
0	0	0.00000
0.006461	0.15	0.00635
0.001393	0.30	0.00134
0.002235	0.44	0.00209
0.006078	0.59	0.00549
0.009895	0.68	0.00871

## Model Isotherms

LAN Isotherm (ton CO <sub>2</sub> /ton Coal)		
X <sub>LAN,LIN</sub>	Y <sub>LAN,LIN</sub>	N <sub>LAN</sub>
0	0	0
0.09367418	157.58473	0.00457022
0.04766081	747.271517	0.00856105
0.03264549	478.33231	0.01197273
0.02475768	182.038682	0.01514281
0.02136661	114.835493	0.01708793

LAN PARAMETERS	
Intercept	198.69140315
Slope	2216.7366059
K <sub>LAN</sub>	0.0050329304
N <sub>mLAN</sub>	0.0896323914

ρ (mol/l)	N <sub>bulk</sub>	N <sub>excess</sub>
		dP (bar)
0.4157	0.0108	0.0003
0.4047	0.0105	0.2851
0.8925	0.0232	0.0001
0.8902	0.0232	0.0437
1.4738	0.0384	0.0001
1.4701	0.0383	0.0545
2.1942	0.0571	0.0002
2.1846	0.0569	0.1190
2.7399	0.0713	0.0004
2.7247	0.0709	0.1698

D-R Isotherm (ton CO <sub>2</sub> /ton Coal)		
X <sub>D-R,LIN</sub>	Y <sub>D-R,LIN</sub>	N <sub>DR</sub>
0	0	0
-5.0599633	3.48098768	0.76877556
-6.6164286	1.41616501	0.87655428
-6.1703057	0.65873466	0.94338174
-5.2042192	0.28628258	0.99542649
-4.7435006	0.15034792	1.02430846

D-R PARAMETERS	
Intercept	0.0993044875
Slope	-0.194164564
N <sub>O</sub>	1.1044025252
D <sub>DR</sub>	0.194164564

V <sub>REF</sub> (l)	0.015975
V <sub>VOID</sub> (l)	0.026039
P <sub>VAP</sub> (bar)	68.97011
V <sub>SAMPLE</sub> (l)	0.003094
V <sub>CELL</sub> (l)	0.029133
ρ <sub>ADS</sub> (mol/l)	22.72211

BET Isotherm (ton CO <sub>2</sub> /ton Coal)		
X <sub>BET,LIN</sub>	Y <sub>BET,LIN</sub>	N <sub>BET</sub>
0	0	0
0.15478155	28.8578752	0.00154283
0.30421295	326.723064	0.00240139
0.44413589	382.187919	0.00330969
0.58563777	257.283898	0.00468888
0.67858384	242.444279	0.00619412

BET PARAMETERS	
Intercept	53.050106979
Slope	424.11033818
C <sub>BET</sub>	8.9945237123
N <sub>mBET</sub>	0.0020957311

Experimental Data		
(ton CO2/ton Coal)		
N <sub>ADS</sub>	P (bar)	N <sub>exc</sub>
0	0	0.00000
0.002348	0.14	0.00231
0.008334	0.29	0.00803
0.014524	0.44	0.01362
0.006398	0.59	0.00578
0.016393	0.70	0.01434

Model Isotherms		
LAN Isotherm (ton CO <sub>2</sub> /ton Coal)		
X <sub>LAN,LIN</sub>	Y <sub>LAN,LIN</sub>	N <sub>LAN</sub>
0	0	0
0.10707613	432.82006	-0.0043682
0.04944351	124.594479	-0.0022132
0.03312037	73.4437838	-0.0019418
0.02478597	172.896152	-0.0018275
0.0207379	69.7256735	-0.0017766

LAN PARAMETERS	
Intercept	-6.0145227831
Slope	3867.8018718403
K <sub>LAN</sub>	-0.1662642301
N <sub>mLAN</sub>	-0.0015550235

ρ (mol/l)	N <sub>bulk</sub>	N <sub>excess</sub> dP (bar)
0.3648	0.0095	0.0001
0.3608	0.0094	0.1087
0.8525	0.0222	0.0004
0.8385	0.0218	0.2682
1.4445	0.0376	0.0006
1.4207	0.0370	0.3594
2.1905	0.0570	0.0003
2.1804	0.0568	0.1254
2.8685	0.0747	0.0007
2.8435	0.0740	0.2738

D-R Isotherm (ton CO <sub>2</sub> /ton Coal)		
X <sub>D-R,LIN</sub>	Y <sub>D-R,LIN</sub>	N <sub>DR</sub>
0	0	0
-6.0703221	3.98389825	0.23139668
-4.8250643	1.4963683	0.32004929
-4.2965203	0.67663613	0.378668
-5.1526911	0.2837782	0.42766144
-4.2445686	0.12559455	0.46089899

D-R PARAMETERS	
Intercept	-0.6258212586
Slope	-0.4197459491
N <sub>O</sub>	0.5348220209
D <sub>DR</sub>	0.4197459491

BET Isotherm (ton CO <sub>2</sub> /ton Coal)		
X <sub>BET,LIN</sub>	Y <sub>BET,LIN</sub>	N <sub>BET</sub>
0	0	0
0.13588172	68.0605118	0.0042727
0.29426889	51.9521932	0.00521049
0.43929727	57.5414594	0.00655072
0.58701297	245.751749	0.00888857
0.70159904	163.938699	0.0122983

BET PARAMETERS	
Intercept	-0.2772598938
Slope	272.887780241
C <sub>BET</sub>	-983.2309918028
N <sub>mBET</sub>	0.003668237

V <sub>REF</sub> (l)	0.015975
V <sub>VOID</sub> (l)	0.026039
P <sub>VAP</sub> (bar)	68.73
V <sub>SAMPLE</sub> (l)	0.003094
V <sub>CELL</sub> (l)	0.029133
ρ <sub>ADS</sub> (mol/l)	22.72211

## Experimental Data

(ton CO <sub>2</sub> /ton Coal)		
N <sub>ADS</sub>	P (bar)	N <sub>exc</sub>
0	0	0.00000
0.00267	0.15	0.00262
0.003092	0.32	0.00297
0.009416	0.46	0.00881
0.012732	0.60	0.01151
0.01215	0.66	0.01079

## Model Isotherms

LAN Isotherm (ton CO <sub>2</sub> /ton Coal)		
X <sub>LAN,LIN</sub>	Y <sub>LAN,LIN</sub>	N <sub>LAN</sub>
0	0	0
0.0964376	381.23735	0.001214
0.047004	336.75008	0.0016302
0.0325615	113.51241	0.0018118
0.0247348	86.8661	0.0019281
0.0223586	92.653724	0.0019664

LAN PARAMETERS	
Intercept	10.2924910648
Slope	4254.9517412657
K <sub>LAN</sub>	0.0971582092
N <sub>mLAN</sub>	0.0024189443

ρ (mol/l)	N <sub>bulk</sub>	N <sub>excess</sub>
		dP (bar)
0.4039	0.0105	0.0001
0.3993	0.0104	0.1188
0.9083	0.0236	0.0001
0.9031	0.0235	0.0963
1.4791	0.0385	0.0004
1.4637	0.0381	0.2297
2.1972	0.0572	0.0005
2.1771	0.0567	0.2495
2.5568	0.0666	0.0005
2.5380	0.0661	0.2176

D-R Isotherm (ton CO <sub>2</sub> /ton Coal)		
X <sub>D-R,LIN</sub>	Y <sub>D-R,LIN</sub>	N <sub>DR</sub>
0	0	0
-5.9434222	3.5061364	0.3030296
-5.819341	1.3312634	0.3912041
-4.7319122	0.6189016	0.4457194
-4.4643679	0.2619211	0.4914651
-4.5288691	0.168743	0.5094256

D-R PARAMETERS	
Intercept	-0.5284873405
Slope	-0.3553798129
N <sub>O</sub>	0.5894960023
D <sub>DR</sub>	0.3553798129

V <sub>REF</sub> (l)	0.015975
V <sub>VOID</sub> (l)	0.026039
P <sub>VAP</sub> (bar)	67.44599
V <sub>SAMPLE</sub> (l)	0.003094
V <sub>CELL</sub> (l)	0.029133
ρ <sub>ADS</sub> (mol/l)	22.72211

BET Isotherm (ton CO <sub>2</sub> /ton Coal)		
X <sub>BET,LIN</sub>	Y <sub>BET,LIN</sub>	N <sub>BET</sub>
0	0	0
0.1537438	69.261364	0.0030282
0.3154346	155.16798	0.0048637
0.4553436	94.89863	0.0066988
0.5994263	129.98812	0.0096071
0.6631306	182.38972	0.011617

BET PARAMETERS	
Intercept	26.9574915848
Slope	214.8806234177
C <sub>BET</sub>	8.9710911804
N <sub>mBET</sub>	0.0041349975



## Experimental Data

(ton CO <sub>2</sub> /ton Coal)		
N <sub>ADS</sub>	P (bar)	N <sub>exc</sub>
0	0	0.00000
0.003643	0.15	0.00358
0.004637	0.30	0.00446
0.017832	0.45	0.01672
0.013539	0.59	0.01225
0.046432	0.68	0.04106

## Model Isotherms

LAN Isotherm (ton CO <sub>2</sub> /ton Coal)		
X <sub>LAN,LIN</sub>	Y <sub>LAN,LIN</sub>	N <sub>LAN</sub>
0	0	0
0.0980334	279.28699	-0.0065447
0.0493084	224.03101	-0.0032753
0.033043	59.816316	-0.0028072
0.0248571	81.619226	-0.0026188
0.0215733	24.353828	-0.0025502

LAN PARAMETERS	
Intercept	-6.8097956859
Slope	3130.1521842855
K <sub>LAN</sub>	-0.1468472838
N <sub>mLAN</sub>	-0.0021755478

ρ (mol/l)	N <sub>bulk</sub>	N <sub>excess</sub>
		dP (bar)
0.3974	0.0103	0.0002
0.3911	0.0102	0.1633
0.8554	0.0223	0.0002
0.8476	0.0221	0.1487
1.4492	0.0377	0.0008
1.4200	0.0370	0.4410
2.1812	0.0568	0.0006
2.1598	0.0562	0.2665
2.6999	0.0703	0.0019
2.6282	0.0684	0.8104

D-R Isotherm (ton CO <sub>2</sub> /ton Coal)		
X <sub>D-R,LIN</sub>	Y <sub>D-R,LIN</sub>	N <sub>DR</sub>
0	0	0
-5.6322399	3.585837	0.2320574
-5.4117845	1.4554429	0.3131769
-4.0912785	0.649848	0.3729279
-4.4020648	0.2719249	0.4222366
-3.192689	0.1442299	0.4491579

D-R PARAMETERS	
Intercept	-0.6347108825
Slope	-0.4362306765
N <sub>O</sub>	0.5300887241
D <sub>DR</sub>	0.4362306765

V <sub>REF</sub> (l)	0.015975
V <sub>VOID</sub> (l)	0.026039
P <sub>VAP</sub> (bar)	67.76712
V <sub>SAMPLE</sub> (l)	0.003094
V <sub>CELL</sub> (l)	0.029133
ρ <sub>ADS</sub> (mol/l)	22.72211

BET Isotherm (ton CO <sub>2</sub> /ton Coal)		
X <sub>BET,LIN</sub>	Y <sub>BET,LIN</sub>	N <sub>BET</sub>
0	0	0
0.1505243	49.488742	0.0043058
0.2992675	95.678749	0.0077623
0.4465823	48.268984	0.011737
0.5936507	119.24053	0.0177162
0.6840146	52.718798	0.0238174

BET PARAMETERS	
Intercept	27.1201130948
Slope	93.2251399194
C <sub>BET</sub>	4.4374908244
N <sub>mBET</sub>	0.0083094262

## Experimental Data

(ton CO <sub>2</sub> /ton Coal)		
N <sub>ADS</sub>	P (bar)	N <sub>exc</sub>
0	0	0.00000
0.00235	0.14	0.00231
0.001541	0.30	0.00148
0.002067	0.45	0.00193
0.003725	0.60	0.00336
0.005122	0.68	0.00452

## Model Isotherms

LAN Isotherm (ton CO <sub>2</sub> /ton Coal)		
X <sub>LAN,LIN</sub>	Y <sub>LAN,LIN</sub>	N <sub>LAN</sub>
0	0	0
0.1033119	432.73645	0.0024033
0.0492502	674.40018	0.0048072
0.0328265	517.00483	0.0069057
0.0246502	297.35314	0.0088231
0.0217314	221.17785	0.0097938

LAN PARAMETERS	
Intercept	208.43844202
Slope	3848.8213436
K <sub>LAN</sub>	0.0047975795
N <sub>mLAN</sub>	0.0541564348

ρ (mol/l)	N <sub>bulk</sub>	N <sub>excess</sub>
		dP (bar)
0.3776	0.0098	0.0001
0.3735	0.0097	0.1073
0.8566	0.0223	0.0001
0.8540	0.0222	0.0493
1.4625	0.0381	0.0001
1.4591	0.0380	0.0506
2.2084	0.0575	0.0002
2.2025	0.0574	0.0726
2.6700	0.0695	0.0002
2.6621	0.0693	0.0892

D-R Isotherm (ton CO <sub>2</sub> /ton Coal)		
X <sub>D-R,LIN</sub>	Y <sub>D-R,LIN</sub>	N <sub>DR</sub>
0	0	0
-6.0701289	3.7877531	0.5382044
-6.5138237	1.4529302	0.6432292
-6.2480522	0.639518	0.7091848
-5.6949205	0.2634239	0.7597903
-5.3989671	0.1499395	0.7831841

D-R PARAMETERS	
Intercept	-0.1512136006
Slope	-0.240622607
N <sub>0</sub>	0.8596640543
D <sub>DR</sub>	0.240622607

V <sub>REF</sub> (l)	0.015975
V <sub>VOID</sub> (l)	0.026039
P <sub>VAP</sub> (bar)	67.77667
V <sub>SAMPLE</sub> (l)	0.003094
V <sub>CELL</sub> (l)	0.029133
ρ <sub>ADS</sub> (mol/l)	22.72211

BET Isotherm (ton CO <sub>2</sub> /ton Coal)		
X <sub>BET,LIN</sub>	Y <sub>BET,LIN</sub>	N <sub>BET</sub>
0	0	0
0.1428136	72.097091	0.0013848
0.2995795	288.45021	0.0018094
0.4494644	422.0894	0.0023502
0.5985481	443.34121	0.003257
0.6789416	467.7243	0.004088

BET PARAMETERS	
Intercept	14.561267942
Slope	740.46914716
C <sub>BET</sub>	51.85196908
N <sub>mBET</sub>	0.00132445

## Experimental Data

(ton CO <sub>2</sub> /ton Coal)		
N <sub>ADS</sub>	P (bar)	N <sub>exc</sub>
0	0	0.00000
0.005574	0.14	0.00548
0.006643	0.30	0.00640
0.009534	0.44	0.00893
0.015162	0.59	0.01370
0.018782	0.70	0.01646

## Model Isotherms

LAN Isotherm (ton CO <sub>2</sub> /ton Coal)		
X <sub>LAN,LIN</sub>	Y <sub>LAN,LIN</sub>	N <sub>LAN</sub>
0	0	0
0.10249645	182.365451	0.00432583
0.04913377	156.362296	0.00717779
0.03283987	112.017687	0.00898694
0.02461984	72.9852376	0.01029614
0.02088184	60.752636	0.01102661

LAN PARAMETERS	
Intercept	31.44042
Slope	1721.258
K <sub>LAN</sub>	0.031806
N <sub>mLAN</sub>	0.018266

ρ (mol/l)	N <sub>bulk</sub>	N <sub>excess</sub>
		dP (bar)
0.3805	0.0099	0.0002
0.3709	0.0097	0.2547
0.8592	0.0224	0.0003
0.8480	0.0221	0.2128
1.4616	0.0381	0.0004
1.4461	0.0377	0.2341
2.2124	0.0576	0.0006
2.1885	0.0570	0.2961
2.8381	0.0739	0.0007
2.8094	0.0732	0.3160

D-R Isotherm (ton CO <sub>2</sub> /ton Coal)		
X <sub>D-R,LIN</sub>	Y <sub>D-R,LIN</sub>	N <sub>DR</sub>
0	0	0
-5.2060126	3.8048949	0.30176832
-5.0521757	1.47703279	0.40076329
-4.7186568	0.66004119	0.46817062
-4.2902572	0.2749307	0.5232157
-4.1068105	0.12935938	0.55753955

D-R PARAMETERS	
Intercept	-0.445443
Slope	-0.385854
N <sub>o</sub>	0.64054
D <sub>DR</sub>	0.385854

V <sub>REF</sub> (l)	0.015975
V <sub>VOID</sub> (l)	0.026039
P <sub>VAP</sub> (bar)	68.61705
V <sub>SAMPLE</sub> (l)	0.003094
V <sub>CELL</sub> (l)	0.029133
ρ <sub>ADS</sub> (mol/l)	22.72211

BET Isotherm (ton CO <sub>2</sub> /ton Coal)		
X <sub>BET,LIN</sub>	Y <sub>BET,LIN</sub>	N <sub>BET</sub>
0	0	0
0.14218675	30.2279659	0.00551049
0.29661141	65.9363004	0.00708803
0.44377873	89.3728273	0.00911572
0.5919469	105.87687	0.01253318
0.69790963	140.354854	0.01699621

BET PARAMETERS	
Intercept	2.997547
Slope	190.4701
C <sub>BET</sub>	64.54197
N <sub>mBET</sub>	0.005169